IPB-CHAPTER 8

PLASMA OPERATION AND CONTROL

TABLE OF CONTENTS

8. PLASMA OPERATION AND CONTROL

Plasma operation and control constitute the ultimate manifestation of the science of tokamak operation, and in the broadest sense encompass the practical application of the physics basis knowledge and plasma operation experience that is embodied in Chapters 2-7 of this Article. This

Chapter addresses the implementation of plasma operation and control means, with emphasis on the operational techniques that are used to effect and control plasmas in tokamaks so as to obtain maximum plasma performance or conduct scientific and technology validation studies. These plasma operation techniques derive both from the science/physics understanding quantified elsewhere in the ITER Physics Basis and from the tokamak operation experience that has been accumulated in what is now more than 30 years of development of tokamak and related toroidal magnetic fusion experiments. This experience basis, which now constitutes a well-defined set of procedures and practices for tokamak operation, falls into a domain which encompasses both scientific and technology/hardware considerations. Assessing how this experience will extrapolate to ITER and reactor tokamaks is the rationale for this Chapter.

This Chapter also addresses the plasma-operation-related subject of how control and monitoring of plasma operation enters into the protection of tokamak systems against the normal and abnormal effects of plasma operation. This aspect of plasma control—already of some import in present tokamaks—will assume a higher level of importance for reactor tokamaks and ITER, since the plasma energies and surface energy deposition levels inherent in reactor-regime operation have a higher potential to effect plasma-facing-component surface damage, and the need for comprehensive protection of reactor tokamak systems against plasma-operation-produced damage is arguably higher—for both economic and safety reasons—in a reactor-scale tokamak.

Much of the basis for plasma operation and control ultimately devolves to the physics basis elements—confinement, MHD stability, beta and density limits, power and particle exhaust optimization and heating and current drive means—that have already been addressed from a scientific viewpoint in Chapters 2-6 of this Article. Plasma control also utilizes the plasma status data provided by the various plasma diagnostics systems described in Chapter 7. There are also tokamak and ancillary hardware system considerations that enter into plasma control and operation, and in many cases it is these design-specific hardware considerations—PF coil configuration, power system controllability and response time, available auxiliary power, deposited power profiles and so forth and the availability of diagnostic data—that ultimately determine how plasma control in reactor tokamaks can be effected and the degree to which the underlying characteristics of the plasma can be controlled—or not controlled. In the discussion that follows, both physics and hardware considerations are addressed. For the hardware aspects, we introduce hardware and characteristics and operation limitations that are specific to the present ITER design concept. It is possible, of course, that some of these specific details may change in the future or may be somewhat different in other embodiments of a future tokamak reactor design.

The content of this Chapter is organized into two Sections. Section 8.1 addresses wall conditioning, an aspect of plasma operation that is the necessary prelude to obtaining the very-low impurity release conditions that are essential for tokamak plasma operation in general and high-

fusion-performance operation in ITER in particular. The subject of tritium retention and removal of retained in-vessel tritium, an operational matter of great importance for reactor tokamaks and ITER, is also addressed in this Section. Section 8.2 addresses what can be thought of as the kernel of tokamak plasma operation: implementation of the various aspects of plasma operation scenario (discharge sequence). The broad outline of the various considerations that enter into determining the scenario are introduced in §8.2. More specialized details of the control of the plasma magnetic configuration and control of the basic plasma kinetic properties (density, fusion power, power and particle exhaust and divertor conditions) are respectively addressed in §8.2.1 and §8.2.2. Specialized aspects of the scenario, including the details of plasma startup, current rampup and rampdown and current termination phases are presented in §8.2.3. The emerging topics of control and optimization means for 'advanced performance' and/or steady-state plasma operation—where modification and active control of the naturally-occurring plasma current profile is required (see §3.2.7)—are addressed in §8.2.4. The presentation here also briefly addresses the further considerations of implementation and control of the various possible internal or edge transport barriers that such 'advanced-performance' modes may incorporate.

The overall projections of wall conditioning and plasma operation and control to ITER are respectively summarized in Section 8.1 and in the corresponding sub-sections of 8.2. How the ITER operation program will be conducted and the scientific and technology issues that ITER operation will address during the course of this program are presented in Chapter 9.

8.1 SURFACE AND WALL CONDITIONING

The plasma facing surfaces in ITER will need to be conditioned before plasma operation commences. For ITER, pre-operation conditioning is required not only to establish a stable discharge, but also to avoid contamination of a burning DT plasma with appreciable levels of both higher-Z impurities and also hydrogen (H). In ITER, excessive levels of either of these impurities will lead to degradation of DT burn and fusion power capability and ultimately termination of sustainable fusion burn and plasma disruption. This Section summaries ITER requirements for surface conditioning, reviews present tokamak condition methods and presents how these methods will extrapolate to the ITER reactor-regime. In the latter regard, extrapolation of presently-used tokamak wall and surface conditioning methods to ITER and to reactor tokamaks in general is not fully straight-forward, since operational limitations inherent in a practical ITER/reactor design will preclude or limit utilization of several of the presently most used surface conditioning techniques. In addition, unlike in most present tokamaks, plasma operation—with sustained current and fusion power— in ITER will comprise the majority of the tokamak operation cycle time. This plasma operation duty factor distinction is expected to result in a substantially different wall conditioning situation than in present tokamaks where the plasma operation duty factor is very low.

8.1.1. ITER Wall/Surface Conditioning Requirements and Constraints

As in present tokamaks, the plasma facing surfaces in ITER will need to be conditioned before plasma operation, after torus vacuum vessel openings, vents, and major leaks and possibly after the occurrence of major disruptions. ITER plasma-facing-surfaces may also have to be conditioned —in a quasi-continuous manner—during the actual course of plasma operation. Conditioning—which broadly defined means achieving surface conditions in which the amount of desorbable hydrogenic species (D and/or T in ITER) is limited and in which the amount of desorbable non-hydrogenic impurities is reduced to very low levels—is necessary in ITER for a variety of reasons. These reasons divide into six categories. The first three categories are familiar in present tokamak operation practice: 1) maintenance of a low torus vacuum base pressure, 2) limitation of the release of non-hydrogenic impurities at startup and during the ensuing plasma discharge so as to maintain acceptable plasma purity, and 3) limitation of the release of surface-absorbed D and/or T so as to maintain plasma density and fusion power control and acceptable edge plasma characteristics (see §3).

In addition to these present-tokamak requirements, in ITER, three additional surface-conditioning considerations become important: (4) limitation of hydrogen (H) levels in the plasma during DT operation, (5) control of surface-generated dust production and inventory, and (6) control/limitation of the tritium (T) inventory in the surface layers of the plasma facing components. Consideration (4) reflects the important nuance for DT burning tokamaks that volume-entrained H—a ubiquitous component of many fabricated metals—constitutes an impurity that can significantly reduce plasma DT reactivity if it (H) finds its way into the plasma during DT operation. Considerations 5) and 6) reflect that fact that surface-generated dust (particulates, loosely bound layers, etc.) and surface- or bulk-absorbed T can separately and collectively constitute appreciable in-vessel inventories of radioactivated or inherently radioactive material. The mobilization and release of these inventories in certain torus vacuum and external confinement barrier integrity failures could raise plant personnel and public safety concerns. In addition, the avoidance of excessive long-term in-vessel T accumulation is critical to the efficient utilization of the limited amounts of externally-supplied T that will be available for ITER operation and the similarly-limited amounts of T that can be breed in ITER or a reactor with a tritium breeding blanket installed.

The detailed operational requirements for ITER plasma-facing-surface conditioning are determined both by the basic plasma operation requirements—pre-discharge base pressure, allowable plasma impurity and H levels, allowable uncontrolled DT release levels, etc.—and by the plasma facing surface materials and the conditions under which they are used. These latter aspects are design specific. The present ITER design incorporates a mixture of in-vessel materials and surfaces: carbon fiber composite (CFC) divertor plates (total in-vessel surface area ~100 m^2), tungsten liners in the divertor and baffle (~ 400 m^2), and a Be-clad first wall (~1200 m^2) and divertor dome. The torus vacuum vessel and major internal structural components are austenitic stainless steel, alloy SS316L (~7,200 m^2). All of the plasma-facing-components are mounted on water-cooled Cu alloy heat sinks. The maximum bakeout temperature of the in-vessel components will be limited to 240˚C. This limit is set by the 4 MPa maximum pressure that can be allowed in the water cooling pipes. There may be a possibility of baking in-vessel components to higher temperatures with hot gas, but the time required to remove completely remove water, introduce gas and then reintroduce water will limit such enhanced-temperature baking to major commissioning and recommissioning periods.

The use of superconducting magnets in ITER will also significantly restrict surface conditioning methods. Owing to the time required to ramp the toroidal field up or down (~3 hours) and the desire to avoid unnecessary TF magnet stress cycles, the ITER toroidal field will be maintained at or near its nominal 5.7 T value for weeks at a time, and present guidelines specify that the TF magnets can be cycled to zero 1000 times during the ~30-year life of the machine. If

half of these magnet cycles are allocated to glow conditioning, this implies about 15 conditioning periods per calendar year. Given that scheduled 'ready for plasma' operation time in ITER will typically be about 25%, weekly (but not daily) glow conditioning appears possible. In addition, since rapid and frequent changes in the poloidal field of the type needed for rapid pulse discharge cleaning or high-repetition-rate low-current tokamak pulses will cause unacceptable heating in the PF and TF coil cases and other cryogenic-temperature structures, the use of pulse discharge cleaning and repetitive low-current conditioning discharges will not be possible.

The means used for conditioning in present tokamaks and the underlying surface conditioning that they effect are briefly summarized in §8.1.2 below. The application of these methods to ITER is addressed in §8.1.3.

8.1.2. Conditioning Methods Used in Present Tokamaks

Conditioning of the tokamak plasma-facing surfaces has been important in reducing the influx of both impurities and hydrogenic species in tokamaks. Effective surface conditioning is an important aspect of maximizing the plasma parameter operation space and is essential in operating a tokamak successfully close to its various operational limits [8.1.1] (see also §3.2 and §3.3) and for minimizing the frequency of disruptions (see §3.4).

The effects of surface and wall conditioning can be categorized into two major areas: reduction of impurity influxes and control of hydrogenic fueling from plasma facing surfaces. Historically, impurity control was the first area addressed in wall conditioning [8.1.2, 8.1.3], followed more recently by techniques to control hydrogenic wall fueling. Uncontrolled impurity radiation can affect energy confinement, increase the ignition threshold or even prevent ignition completely. In more extreme cases impurity radiation can lead to radiative collapse and disruption (see §3.3 and §3.4.1).

Wall conditioning plays a particularly important role in the control of oxygen (O) as a plasma impurity [8.1.1, 8.1.2]. Oxygen is present in tokamak wall materials as metal oxides and hydroxides, as water, and various compounds which are byproducts in oxygen passivation, such as B_2O_3 after boronization. The sources of oxygen contamination in tokamaks are many and include air and water leaks, water vapor absorbed on surfaces and in materials during prolonged torus vacuum vessel openings, and long-term diffusion from the bulk to the surface of the plasma-facing-component and vacuum vessel wall materials. Oxygen readily forms volatile gases (e.g., CO, CO_2 and H_2O) which can subsequently be released during plasma formation and operation. Oxygen contamination is particularly troublesome during plasma startup, since partially-ionized oxygen is a strong atomic radiator for plasma temperatures in the 100 eV range. It is therefore necessary to limit oxygen contamination of startup plasmas in ITER to $\leq 10\%$ (see §8.2.4).

The means available for control of oxygen include vacuum baking (to liberate surface-absorbed water, CO and CO_2), plasma discharge cleaning, which can remove more tightly-bound chemical and atomic oxygen, and gettering, which controls oxygen by passivation to form stable compounds which are not easily dissociated. A figure of merit for candidate getters is the free energy of formation per oxygen atom for the formed oxides. A wide variety of materials make effective getters: Be and B, with respective free energies of 581 and 397 kJ/mol, Al and Si, 527 and 428 kJ/mol, and Ti and Ta, 444 and 352 kJ/mol.

Excessive hydrogenic influxes from the wall can also affect plasma performance, particularly in present tokamaks without active during-discharge pumping as is embodied in a pumped limiter or pumped divertor (see §3 and §8.2.2.2 below). Wall-released hydrogen (H or D) can be particularly troublesome in present day tokamaks with large areas of plasma facing graphite, and in many cases the highest plasma confinement and DD neutron production has been obtained in low-density discharges with low hydrogenic recycling such as negative central shear (NCS), Supershot, hot-ion H–mode and VH–mode discharges [8.1.4–7]. In all of these cases, the attainment of high-performance has followed upon implementation optimized wall-conditioning procedures that limit uncontrolled hydrogen fueling.

A variety of tokamak wall conditioning techniques have been developed over the last two decades. Nearly all of these techniques are still used, so we discuss them below in the approximate chronological order in which they were developed. In most presently-operating tokamaks, combinations of several of these techniques are used, serially or simultaneously, to provide a wall-conditioning regimen that allows reliable high plasma performance operation to be obtained on a routine basis. A somewhat different combinations of techniques are typically used for recommissioning, vacuum leak recovery and sometimes for recovery after major disruptions.

Metal-Film Gettering. Gettering, one of the earliest techniques used for wall conditioning in tokamaks consists of the controlled evaporation of metals which are deposited as thin films on in-vessel and plasma facing surfaces. The metals used for gettering, primarily Ti, Cr, and more recently Be, passivate oxygen and other volatile impurities and thus reduce the influx of these impurities into the plasma discharge. Initial gettering in a previously-ungettered tokamak typically produces immediate improvements in plasma performance and stability—higher attainable density, lower Z_{eff}, reduced levels of MHD instability and occurrence of disruption and so forth.

The JET tokamak has used Be as a getter which has the additional advantage of low Z, so potential problems with influxes of the getter material into the plasma are minimized [8.1.9]. In JET, Be gettering resulted in slower plasma current quenches and more benign disruption effects. However, long-term use of gettering can have detrimental consequences. For example, Ti, applied extensively in the ATC tokamak to reduce both oxygen and higher-Z impurities [8.1.8] also stores

large amounts of hydrogen, and the thick layer of deposited Ti with oxides and hydrides included tends to separate from the underlying gettered surfaces. Such flaking problems, the inhibitory effect that gettering has on impurity removal by pulsed discharge cleaning and the ultimate tendency of heavily-gettered surfaces to begin to release previously-gettered materials has resulted in abandonment of massive metal-film gettering as a long-term tokamak conditioning/operation technique.

Pulsed Discharge Cleaning. Taylor discharge cleaning (TDC)) [8.1.10], repetitively pulsed low temperature discharges, is another early wall conditioning technique. Pulsing results in improved impurity removal efficiency: the dwell time between pulses allows for the volatile impurity gases to be pumped out of the vessel. TDC is especially effective in reducing surface oxygen to less than one atomic monolayer in metal-wall tokamaks, in particularly when it is used at elevated wall temperatures. In many applications, the ohmic heating of resistive torus vessels or in-vessel structures that TDC produces also raises vessel and in-vessel temperatures to high levels; in other cases hot gas or external heaters are added to obtain the desired temperatures (see below).

Baking, another early wall conditioning technique, is especially effective in removing water, volatile hydrocarbons, and hydrogen from graphite and other materials. Fig. 1 shows the volatile gas desorption for graphite during baking [8.1.11]. Many fusion devices have the capability of baking vacuum vessels and in-vessel components to temperatures greater than 250°C, including DIII–D, TEXTOR, JT–60U, Tore-Supra and JET, and reductions in both recycling and impurity influxes are obtained when baking is used. Baking is, of course, part of the standard regimen for the ultra-high-vacuum practice that forms the starting point for tokamak surface conditioning. However baking alone, without simultaneous or following plasma conditioning, does not usually produce satisfactory results. In-situ baking temperatures in present tokamaks fall in the range of 150-500 °C. Higher temperatures are more effective, particularly when large quantities of graphite or carbon-composite in-vessel material is present. Figure 1 demonstrates that for graphite, while ≥400 °C baking is more efficient than lower temperatures in releasing water and surface-bound H, 250 °C is still adequate, and thermal and structural difficulties of higher temperature baking can, if necessary, be traded off against the faster release that higher temperatures allow. For ITER, where thermal and structural limitations set an in-vessel baking temperature limit of ~240 °C, adequate removal of water, volatile hydrocarbons and the first increment of surface-bound H/D/T.

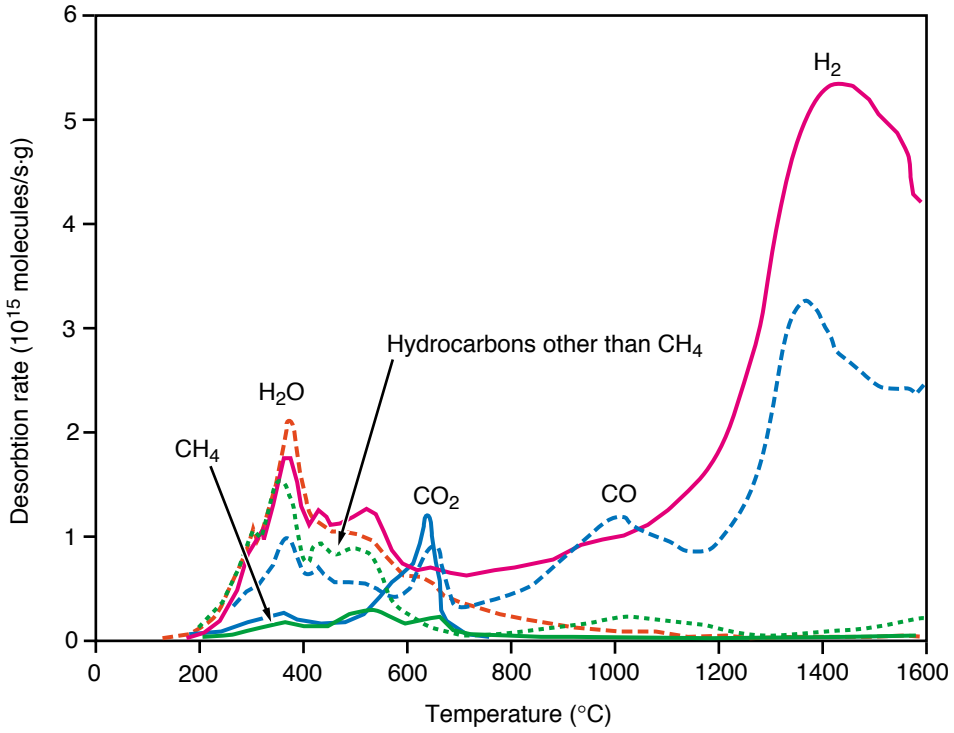

FIG. 1. Thermal desorption of volatile gases from graphite (from Ref. [8.1.11]).

Vacuum Pre-Baking of small metallic and graphite components to higher temperatures (≥ 600 °C) has also come to be a standard tokamak construction and commissioning practice. Here experience has shown that back-filling the baking chamber with an inert gas after the baking is complete and maintaining the baked component in a modestly sealed inert gas environment until installation preserves most of the initial impurity removal benefit that such pre-processing provides.

Disruptive Discharge Cleaning provides an alternate to high temperature baking that combines certain features of baking and pulsed discharge cleaning. In tokamaks in which the in-situ baking temperature of the torus vessel is limited, thermal desorption of volatile impurities and hydrogenic species has been facilitated by heating only the plasma facing surfaces using disruptive discharge cleaning (DDC). The method has been extensively used in TFTR [8.1.12]. A series of low-density helium discharges that terminate in disruption are used to provide high transient surface heat and particle fluxes that “flash desorb” impurities and also eventually raise the bulk temperatures of thermal-isolated in-vessel components (e.g., graphite tiles) appreciably above the equilibrium temperature of the vacuum vessel wall. Although this DDC process requires operation

of all tokamak systems and is more complicated and time-consuming than simple baking, it is effective in conditioning the first wall.

Glow Discharge Cleaning has proven to be useful for both impurity and hydrogen recycling control. The method, which uses a dc anode inserted into the torus vessel to produce a steady-state low-pressure 'cathode glow' discharge that more-or-less uniformly covers the torus/wall surface. The method is simple to implement either for between-plasma-operation (overnight) or between-plasma-discharge wall conditioning. The anode voltage is typically ~500 V and a current-limiting series resistor or inductor is used to stabilize the discharge current and to limit current during arcing that can occur during initial periods of glow conditioning. Discharge pressures are typically about 0.1 Pa (10^{-3} Torr).

Depending on the intent of the glow conditioning, various inert or reactive gases can be used. For initial removal of oxygen and/or volatile impurities, hydrogen or sometimes argon is used. For control of hydrogen, helium is the preferred gas. Hydrogen recycling control is especially important for graphite wall machines, since graphite can be a large reservoir of hydrogenic atoms, providing excessive and unwanted fueling during tokamak. Helium glow cleaning decreases the hydrogen that is released from conditioned surfaces and any helium that is subsequently released has generally minimal effect on the plasma discharge. For hydrogen recycling control, helium glow discharges have been used prior to operations, or before every discharge to provide reproducible wall conditions [8.1.13]. This technique is routinely used on many fusion devices, also between discharges (ASDEX-U, DIII–D, and TEXTOR). In addition, it has been used for disruption recovery on JET, TFTR and JT–60U.

For the most effective He conditioning, the energy of the incident ions needs to be greater than a few hundred eV. Desorption of hydrogenic particles only occurs within the range of the He atoms in the near-surface region. Thus, in order to effectively desorb hydrogenic particles from graphite, the energy of the helium atoms striking the wall must be several hundred eV, as shown in Fig. 2. Both laboratory and in-situ tokamak data illustrate the effect of energy.

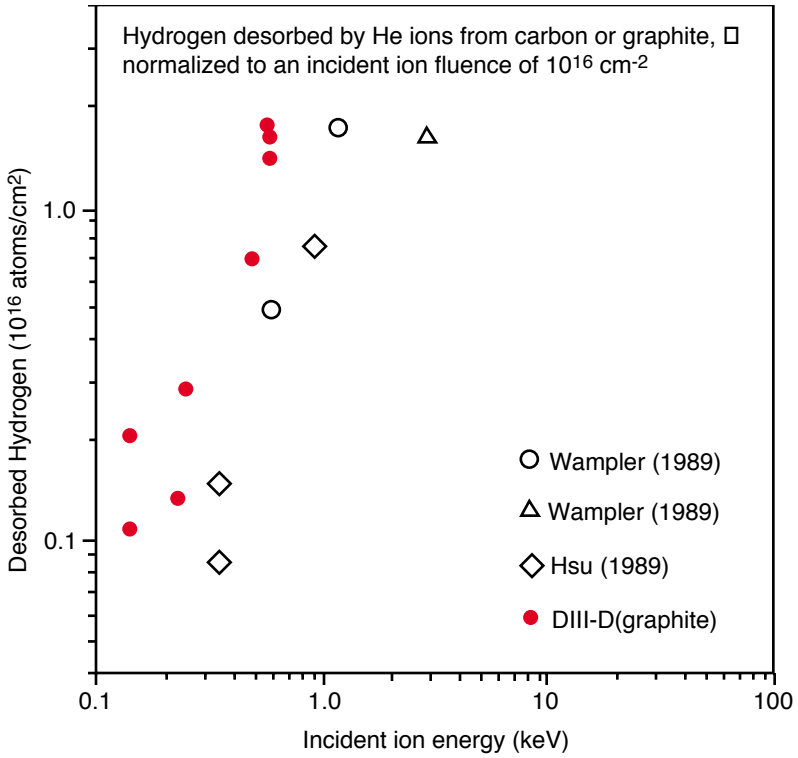

FIG. 2. Helium-induced desorption of hydrogenic species from hydrogen-saturated carbon films (laboratory data, indicated by open symbols, see [8.1.13] for references) and DIII–D graphite tiles (in-situ glow conditioning data, filled symbol) as a function of incident He ion energy. The desorbtion is normalized to a He ion fluence of 1×10^{16} ions cm^{-2}.

In DIII-D between-pulse glow cleaning has been found to significantly improve plasma operation reliability in low-field/high-beta experiments where $q_{95} < 3$ is required. Between pulse conditioning is also found to reduce the frequency of disruptions during such experiments [8.1.13]. For an experimental session without between-pulse conditioning, only 36 out of 106 discharges attained $q < 3$ without disruption or intentional limitation of current to maintain $q > 3$ (higher q discharges were used for recovery after a low-q disruption occurred). With between-pulse He conditioning, the $q < 3$ 'success ratio' was 75 out of a total of 110 discharges. Improvements in error-field-induced-locked-mode tolerance were also observed with between-pulse conditioning.

Deposition of thin films of various materials on the entire plasma facing wall is a more-recent development in wall conditioning. The method serves to modify the composition and surface characteristics of the plasma facing surfaces. Techniques to apply these films consist of chemical vapor deposition (CVD), solid target erosion and deposition, and pellet injection [8.1.3]. However

the most used technique is the plasma-assisted deposition of thin films, initially in form of amorphous carbon films (carbonization) to reduce sputtering of metal impurities [8.1.14]. Although carbonization is successful in reducing metal influxes, the effect on oxygen is not very pronounced and carbon influxes increase. The use of boron films (boronization) has been found to be more optimal, since it simultaneously reduces oxygen, carbon and metal influxes. Boronization is presently used on nearly all fusion devices throughout the world. In the DIII–D tokamak boronization has led to a very high confinement mode, (VH–mode) [8.1.7]. Deposition of silicon (siliconization) has been done in TEXTOR and was very effective in reducing oxygen influx and recycling, but under certain conditions has also increased the edge radiation by physical sputtering of silicon [8.1.15].

Lithium has also been used as a wall coating material. The most successful application of lithium has been on TFTR where lithium pellet injection increased the fusion triple product and energy confinement time in supershot discharges [8.1.16].

Radio-Frequency Discharge Cleaning has been used for impurity removal in limited number of applications, generally as an alternate to more conventional glow or pulsed discharge cleaning methods. Electron cyclotron resonant (ECR) heating was successfully applied in the Gamma 10 mirror device, which has a very complex inner geometry, to improve wall conditions [8.1.17]. Recently, ECR discharges have been used on Alcator C-Mod for boronization, and discharges produced by pure ion cyclotron resonant heating have been used in the TEXTOR tokamak for in-vessel conditioning [8.1.18]. Although these techniques have been demonstrated to produce significant conditioning, their conditioning efficiency needs to be compared directly to more conventional techniques such as glow discharge conditioning. While rf heating discharges can be used in a magnetic field, the energy of helium or hydrogen atoms striking the wall is usually considerably lower than glow discharges and hence, as shown in Fig. 2, the desorption efficiency is expected to be lower. In addition, the uniformity of the incident particles produced by these discharges needs to be determined.

Hydrogen (Tritium) Removal. Removal of hydrogenic species absorbed and/or co-deposited in plasma-facing-surfaces after a sustained period of plasma operation is needed in present tokamaks when the isotopic species is to be changed (e.g., D operation following H operation or vice versa) or more recently when experiments with T initiated . For isotopic ‘switchover’ in JET tritium experiments, glow pre-conditioning with the desired species followed by Ohmic and low-power auxiliary-heated discharges is found to be sufficient to obtain adequate ‘isotopic purity’ in subsequent operation with 100% T or 50%-50% DT [8.1.21]. In TFTR, there has also been demonstration of tritium removal following T operation campaign periods by D_2 GDC and by He-O GDC (He + 10% O) and also by venting the torus to [subsequently exhausted] air [22]. He-O glow cleaning was found to be significantly more effective in the long term than D_2

glow cleaning, but was not pursued owing to concerns about its effect (oxygen addition) on subsequent plasma operation The JET and TFTR results support the general paradigm for tokamaks of being able to use hydrogen, He and/or reactive gas glow or discharge cleaning plus atmospheric flushing to remove significant quantities of the accumulated in-torus tritium inventory. Reactive gas (oxygen, water vapor) at high temperatures is clearly more effective, but of course leads to de-conditioning (with regard to oxygen and water connect) of the surfaces cleaned.

The tritium inventory that can accumulate in co-deposited first-wall and divertor target surface material in reactor tokamaks and in ITER is projected to be appreciable (~ 1 kg). For this reason, tritium removal becomes an important wall- and torus conditioning issue for such tokamaks. The physics basis for tritium retention and removal in present and reactor tokamaks is discussed at further length in §8.1.3 below.

In-situ Limiter and Divertor Pumping. All of the techniques discussed above apply to present day tokamaks, which operate transiently, with plasma on/off duty-cycle ratios <<1. In-situ pumping can remove impurities on a steady-state basis and also provide recycling control, important for long-pulse and steady-state fusion reactors. Several tokamaks have implemented in-situ pumps in conjunction with pump limiters (e.g., TEXTOR and Tore Supra) or in the divertor region (JET, DIII–D and ASDEX-U). These systems have demonstrated the ability to lower the wall inventory of hydrogenic particles, at least in graphite wall machines [8.1.19, 8.1.20]. For example, the in-situ cryopump in DIII-D has been used in lieu of inter-shot helium glow discharge conditioning [8.1.19]. In the DIII-D experiment, the partially-saturated hydrogenic wall inventory was reduced by 1250 Torr-liters using the pump for 10 consecutive discharges, equivalent to 50-60 times the particle inventory in a typical DIII-D discharge. Wall inventories as low as those maintained by the helium glow were obtained. Thus pumping has demonstrated the ability to achieve low recycling wall conditions equivalent to other conditioning techniques. While reproducible discharges were obtained with pumping in DIII-D, the ability of the cryopump to control impurities, especially after disruptions, was not addressed and is an area requiring further investigations before in-situ pumping can be considered as a replacement for other techniques such as He glow conditioning. Nevertheless, pumping is a promising conditioning technique for devices with a continuous magnetic field and long pulses such as ITER.

8.1.3 Tritium Retention and Removal

As has been noted above, the amount of tritium retained in the surface and bulk materials facing the plasma in ITER and the means required to periodically remove retained tritium become important considerations for the design of ITER systems and plasma operation procedures. Projections of the amount of retained tritium are required for several reasons: assessment of the

radiological hazard associated with routine operation and with potential accident scenarios; determination of the plasma fueling requirements and DT supply; and establishment of detritiation requirements for coolant water. Present understanding of the mechanisms by which hydrogenic isotopes are retained in PFCs as well as quantitative estimates of the fraction of injected plasma fuel which is retained comes both from experiments in existing tokamaks and from laboratory experiments designed to probe fundamental processes [8.1.23]. Results from these tokamak and laboratory experiments are being used to validate models which are utilized in predicting tritium retention in ITER [e.g. 8.1.24].

Some appreciation of the magnitude of the tritium retention effect in ITER can be had from present predictions of these models, which indicate that more than 1 kg of tritium can accumulate in PFCs in less than 1 year of the 'full duty cycle' nuclear testing operation that is planned to take place during the final 5 years of the ITER Basic Performance Phase (BPP). The projected tritium burn-up rate will be about 5 kg per year for such operation (1500 pulses/year x 3.5 g/pulse). For reference, the projected total tritium burnup for the BPP will be about 27 kg, and the annual world-wide tritium production rate projected to be available for ITER will be about 2 kg/year. So the projected 'per-annum' rate of tritium retention in ITER will be appreciable compared to the annual utilization rate (to be derived primarily from already-accumulated commercial tritium reserves) and will comparable to the projected production rate in the period where ITER operates. These supply-related considerations alone mandate that retained tritium in ITER be limited to levels of ~1 kg and that any long-term secular increase in retained tritium be prevented.

Tritium Retention Mechanisms. Hydrogenic isotopes will be retained in plasma facing components of ITER by three principal mechanisms [8.1.23 and references therein]: (*i*) direct implantation of ions escaping from the plasma, which leads to hydrogen retention primarily in a shallow surface region and possibly also diffusion into the bulk (depending on the material used and temperature) (*ii*) co-deposition of hydrogen isotopes with eroded carbon or beryllium (the latter only if abundant O is present) on plasma facing surfaces, which produces co-deposited surface layers with significant hydrogenic content, (*iii*) production of tritium by transmutation nuclear reactions in beryllium which results in tritium inventory within the bulk material, principally in microscopic defect sites and bubbles containing helium. There is still a significant uncertainty in quantifying the in-vessel tritium inventory of ITER. Hydrogenic retention is influenced by such factors as the materials used (e.g. carbon, beryllium, tungsten), as well as their crystalline structure, the temperature, and neutron irradiation history, by the presence of other impurities such as oxygen, by plasma conditions close to the PFC, and by the spatial distribution of erosion and redeposition. The use of more than one PFC materials (Be, C, W) in ITER will lead to the formation of complex redeposition layers involving several materials with retention properties which are not well known.

Retention in Present Tokamak Experiments. Quantitative estimates of hydrogen retention are routinely obtained in tokamak experiments using hydrogen or deuterium. The basic mechanism by which the hydrogen species are retained have been identified in several tokamaks. Under carbon wall conditions the dominant mechanism for hydrogenic retention is co-deposition of carbon with deuterium. In-vessel surveys in TFTR by beta back-scattering and ion beam analysis of tiles removed from the vessel show that the dominant regions of redeposition are located away from the plasma-limiter interaction regions, with co-deposited films of up to 10 μm thickness developing in low flux regions of the SOL. Significant co-deposition was also observed in gaps between the limiter tiles. In TFTR deuterium-fueled discharges over a five year period, the fraction of injected deuterium retained in the first wall was found to be 44% (with uncertainty ±17%).

More recently, TFTR and JET have provided precise measurements based on the accounting of tritium in D-T experiments. During the D-T experiments in TFTR, which lasted 3 years, the fraction of tritium retained in the vessel was found to vary with discharge type, clean-up history and the period studied [8.1.28, 8.1.29, 8.1.30]. Overall, the long-term retention was in the range of 30-55% depending on discharge history. This fraction is in excellent agreement with the retention observed in deuterium experiments. Of the 2.7 g of tritium introduced by NBI and 1.7 g introduced by gas-puffing, 1.6 g remained in the vessel at the end of D-T operations.

Several removal techniques including DC discharges in oxygen and deuterium, pulsed discharges and ventilation with room air were applied to remove tritium during this period, with varying degrees of success. It was noted, in particular, that He/O-GDC was substantially less efficient than observed in laboratory experiments [8.1.30]. In addition, later removal campaigns were less effective than the initial campaign, presumably because the majority of the retained tritium was more deeply buried. Following termination of TFTR experiments, the residual tritium retention in the torus after various removal techniques had been exhausted was approximately 1.3 g, with a residual outgassing rate of <1 mg per day.

To evaluate the consequences for ITER of the large hydrogenic retention observed in TFTR one has to keep in mind that this tokamak operated at low wall temperatures of about 300 (?) K and has no external pumping capability relying thus only on wall pumping. Low wall temperatures enhance the amount of deuterium stored in the co-deposits and decrease the efficiency of clean-up removal techniques, and a low pumping capability reduces the gas throughput and increase the fraction of retention. In addition, plasma scenarios with high edge temperatures as used routinely in TFTR result in large carbon impurity release rates which results in thicker carbon deposits.

Although D-T experiments in JET have, to date, been of much briefer duration than in TFTR, the use of both beryllium and carbon in PFCs is of particular relevance to ITER. JET operates at wall temperatures of about 600 K with diverted plasmas with much colder plasma temperatures in front of the target. Prior to 1989 PFCs in JET were fabricated from carbon-based

materials or Inconel (from which the vacuum vessel was constructed).and carbonization [8.2.31] was used to cover metallic areas.

In this phase, 13 mg of deuterium was typically required to fuel a JET discharge, of which a total of 60% was recovered after a full day of plasma operations [8.1.32]. Overnight and weekend outgassing increased this recovery to up to 80 %. Analysis of in-vessel components [8.1.33]. revealed similar retention. After beryllium was introduced in 1989, both as a gettering medium and in the form of two toroidal belt limiters, increased wall pumping led to a reduced fueling efficiency but also to an increased recovery rate of deuterium after the discharge, so that the amount of deuterium per plasma pulse retained in the vessel remained approximately the same as with an 'all-carbon' first wall.

Analysis of carbon divertor tiles removed from the JET torus after the experimental campaign in the MkI Pumped Divertor indicated a deuterium retention of ~3.3 g for the entire vessel, very similar to that observed in previous campaigns [8.1.35]. Moreover, following experiments using a beryllium divertor target [8.1.36], similar levels of deuterium were found on beryllium tiles from the inner divertor strike region as on equivalent carbon tiles [8.1.35]. Significant carbon deposition was also observed in this region, presumably due to redeposition of carbon eroded from the PFCs of the main plasma chamber. Deuterium deposition on the beryllium tiles of the outer divertor strike region was significantly below that observed in equivalent carbon tiles. Initial analysis of carbon tiles removed from the MkII Pumped Divertor, which approximates much more closely a continuous toroidal target, showed a very similar pattern of deuterium deposition on the target tiles to that observed in the MkI target, with the dominant deposition in the inner leg of the divertor [8.1.37]. However, the average D concentrations on all the plasma exposed areas of the divertor floor had fallen by a factor of 2, possibly due to the higher operating temperature (200-350°C) of the MkII tiles as compared to that of the MkI tiles (~50°C, with limited excursions to higher temperatures). Of particular significance was the observation for the first time of films and flakes of deuterium-saturated material in cooled regions behind the divertor pumping slot. If these deuterium-saturated flakes are assumed to be formed with toroidal uniformity, they contain an inventory corresponding to 3% of the throughput. Formation of such flakes is thought to be due to the interaction between strong deuterium gas flows and high impurity influxes. This condition may be representative of certain regions of the ITER divertor.

Analysis of tritium retention and removal was a key aim of the JET preliminary tritium experiment (PTE) in 1991, during which 5.5 mg of tritium were injected into plasmas via the NBI system. Although 67% of the injected tritium remained in the torus two days after the experiment, specialized clean-up procedures succeeded in reducing this fraction to ~10% [8.1.38]. This high removal efficiency may be explained by the brevity of the experiment, so that virtually all of the tritium was close to the surface and hence readily removed by isotope exchange. JET is now

conducting a more extensive D-T experiment using optimal D-T mixtures in which up to 10 g of tritium will be introduced into the vacuum vessel. In a preliminary 'experiment-in-progress' account of the tritium retention behavior, of the 40 g of total injected tritium used in the experimental period, about 4 g was retained in-vessel and 1.3 g of the retention was subsequently removed in a 4-day clean-up period [8.1.21]. At this point, about 7% of the tritium used during the first period of T and DT experiments remained in-vessel

Other Retention Data From Present Experiments. Studies of hydrogenic retention in other large and medium tokamaks have also been made via analysis of retained tritium produced by DD. reactions. However these tritons are produced with 1 MeV and can impinge directly on the first wall with high energy and thus a high retention probability.

In JT-60U. analysis of exhaust gases showed that 80-90% of tritium produced in D-D reactions was initially retained in the torus [8.1.39]. Hydrogen plasma pulsing and helium DC with the vessel at 150-300°C reduced this fraction to 70-80%. Analysis of sample tiles from the first wall and divertor accounted for 50% of the tritium produced [8.1.40], with the remainder thought to be accounted for by dust, toroidal asymmetries and in sections other than the immediate first wall.

Tritium produced by deuterium plasmas in DIII-D accumulated in a narrow surface layer on the carbon PFCs on the first wall. The fraction of tritium thus retained corresponded to 20% of the tritium production in the 1991-92 period, or ~10% of the integrated tritium production in DIII-D to that time [8.1.41]. It was found that the tritium could be removed from the tiles as DT gas by baking in an oven to 1000°C.

ASDEX Upgrade has investigated both graphite and tungsten-coated graphite as divertor target materials and the inventory of hydrogenic species following plasma operation has been analyzed by quantitative thermal desorption spectroscopy, nuclear reaction analysis and calibrated secondary ion mass spectroscopy [8.1.42, 8.1.43]. The measured inventory, equivalent to ~0.33 g/m^{-2} of deuterium, was found to be predominantly in co-deposited layers, which form on the inner divertor strike region, and in near surface regions (10-25 μm) beyond the implantation zone. Inventories at the divertor strike points were a factor of 10-100 larger than at the inner wall limiter. Measurements of the tritium inventory of sample tiles from the inner wall limiter and the outer divertor strike point were consistent with the tritium production estimated from the D-D neutron yield. As in the cases of hydrogen and deuterium, the tritium was found to be present at depths (up to 25 μm) well beyond the ion implantation zone, indicating that diffusion into the bulk occurs.

Extrapolation of Tokamak Data to ITER. Great caution is necessary in directly extrapolating the hydrogenic deuterium and tritium retention data from present machines to ITER. The short pulse lengths of present devices—typically 1–10 s—and the significantly smaller ratios of plasma volume to wall surface area favor wall pumping compared with external pumping and hence lead to

higher retention. In present day devices, the wall-retention fraction decreases with increasing gas throughput (JET). Thus it seems that extrapolations of present retention behavior to ITER should be based more upon the absolute amount of fuel retained rather than on the retained fraction. Moreover, owing to the short pulse length, measurements in present devices are influenced disproportionately by transient effects such as impurity generation and transport, and their affect on erosion/redeposition, during the start-up and shutdown periods. Finally, the ITER edge plasma conditions are expected to be significantly different from those in present experiments: ITER divertor densities are expected to be substantially higher than those in JET or TFTR, with correspondingly lower divertor target or edge temperatures. Furthermore the wall surface temperature in the divertor region will be higher, and the amount of oxygen contamination may well be lower owing to the large surface area of beryllium present in ITER.

Retention Data from Laboratory Experiments. The interaction of hydrogenic species with plasma facing-components has also been extensively studied in laboratory experiments, where individual processes can be investigated and understood in isolation and where conditions are better controlled and diagnosed than in tokamaks. New implantation and co-deposition data are available, particularly for beryllium and for tungsten alloys, for conditions representative of ITER [see e.g. 8.1.23]). Results from laboratory experiments and modeling must be coupled to edge plasma codes to test predictions of retention against measurements on existing tokamaks. Furthermore tests are required on tokamaks with the proper impurities and wall materials to provide a realistic test bed which would closely mirror the situation proposed for ITER (i.e. beryllium walls and carbon and tungsten in the divertor).

ITER Tritium Retention Estimates. Neglecting transient wall pumping effects by implantation and saturation of a shallow near- surface region with tritium, which should be of minor importance for ITER, the tritium inventory in the vacuum vessel of ITER will be mainly determined by co-deposition of tritium with carbon, and possibly beryllium, eroded from the wall on the cold surfaces of the divertor. This process has been simulated for ITER divertor conditions, based on modeling studies by Brooks *et al.* of the plasma edge parameters at the strike zones, impurity release from the target (mainly chemical erosion) and near-wall transport and redeposition of eroded molecules based on molecular break-up data of methane [8.1.44]. These studies predict tritium co-deposition ranging from 1-20 g/pulse (= 0.3-6 $\times$ burn-up per pulse), depending mainly on the divertor operation regime. For the nuclear testing phase of the BPP (1500 pulses/year), the corresponding per annum accumulation would be (without removal) 1.5-30 kg. Depending on the accumulation rate, 1 kg of retention would develop after 50-1000 pulses (31-600 hours of continuous operation at 1.6 pulses/hour). If an administrative limit of 1 kg were to apply (this is an arbitrary but not unreasonable assumption), then tritium removal action would be required after this number of pulses.

There is a great variation in the range of predictions. With respect to the causes of the variation, attached divertor scenarios with high local redeposition probability are favorable (lead to low retention), whereas detached scenarios are unfavorable, with high retention, since the resulting low-temperature are more transparent for escape of the hydrocarbons formed at the target and are found in the modeling to result in thick co-deposits on side areas with large amounts of stored tritium. The estimated amount of tritium retention in these detached scenarios is consistent to some extent with the retention observed in present short-pulse tokamaks. It is therefore conceivable that per-annum retention rates in ITER will be of the order of 10 kg. At this rate of accumulation, periodic removal during a sustained operation (fluence accumulation) campaign will likely be required, if only for reasons of the need to recover and recycle in-vessel tritium.

There is presently major uncertain about tritium accumulation and removal in an ITER-class tokamak. However, present data and the simulation considerations presented above highlight the potential magnitude of in-vessel retention and a critical need to develop and test in-situ cleaning techniques for the efficient control and removal of the co-deposited tritium in ITER. High temperature (> 300˚C) baking of the divertor system in an oxygen atmosphere, low-pressure plasma discharges with oxygen (ECR, ICR, GD) show potential, but further R&D is required to determine the ability of these methods to efficiently and reliably detritiate and/or remove co-deposited layers. The effect of detritation measures on subsequent wall conditions and better quantification of the wall reconditioning needed after each detritiation also require further study. It appears likely that the need for periodic detritation and subsequent wall reconditioning will be a significant factor in the 'ready-for-DT-plasma-operation' availability of ITER and reactor tokamaks.

8.1.4. Implications for ITER: Summary

The wall conditioning needs for ITER are generally similar to those for present tokamaks. The principal addition is a need for periodic tritium removal to recover plasma-facing-surface entrained tritium. Five general types of conditioning needs have been identified:

1. Preparation (commissioning) for initial operation.
2. Recommissioning following major openings, vents, in-vessel component replacements and significant leaks.
3. Daily or weekly conditioning during operation.
4. During and between-shot conditioning.
5. Tritium inventory removal

Wall conditioning in ITER, as in present day fusion devices, is projected to involve a variety of different methods. As has been noted above, ITER has several unique features including superconducting magnets which produce continuous magnetic field for months at a time, long-pulse operation, and a variety of wall materials. Initially, there will be no magnetic field, so most of the conditioning techniques used on present day devices can be applied to ITER during the commissioning phase and during major recommissionings. The applicable techniques include: pre-cleaning and pre-baking of individual components, in-situ baking, glow discharge cleaning, and also thin film deposition (possibly boronization). These methods have been shown to be effective under a variety of conditions and are expected in ITER to be adequate to initially condition the machine for initial plasma operation. The plasma-facing-components will be baked at higher temperatures (> 600 K) before installation. After assembly and prior to first plasma all of the plasma facing components will be baked in-situ at 240˚C followed by glow discharge cleaning (B = 0) and/ or ECR cleaning (B > 0)

Once the ITER toroidal field magnets are energized, however, different techniques are required. Conditioning might be necessary after strong leaks, disruptions or other events in order to provide reproducible initial conditions and ensure a current ramp-up with low impurity influxes and no deleterious MHD, such as locked modes. The presence of full or nearly-full toroidal field will preclude glow discharge cleaning. While the details of possible pulsed discharge cleaning scenarios remain to be studied, the need to implement such scenarios at nearly full toroidal field (and hence with relatively high plasma current) will likely also limit the applicability of standard pulse or Taylor discharge cleaning methods. Therefore, the principal means envisioned for between-plasma-operation and between-pulse cleaning in ITER is ECR and/or ICRH conditioning. The ability of both of these method to effect conditioning in present tokamaks has been demonstrated. However, the efficacy in both techniques in impurity removal and recycling control and the exact requirements for application to ITER and reactor tokamaks needs more research.

Baking in ITER can be performed with or without a magnetic field and will undoubted be an important conditioning technique, but during routine operations it would probably have to be scheduled for periods when no experiments are planned, possibly on weekends. Diborane "flushing" [8.1.1], i.e. chemically passivating oxygen by injecting B_2D6 gas, is not affected by magnetic fields and may be a useful technique between ITER pulses.

In addition to the conditioning procedures discussed above, operation during discharges will be maintained in ITER with divertor pumping which will provide continuous exhaust of impurities from the walls that are ionized in the scrape off layer and swept into the divertor. Such pumping will also control the hydrogenic particle inventory in the plasma facing surfaces, particularly the graphite material. When ITER operates with its design duty cycle of a 1000-s burn every 2200 s, the total plasma on/off ratio (with startup shutdown periods included) will reach 0.6,

so in-situ ‘plasma operation conditioning’ is expected to become (must become) the dominant conditioning [maintenance] process. In this sense, ITER operation will differ dramatically from present experiments where opportunities for before- or between-plasma-operation conditioning dominate the utilization of plasma operation time.

The use of other wall conditioning techniques for ITER are more speculative. The effect of thin film deposition such as boron or lithium is at most transient. Such transient deposition could be important for discharge initiation or real-time erosion control, but the latter will require additional investigations. The use of beryllium as an ITER first wall material may provide oxygen control, since some of this wall material will be sputtered and could act as a natural getter.

Finally, as noted above, appropriately modified wall conditioning techniques (e.g., He/O discharges or the introduction of high-pressure oxygen or steam) are also being discussed for lowering the T inventory in ITER after peroids of sustained plasma oiperation. It is, of course, quite clear that measures to remove tritium inventory will compromise the surface conditions needed for plasma operation, so a long-term cycle of initial preparatory conditioning, plasma operation possibly supplemented with between-operation conditioning, tritium removal, optional replacement of divertor and other plasma-facing surfaces and reconditioning is envisioned. Continued study of ITER-relevant wall-conditioning and tritium removal methods in present tokamaks and simulations of ITER-revelant conditioning and operation scenarios are also urgently needed to support final quantification of ITER conditioning and tritium removal means and better quantification of the projected availability for ITER and reactor tokamaks to conduct prolonged campaigns of DT-burning plasma operation.

References to Section 8.1

[8.1.1] Winter, J., J. Nucl. Mater. **176–177** (1990) 14.

[8.1.2] McCracken, G.M., P.E. Stott, *Plasma surface interactions in tokamaks* [Review Paper], Nucl. Fusion **19** (1979) 889-891.

[8.1.3] Winter, J., Plasma Phys. Control. Fusion **38** (1996) 1503.

[8.1.4] Lazarus, E.A., G. A. Navratil, C. M. Greenfield, E. J. Strait, M. E. Austin, K. H. Burrell, T. A. Casper, D. R. Baker, J. C. DeBoo, E. J. Doyle, R. Durst, J. R. Ferron, C. B. Forest, P. Gohil, R. J. Groebner, W. W. Heidbrink, R.-M. Hong, W. A. Houlberg, A. W. Howard, C.-L. Hsieh, A. W. Hyatt, G. L. Jackson, J. Kim, L. L. Lao, C. J. Lasnier, A. W. Leonard, J. Lohr, R. J. La Haye, R. Maingi, R. L. Miller, M. Murakami, T. H. Osborne, L. J. Perkins, C. C. Petty, C. L. Rettig, T. L. Rhodes, B. W. Rice, S. A. Sabbagh, D. P. Schissel, J. T. Scoville, R. T. Snider, G. M. Staebler, B. W. Stallard, R. D. Stambaugh, H. E. St. John, R. E. Stockdale, P. L. Taylor, D. M. Thomas, A. D. Trunbull, M. R. Wade, R. Wood, D Whyte, *Higher Fusion Power Gain with Current and Pressure Profile Control in Strongly Shaped DIII-D Tokamak Plasmas*, Phys. Rev. Lett. **77** (1996), 2714-2717.

[8.1.5] Strachan, J.D., et al., Phys. Rev. Lett. **58** (1987) 1004.

[8.1.6] Koide, Y., and the JT–60U Team, Phys. Plasmas **4** (1997) 1623.

[8.1.7] Jackson, G. L., J. Winter, T. S. Taylor, et al., Phys. Rev. Lett. **67** (1991) 3098.

[8.1.8] Stott, P. E., C. C. Daughney, R. A. Ellis, *Control of re-cycling and impurities in the ATC tokamak by means of gettered surfaces*, Nucl. Fusion **15** (1975) 431-440.

[8.1.9] Campbell, D. J., et al., submitted to Fusion Energy Design (1997).

[8.1.10] Oren, L., R. J. Taylor, *Trapping and removal of oxygen in tokamaks*, Nucl. Fusion **17** (1977) 1143-1152.

[8.1.11] Pontau, A. E., and D.J. Morse, J. Nucl. Mater. **141–143** (1986) 124.

[8.1.12] Dylla, H. F., J. Nucl. Mater. **145–146** (1987) 48.

[8.1.13] Jackson, G. L., T. S Taylor, P. L. Taylor, *Particle control in DIII-D with helium glow discharge conditioning*, Nucl. Fusion **30** (1990) 2305-2317.

[8.1.14] Winter, J., J. Nucl. Mater. **145–147** (1987) 131.

[8.1.15] Winter, J., H.G. Esser, G.L. Jackson, *et al.*, Phys. Rev. Lett. **71** (1993) 1549.

[8.1.16] Strachan, J.D., D.K. Mansfield, M.G. Bell, *et al.*, J. Nucl. Mater. **217** (1994) 145.

[8.1.17] Nakshima, Y., M. Ichimura, Y. Imai, *et al.*, J. Nucl. Mater. **162–164** (1989) 812.

[8.1.18] Esser, H.G., A. Lyssoivan, M. Freisinger, *et al.*, Proc. 12th International Conf. on Plasma-Surface Interactions in Fusion Devices, St. Raphael, France, May 1996, to be published in J. Nucl. Mater.

[8.1.19] Maingi, R., G. L. Jackson, M. R. Wade, M. Ali Mahdavi, P. K. Mioduszewski, G. Haas, M. J. Schaffer, J. T. Hogan, C. C. Klepper, *Control of wall particle inventory with divertor pumping in DIII-D* Nucl. Fusion **36** (1996) 245-253.

[8.1.20] Mioduszewski, P.K., J.T. Hogan, L.W. Owen, *et al.*, J. Nucl. Mater. **220–222** (1995) 91.

[8.1.21] Keilhacker, M., for the JET Team, *JET D-T Experiments and Their Implications for ITER*, in *17th IEEE/NPSS Symposium on Fusion Engineering*, (Proceedings 17th SOFE, San Diego 1997), IEEE, Piscataway New Jersey (1998), **Vol. 1** 3-9.

[8.1.22] Mueller, D., W. Blanchard, B. L. Doyle, J. C. Hosea, A. Nagy, G. Pearson, C. H. Skinner, M. A. Ulrichson, W. R. Wampler, S. J. Zweben, *Tritium Retention and Removal on TFTR*, in *17th IEEE/NPSS Symposium on Fusion Engineering*, (Proceedings 17th SOFE, San Diego 1997), IEEE, Piscataway New Jersey (1998), **Vol. 1** 279-285.

[8.1.23] G. Federici, R. Anderl, J. N. Brooks, R. Causey, J. P. Coad et al, Proc. ISFTN-4, Tokyo, 1997 (to appear in Fus. Eng. Design).

[8.1.24] G. R. Longhurst, D. F. Holland, J. L. Jones, B. J. Merrill, *TAMP4 User's Manual*, EGG-FSP-10315, Idaho National Engineering and Environmental Laboratory, June 1992.

[8.1.25] H. F. Dylla and K. L. Wilson editors, *Tritium retention in TFTR*, Princeton Plasma Physics Laboratory Report, PPPL-2523 and Sandia National Laboratory Report, SAND 88-8212, (April 1988).

[8.1.26] W. R. Wampler, B. L. Doyle, S. R. Lee, A. E. Pontau, B. E. Mills, R. A. Causey, D. Buchenauer, H. F. Dylla, M. A. Ulrickson and P. H. LaMarche, *Deposition of carbon, deuterium and metals on the walls and limiters of the Tokamak Fusion Test Reactor*, J. Vac. Sci. Technol. **A6** (1988) 2111-2115.

[8.1.27] M. Ulrickson, H.F. Dylla, P.H. LaMarche and D. Buchenauer, *Particle balance in the Tokamak Fusion Test Reactor,* J. Vac. Sci. Technol. **A6** (1988) 2001-2003.

[8.1.28] C.H. Skinner, W. Blanchard, J. Kamperschroer, P. LaMarche, D. Mueller, A. Nagy, S. Scott, G. Ascione, E. Amarescu, R. Camp, M. Casey, J. Collins, M. Cropper, C. Gentile, M. Gibson, J. Hosea, M. Kalish, J. Langford, S. Langish,R. Mika, D.K. Owens, G. Pearson, S. Raftopoulos, R. Raucci, T. Stevenson, A. Von Halle, D. Voorhees, T. Walters, J. Winston, *Measurements of tritium retention and removal on the Tokamak Fusion Test Reactor*, J. Vac. Sci. Technol. **A14** (1996) 3267-3274.

[8.1.29] C. H. Skinner and the TFTR team, *Plasma wall interactions and tritium retention in TFTR"*, J. Nucl. Mat. **242-243** (1997) 214-226.

[8.1.30] D. Mueller, W. Blanchard, J. Collins, J. Hosea, P.H. LaMarche, D.K. Owens, and C. H. Skinner, *Tritium removal from TFTR*, J. Nucl. Mat. **242-243** (1997) 897-901.

[8.1.31] J Winter, *Carbonisation in tokamaks,* J Nucl. Mat. **145-147** (1987) 131-144.

[8.1.32] R Sartori, G. Saibene, D.H.J. goodall, E. Usselmann, J.P. Coad and D. Holland, *Deuterium release measurements in the Be phase of JET and determination of tritium content in the exhaust gas*, J Nucl. Mat. **176-177** (1990) 624-629.

[8.1.33] J.P. Coad, R. Behrisch, H. Bergsåker, J. Ehrenberg, B. Emmoth, J. Partridge, G. Saibene, R. Sartori, J.C.B. Simpson, and Wen-Min Wang, *The retained deuterium inventory in JET and implications for tritium operation*, J. Nucl. Mat. **162-164** (1989) 533-541.

[8.1.34] J. Ehrenberg, V. Philipps, L. De Kock, R.A. Causey and W.L. Hsu, *Analysis of deuterium recycling at JET under beryllium first-wall conditions*, J. Nucl. Mater. 176-177 (1990) 226-230.

[8.1.35] J.P. Coad, M. Rubel, C.H. Wu, *The amount and distribution of deuterium retained in the JET divertor after the C and the Be phases in 1994-5*, J.Nucl. Mat. **242-243** (1997) 408-413.

[8.1.36] D.J. Campbell and the JET Team, *Experimental comparison of carbon and beryllium as target materials in JET*, J. Nucl. Mat. **242-243** (1997) 379-384.

[8.1.37] J. P. Coad, *Report of the ITER Contract: Deuterium content of material redeposited in tokamaks*", for the period Jan. 1996 to Jan. 1997, JET Report JET-IR(97)02, 3. 1997.

[8.1.38] P. Andrew, J.P. Coad, J. Ehrenberg, D.H.J. Goodhall, L.D. Horton, O.N. Jarvis, P.L. Lomas, M.J. Loughlin, G.M. McCracken, A.T. Peacock, M.A. Pick, G. Saibene, R. Sartori, P.R. Thomas, *Experiments on the release of tritium from the first wall of JET*, Nucl. Fusion **33** (1993) 1389-1404.

[8.1.39] N. Miya, M. Nemoto and N. Toyoshima, *Tritium release from JT-60 vacuum vessel following high-power heated deuterium operations*, Fus. Techn. **26** (1994) 507-511.

[8.1.40] K. Masaki, K. Kodama, T. Ando, M. Saidoh, M. Shimizu, T. Hayashi, K. Okuno, *Tritium retention in graphite inner wall of JT-60U*, Fus. Eng. & Des. (1996) 181-187.

[8.1.41] P.L. Taylor, A.G. Kellman, and R.L. Lee,*Tritium in the DIII-D tiles*, J. Fus. Engin., **12** (1993) 35.

[8.1.42] P. Franzen, R. Behrisch, C. García-Rosales, ASDEX-U Team, D. Schleussner, D Rösler, J. Becker, W. Knapp, C. Edelmann, *Hydrogen isotope inventory in the graphite divertor tiles of ASDEX-Upgrade as measured by thermal desorption spectroscopy*, Nucl. Fusion **37** (1997) 1375-1393.

[8.1.43] P. Franzen, H. Maier, D. Schleußner, R. Behrisch, M. Balden, and the ASDEX Upgrade Team, *Hydrogen isotope inventories in the ASDEX Upgrade Tungsten Coated Divertor Tiles*", presented at the 24th European Physical Society Conference on Controlled Fusion and Plasma Physics, 9-13 June, 1997, Berchtesgaden, Germany.

[8.1.44] J.N. Brooks, R. Causey, G. Federici, D.N. Ruzic, *Assessment of erosion and surface tritium issues for the ITER divertor*, J Nucl. Mat., 241-243 (1997) 294-298.

8.2. PLASMA CONTROL

Broadly speaking, plasma control in tokamaks can be defined to comprise the implementation of the scientific and technological understanding that is required to produce, sustain and terminate a tokamak discharge and to optimize the performance of the plasma that is obtained during the central 'flattop' portion of the resulting plasma operation sequence. Given this all-embracing scope, plasma control draws upon all of the physics basis elements that are presented in the various Chapters of this paper, plus other considerations—for example, vacuum technologies and the control of pulsed electrical power systems—that are essential to implementation of the tokamak concept. In a more limited sense, plasma control is frequently defined to comprise the operational implementation of the control procedures and algorithms that lead to initiation, sustainment, performance optimization and benign termination of a given discharge, and to being able to repeat such a discharge in a reliable and reproducible manner. It is in this sense that the subject is addressed herein, with emphasis on the physics aspects that underlie the various plasma control and operation procedures that are implemented in present tokamaks and that are foreseen to be applicable to future reactor tokamaks and specifically to ITER.

The remainder of Section 8.2 is organized in four Sub-Sections (§8.2.1-§8.2.4) that respectively present details of the physics and operational experience basis for *i)* magnetics control, *ii*) kinetics and divertor control, iii) scenario control, and *iv*) 'advanced performance' control—involving active current profile modification and control of the details of the current profile. These specialized presentations in the following Sections are preceed in this introduction by *i)* a brief historical overview of plasma control methodology and progress and *ii*) a presentation of the presently-envisioned concepts and logic for ITER plasma control. With regard to presentations here and in following Sections about the envisioned characteristics and implementation ITER plasma control, it should be recognized that the present status of ITER plasma control design is largely conceptual and scientific in nature, with a focus on identication of the physics basis for the desired plasma control characteristics and development of a plasma control and machine protection system design concept within which detailed control algorithms, event control logic and data processing can ultimately be implemented as final design and construction of ITER proceeds.

Plasma Control: A Historical Overview

From a historical perspective, there has been major progress since the beginning of tokamak experimentation in the area of plasma control, and there has been a evolution of approach from the pre-programmed 'passive' electrical pulsed power control of the first pioneering tokamaks to 'active' (feedback-enabled) real-time control of key device operation and plasma attributes in the

present generation of tokamaks. In the course of this plasma control development, a great deal of operational experience has been accumulated in the control of the various parameters involved: plasma current, plasma position, plasma shape and plasma density and, with the advent of auxiliary heating, global control of plasma temperature and pressure. Many of the control solutions developed in these tokamaks reflect the specific details of the hardware systems involved, but broadly speaking, the plasma control experience obtained can be categorized as comprising independent and separate control of the magnetic (current, position, shape) and kinetic (density, temperature, pressure) attributes of the plasma.

More recently, experiments have begun to address more-sophisticated localized and direct modification and control the plasma density and current profiles, localized control of MHD instabilities and direct control of the power and particle exhaust characteristics of the divertor plasma. Furthermore, with the advent of a combination of a well-controlled magnetic configuration, controllable auxiliary heating and controllable wall conditioning and particle exhaust (see §8.1), it has been possible to 'control' or optimize the plasma operational regime so as to obtain operation modes with enhanced energy confinement relative to that obtainable in the 'standard' auxiliary-heated L-mode regime (see Chapter 2). This 'operational regime-control' capability combined with the implementation of closed-loop feedback of the subordinate control elements involved—especially plasma shape and position, auxiliary power level and gas fueling for density control—has allowed high plasma energies to be obtained more regularly and reproducibly and sustained in many cases for durations that are set by hardware pulse-length considerations rather than any inherent secular 'uncontrolled' evolution of the plasma itself. In this regard, the increasing long characteristic times scales of the discharges obtained in the most-recent generation of tokamaks has helped in the implementation of the feedback control concepts that make such attainment of such 'stationary' plasmas possible.

There has also been continuing progress in the availability of plasma diagnostics with radial or spatial profile resolution (see §7) and in the coupling of these diagnostics to the corresponding plasma control 'actuators' (poloidal field power supplies, gas injection valves, pellet injectors, auxiliary heating systems, etc.) that affect the measured quantity. There has also been progress in the quantification of the physics and control modelling bases for the key physics elements for real-time plasma control. These bases are expected to ultimately be important for final optimization of the ITER plasma control system, which is presently at the concept definition stage [8.2.0.1].

With regard to future design refinements, plasma control design for ITER and other future machines requires not only a set of suitable plasma diagnostics and control actuators but also a model of the effect that these actuators have on the plasma parameters. A model is not explicitly required for present experiments, since empirical development and tuning of a control system or algorithm can still proceed "manually" by experimental trial and effort. However, this procedure,

which is time-consuming at best, is most applicable to simple systems and becomes increasingly difficult—or can fail completely—in a more-complex 'multi-variable' control situation. In such cases the availability of an adequate model of the plasma response can become useful or essential to the implementation of improved or optimal control. And a model is, of course, needed for future designs. Here it is often necessary to reduce the essential features of a complex physics model or behavior inferred from an experimental database into a simplified 'plasma control' model that can used for control system design and optimization.

Finally, in understanding the present status of plasma control capabilities and the control prospects for ITER or for future reactor tokamaks, it is important to recognize that tokamak operation and control is ultimately a highly-coupled "multiple-input/multiple-output" problem in which the global plasma state derives from elements that are not necessarily fully or separately controllable. Improved physics understanding and modelling and the availability of control methods ('actuators') that can more-directly affect key plasma attributes can result in better control and optimization of plasma performance. However, there will always remain inherent limits to the controllability of certain parameters, even with perfect modelling understanding and perfect diagnostic information.

ITER Control Requirements and Concepts Overview

As has been presented throughout the preceeding Chapters of this Article, the ITER design concept is based upon physics results and operational experience achieved in the past and present generations of tokamaks, most directly those with shaped plasma cross-sections and divertors, e.g., Alcator C-MOD [8.2.0.2], ASDEX Upgrade [8.2.0.3], DIII-D [8.2.0.4], JET [8.2.0.5] and JT-60U [8.2.0.6]. Many of the plasma control requirements and concepts proposed for ITER [8.2.0.1] are identical to those that are already implemented in these devices and other presently operating tokamaks. However, the need for ITER to operate with a burning DT plasma under stationary (time-independent) conditions with pulse lengths of more than 1000 s — 100 times the pulse lengths attained in present devices — and with high levels of plasma thermal and magnetic energy — more than 1 GJ — results in additional plasma control requirements that pose certain new physics and control challenges. Furthermore, as the world's first fusion reactor, ITER will be subject to a high level of public and regulatory scrutiny, especially with regard to issues of robust control of the fusion burn conditions and provision of reliable means to rapidly terminate the fusion burn should off-normal conditions develop.

To first approximation, the plasma control requirements for ITER are similar to those successfully addressed in the presently-operating generation of single-null-divertor tokamaks. As in these tokamaks, the ITER plasma must be initiated, controlled and stabilized magnetically (R, Z,

a, κ, δ) and brought to near-stationary or stationary kinetic conditions (n, T, Z_{eff}, n_{He}/n_e, n_{imp}/n_e and P_{fus}) for a period sufficient to allow attainment of the experimental objective at hand. Owing to the large size and high temperature of the ITER plasma, the time to reach near-stationary plasma conditions (including a fully-equilibrated current profile) can be as long as 1000 s. Accordingly, plasma control methods for ITER will generally have to be 'steady-state': this requirement eliminates many of the transient 'control' techniques (current or shape ramping, transient gas puffing, transient pellet injection, between-pulse wall conditioning) now employed in present experiments. Such transient methods will be useful in ITER for physics experiments or as means to more quickly approach a stationary plasma condition. However, ITER control means must ultimately be compatible with maintaining a stationary plasma condition and with true steady-state operation. This requirement limits the number of control options.

Following attainment of the required plasma conditions, the ITER plasma must be terminated in a controlled manner, in which first the fusion burn and then the plasma current are shut down without disruption. The requirement for a controlled shutdown and for disruption and VDE (vertical displacement event) avoidance throughout the plasma operation scenario is particularly important owing to the high magnitudes (~1 GJ) of plasma thermal and magnetic energy inherent in burning plasma operation.

Finally, the high level of fusion power that ITER will operate at and the relatively short thermal time constants (~3-10 s) of the actively-cooled in-vessel heat removal surfaces make both reliable burn (fusion power) control and a backup fast fusion power and current shutdown mechanism essential for machine component protection. Present concepts for fast shutdown in ITER focus on injection of a relatively massive impurity pellet (~ 10^{22} atoms) leading to a rapid fusion power and current quench on a time-scale of ≤ 300 ms (see §3.4.5).

ITER Requirements and Control Categories. In summary form, the scope of plasma control for ITER and the corresponding requirements for the ITER plasma control system comprises four major requirements [8.2.0.1]:

1) Plasma Operation Scenario Sequencing: Poloidal Field (PF) coil system premagnetization, plasma initiation, current rampup, divertor formation, auxiliary heating, ignition and burn, fusion power shutdown, current rampdown and termination and PF reset and recool

2) Plasma Magnetics Control: plasma current control, plasma shape control (R_o, a, κ, δ versus time, plus control of selected plasma-to-first-wall clearance gaps, including ion-cyclotron antenna coupling gap and the nominal divertor magnetic configuration

during the divertor/heating/ ignition/burn/de-ignition portion of the plasma scenario); also non-axisymmetric error field compensation and control

3) Plasma Kinetics and Divertor Control: core plasma kinetics control (density and/or fusion power, impurity content and/or radiated power fraction, core plasma impurity injection); core plasma profile control: (auxiliary heating and/or current drive), and divertor control (pumping, in-divertor gas and/or impurity injection, magnetic configuration optimization for divertor performance)

4) Fast Plasma Shutdown (fusion power and current shutdown by means of impurity injection)

The division of the ITER control requirements into four categories reflects the relative independence of the four categories and the hierarchical nature of the ITER plasma control concepts. The plasma operation scenario — the superior category in the control hierarchy — provides the overall framework within which plasma operation and control takes place. The overall scenario concept, the order of events and the sequencing of the transitions between the various phases of the scenario are the principal considerations. The same hierarchical control categories and control system organization are already implemented in the control systems of essentially all presently operating tokamaks.

ITER discharge operation will follow a sequence of scenario phases, characterized by distinct technical or physical goals: EC-assisted breakdown, current ramp-up and shape expansion, divertor formation, plasma fueling and auxiliary heating and H-mode transition, ignition and quasi-stationary sustained DT burn. Burn termination and current ramp-down will follow when the maximum PF flux is reached. For optimal control, each scenario phase will require distinct control methods, with a specific set of quantities to be controlled and a specific set of control algorithms to be applied for the actuators. The presently envisioned ITER control strategy is envisioned to involve a mix of sequencing logic, pre-programmed (feed-forward) and closed-loop plasma-parameter-based feedback control of the various hardware actuator systems involved.

In addition to direct control of the scenario phases and parameters, it will be necessary to control the plasma parameters such that operational limits (beta and density limits) are avoided and the various engineering limits of the ITER device and systems are respected. Present understanding is that it may also be necessary to stabilize or control (limit the growth of) certain MHD instabilities (neoclassical modes and sawteeth), to avoid disruption. Finally, if disruption does occur, mitigative actions are desirable to reduce thermal and electromechanical loads on the affected in-vessel systems. This latter function is one of a class of ITER machine protection' functions where

the actions of the plasma control system will overlap the hardware protection functions that have in past tokamaks have traditionally been addressed by separate interlock and/or fault detection systems. To some degree in present tokamaks and to much larger degree in ITER, these ‘protection’ functions are becoming increasing integrated with the more traditional ‘control’ functions ogf the plasma control system.

References to Section 8.2

[8.2.0.1] J. Wesley, H-W. Bartels, D. Boucher, A. Costley, L. DeKock, Yu. Gribov, M. Huguet, G. Janeschitz, P-L. Mondino, V. Mukhovatov, A. Portone, M. Sugihara, and I. Yonekawa, *Plasma Control Requirements and Concepts for ITER*, Fusion Technology **32** (1997) 495-525.

[8.2.0.2] Porkolab, M., R. L. Boivin, F. Bombarda, P. T. Bonoli, C. Christensen, D. Garnier, S. Fairfax, C. Fiore, J. A. Goetz, S. Golovato, M. A,. Graf, R. S. Granetz, M. J. Greenwald, D. Gwinn, S. Horne, T. Hsu, A. Hubbard, I. H. Hutchinson, J. Irby, D. Jablonski, C. Kurz, B. LaBomabard, B. Lipschultz, T. Luke, E. S. Marmar, M. J. May, A. Mazurewnko, G. M. McCracken, R. Nachtrieb, A. Niemczewski, P. O'Shea, J. Reardon, J. E. Rice, J. Schachter, J. A. Snipes, J. Sorci, P. Stek, Y. Takase, J. L. Terry, G. Tinios, J. Urbahn, Y. Wang, R. Watterson, B. Welch, S. Wolfe, *Overview of Recent Results for Alcator C-MOD*, in *Plasma Physics and Controlled Fusion Research 1994* (Proceedings 15th IAEA Conference, Seville 1994), IAEA Vienna (1995) **Vol. 1** 123-135.

[8.2.0.3] Köppendorfer, W, F. Ryter, H. Zohm, M. Alexander, K. Büchll, D. Coster, C. Fuchs, O. Gehre, O. Gruber, A. Herrmann, A. Kallenbach, M. Kaufmann, F. Mast, V. Mertens, R. Neu, W. Suttrop, A. Stäbler, O. Vpllmer, ASDEX Upgrade Team, NI Team, ICRH Team, *H-Mode in ASDEX Upgrade: Physics and Operating Regimes*, in *Plasma Physics and Controlled Fusion Research 1994* (Proceedings 15th IAEA Conference, Seville 1994), IAEA Vienna (1995) **Vol. 1**241 (1995).

[8.2.0.4] Stambaugh, R. D., [for the] DIII-D Team, *DIII-D Program Overview*, in *Plasma Physics and Controlled Fusion Research 1994* (Proceedings 15th IAEA Conference, Seville 1994), IAEA Vienna (1995) **Vol. 1** 103 (1995).

[8.2.0.5] Stork, D., [for the] JET Team, *The New Experimental Phase of JET and Prospects for Future Operation*, in *Plasma Physics and Controlled Fusion Research 1994* (Proceedings 15th IAEA Conference, Seville 1994), IAEA Vienna (1995) **Vol. 1** 51-81.

[8.2.0.6] Kikuchi, M., [for the] JT-60U Team, *Recent JT-60U Results Toward Steady State Operation of Tokamaks,* in *Plasma Physics and Controlled Fusion Research 1994*

(Proceedings 15th IAEA Conference, Seville 1994), IAEA Vienna (1995) **Vol. 1** 31-49.

8.2.1. Magnetic Control and Plasma Disturbances

Magnetic control comprises quasi-static and dynamic control of the global parameters of the tokamak plasma equilibrium—current, shape and position—by magnetic means, effected through control of the currents in the array of Poloidal Field (PF) coils that all modern tokamaks incorporate. Control of the PF coil currents is implemented via feedback control—derived from magnetic diagnostic measurements—of PF coil power supply currents or voltages. The plasma data used as the basis for this feedback control of the PF currents is in turn derived from plasma current, position and shape measurements made with a suite of magnetic diagnostics (Rogowski coils, magnetic probes, flux loops and diagmagnetic loops) that are a common feature of all operating tokamaks. The resulting ability of such feedback-based 'magnetic control' procedures to reliably and precisely control the magnetic attributes of tokamak discharges has become a key contributing factor to the routine attainment of repeatable and reliable plasma performance that modern tokamaks can achieve. The ability to arbitrarily manipulate plasma shape and current (within certain limits) essentially at will has also been instrumental in the conduct of experiments to determine the effect of key plasma parameters (e.g., the q- and j(r) profile) on fundumental plasma transport and MHD stability considerations (see §3.2.7). The state of magnetic control in tokamaks has been refined to such a degree that such control is usually regarded to fall into the domain of engineering operation rather than plasma physics.

In addition to determining global plasma shape, position and current during the course of a given discharge, plasma magnetic control also has the essential additional functions of stabilizing axisymmetric (n = 0) instabilities of the plasma cross-section (especially the m = 1 vertical instabililty inherent in elongated cross-sections) and in maintaining the plasma shape, position and current nearly fixed despite the occurance of internal plasma disturbances—sawteeth, minor disruptions, ELMs and other internal relaxation transients—that would otherwise compromise maintenance of the plasma equilibrium. Quantification of the expected characteristics of such disturbances and design of appropriate control procedures to limit the ensuing effect is thus an important aspect of the science and art of plasma magnetics control.

The same plasma magnetic control diagnostics and procedures that are sucessfully used in present tokamaks are envisioned to be fully adequate for the magnetic control of ITER plasmas with fusion burn durations of 1000 s or greater, and neither the longer plasma discharge duration nor the higher levels of plasma magnetic and kinetic energy that are inherent in ITER plasmas will affect the underlying present physics basis for plasma magnetic control. However, as will be addressed below, the ultimate need to extend magnetic control of ITER plasmas to burn and current durations that are ultimately steady state will eventually require that non-magnetic diagnostic data and/or true dc magnetic measurements of the plasma current, shape and position be added to the

overall plasma magnetics control system. In addition, while the larger size and energy content of ITER plasmas will not affect the physics basis of plasma magnetic control, considerations of limiting peak control power demand and the greater similarity of the time-scales in ITER for vertical instability control and plasma shape variance control and for response to the effects of internal plasma disturbances all argue for the application of 'modern' control system design methodologies to develop a highly optimized plasma magnetics control system for ITER.

8.2.1.1. Physics basis for plasma control

The underlying physical basis of plasma current shape, position control in tokamaks and other similar axisymmetric magnetic confinement configurations is ideal MHD equilibrium, as embodied in the Grad-Shafranov plasma equilibrium equation (see §3.2.1), which describes 2-D magnetostatic plasma equilibrium in the absence of significant mass flow, plasma rotation or pressure anisotropy. As is described in §3.2.1 and references therein, solution of the Grad-Shafranov equation in conjunction with specification of parameters that characterize the plasma pressure and current profile and toroidal field yields both the plasma equilibrium flux surface configuration and the corresponding PF coil currents. Although analytic solutions for the plasma equilibrium can be obtained in certain idealized cases, numerical methods are typically employed for tokamak design and operation planning and for analysis of experimental data, and numerical models are essential for the design of tokamaks with discrete PF coil systems and divertor geometries. A variety of well-benchmarked numerical Grad-Shafranov design and data analysis codes are presently in use. For the design of future tokamaks, when care is taken to use the same perscriptions for the plasma pressure and current profiles and to obtain the same plasma boundary shape, excellent agreement among codes with regard to both the plasma flux surface configuration and the PF currents is obtained. When these Grad-Shafranov models are used for data analysis, good agreement among calculated flux surface geometry and the corresponding experimentally measurable attributes of the plasma can be obtained, and it is also possible to determine the normalized plasma pressure (poloidal beta, β_p) and the approximate degree of current profile peaking (as quantified in terms of the dimensionless internal inductance l_i) [8.2.1.1]. In the same vein, specification of these two parameters for future plasmas is sufficient to obtain an accurate estimated static flux surface configuration and PF currents.

Figure 8.2.1-1 illustrates a ITER plasma equilibrium calculation for the 1.5 GW fusion power phase of the ELMy H-mode operation scenario, where the plasma is optimally postioned within the first-wall and divertor surfaces. The nominal internal inductance and poloidal beta assumed for the calculation are $l_i = 0.9$ and $\beta_p = 0.9$. Table 8.2.1-1 gives the corresponding plasma and PF coil currents for the start-of-burn (SOB) and end-of-burn (EOB) 'fiducial' flux

states of the plasma operation scenario (see §8.2.3). The ITER PF coil locations and nomenclature are illustrated in Fig. 2 below.

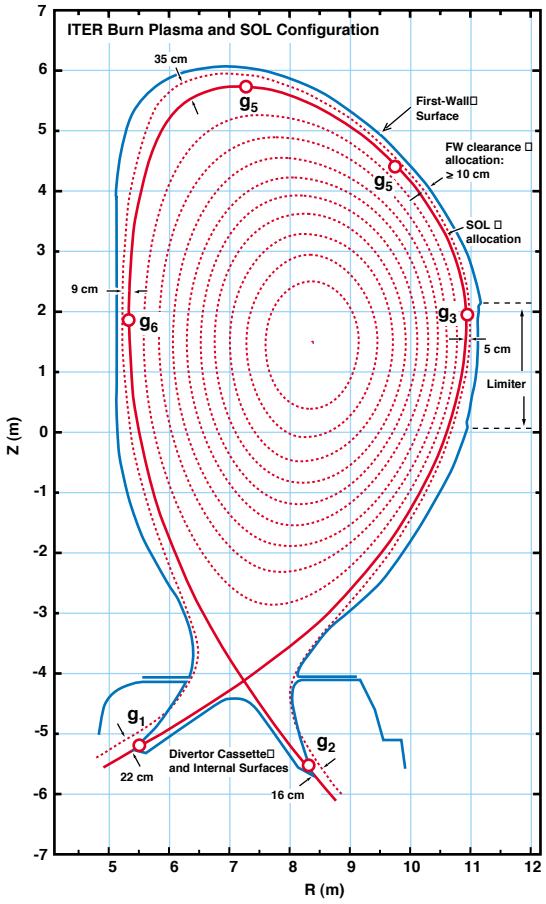

FIG. 8.2.1-1. ITER static plasma equilibrium for 1.5 GW burn.

TABLE 8.2.1-1: ITER Burn-Phase Plasma and Poloidal Field Coil Currents

Plasma and PF Coil System Parameters	Start-of-Burn (SOB)	End-of-Burn (EOB)
Ψ_{PF} (Wb)	-246.8[(a)]	-329.5[(b)]
I_p (MA)	21.0[(a)]	21.0[(a)]
I_{CS} (MA)	-88.3	-138.3
I_{PF1} (MA)	5.81	-5.75
I_{PF2} (MA)	1.18	0.12
I_{PF3} (MA)	-8.64	-8.97
I_{PF4} (MA)	0[(a)]	0[(a)]
I_{PF5} (MA)	-9.74	-10.16
I_{PF6} (MA)	-13.52	-13.78
I_{PF7} (MA)	9.92	11.98
I_{PF8} (MA)	13.34	6.21
I_{PF9} (MA)	5.75	-0.84

a) Specified (input) requirement for Grad-Shafranov equilibrium calculation

b) Flux linkage to give B_{CS} = 12.75 T (maximum allowable field)

Figure 1 illustrates several features that are important to the design basis for the ITER plasma configuration: *i)* the nominal burn-phase ITER plasma equilibrium configuration and the surrounding first-wall (FW) and divertor plasma-facing-surfaces are—for reasons of efficient utilization of in-vessel and in-magnet volume—necessarily quite carefully matched, *ii)* there is a modest (~10 cm) allowance for clearance between the bounding extent of the plasma SOL (scrape-off-layer) and the FW surfaces, and *iii)* the plasma shape is defined (specified) by 6 fiducial 'gaps', labeled g_1-g_6 in Fig.1. Gaps g_1 and g_2 set the location of the inner (small-R) and outer (large-R) divertor strikepoints (intersection of the separatrix with the target surface): gaps g_3 through g_6 control the shape of the plasma within the FW plasma-facing-surfaces. For ITER plasma equilibrium and PF design, these six fiducial control points (gaps) are used as the basis for both static equilibrium specification in Grad-Shafranov design calculations and as the 'reference' basis for dynamic equilibrium control (to be discussed shortly). Simply put, the requirement for magnetic equilibrium control is to keep quasi-static and dynamic variances in the six gaps to within about ± 10 cm, *i.e.*, within the SOL-to-FW clearance allowance. The specifics of what constitutes 'acceptable' and 'optimal' control performance within this requirement are addressed below.

Static equilibria computed with a Grad-Shafranov solver can form the basis for plasma operation scenario development (§8.2.3) and for the development of magnetic control dynamic modelling codes that self-consistently calculate the interaction among the plasma, the PF coil system and any nearby toroidally-conducting structures (see §3.4.7). For dynamic modelling, the need for connected plasma equilibria becomes important: for physically-meaningful results, it is essential to either calculate the evolution of the plasma equilibrium in a fully self-consistent manner based on solution of the ideal MHD pressure balance equation (as is done, for example in the Tokamak Simulation Code, see §3.4.7 and [8.2.1.2]) or to prescribe or devise equivalent constraints for equilibrium codes that employ *ad hoc* profiles to maintain correspondence between the reference and perturbed equilibrium states. When such constraints are properly imposed, the resulting dynamic equilibrium models become useful tools for the analysis of plasma magnetic control experiments and for the plasma control design of future tokamaks, including ITER. This usage is discussed further below.

8.2.1.2. Dynamic equilibrium control and plasma distubances

Successful magnetic control requires that the control system be able to maintain (within acceptable limits) the specified plasma current, shape and position parameter despite *i*) slow evolution of the plasma temperature and resistivity, current profile and pressure as the plasma scenario proceeds, and also despite *ii*) the occurance of faster transient disturbances to the current and pressure profiles that plasma MHD activity or transient external disturbances (impurity release by the initiation of auxiliary heating, pellet injection, flaking of first-wall material, etc.) produce. From the viewpoint of plasma control design, three types of repetitive MHD-initiated disturbances seen in present plasmas are potentially important: sawteeth, minor disruptions and ELMs. The underlying physics basis and charactristics of these 'plasma' disturbances are addressed in the various parts of §3.2 and §3.4. All of these disturbances affect the equilibrium-determining parameters — l_i and β_p — of the plasma and hence potentially lead to a need for magnetic control action. However, these disturbances are inherently self-recovering: if left to its own devices, the plasma will eventually recover to the pre-disturbance state. But in the meantime, if lack of plasma control results in excessive plasma-wall interaction, recovery will be thwarted and a disruption will ensue. Hence there may be some need following a disturbance for the magnetics control system to take interim corrective action to avoid plasma termination.

The effects of minor disruptions and ELMs on plasma shape, position and current can, with careful scrutiny of the control response data, be seen in all presently-operating tokamaks with feedback control of the respective plasma attributes. For minor disruptions and large 'compound' Type I ELMs, there is a readily detectable effect on the plasma inductance, position and current,

but the discharge typically survives without immediate control reaction. In some cases (e.g., in JET) control becomes more problematical when so-called 'giant' disturbances—large Type I ELMs or 'monster' sawteeth—arise, and such disturbances can act a sources of 'loss-of-equilibrium-control' initiated plasma termination, for example, a vertical displacment event (VDE) (see §3.4.3). The need for control following a plasma disturbance is clearly a matter of degree that is related to the effect of the shape disturbance relative to the size of the pre-disturbance clearance gaps: if the shape perturbation effects are small and if the disturbance heals itself rapidly, no immediate control response is needed and control response may—because of finite response time—actually exacerbate the shape perturbation effects of the disturbance. But if the shape perturbation effects approach or exceed the pre-existing gaps, then effective control response following the disturbance becomes important and/or manditory.

Because of this sensitivity of control requirements to the comparative magnituide of potential disturbances, quantification of the expected nature of plasma distrubances is an important issue for the design of future tokamaks, particularly for those tokamaks (like ITER) in which the relative size of the static plasma-to-first-wall clearance gaps is necessarily limited and where relatively precise dynamic control of the plasma configuration is projected to be required to maintain optimal divertor operation and optimal coupling of rf heating power. For ITER, quantification of the expected types and magnitudes thus becomes an important basis consideration for the design of the PF power supplies and PF controller: the requirement is to have sufficient control response (installed PF power) to avoid fatal plasma-wall interaction up to some design-basis disturbance level. Table 8.2.1-2 summarizes the disturbance types and paramaters that have been developed from experimental data for ITER design [8.2.1.3]. The resulting simulated response of a candidate ITER control system is presented below in §8.2.1.7.

TABLE 8.2.1-2: Plasma Disturbance Parameters for ITER Control System Response Evaluation

Disturbance	$\Delta l_i(3)$ (decrease)	$\Delta\beta_p$	Waveform/frequency/ recurrence
Vertical drift	0	0	0.1-m 'control-off' drift phase
Minor disruption (A)	0	≤ 0.2 (decrease)	Step/0.2 Hz/< 10 per pulse
Minor disruption (B)	≤ 0.1	≤ 0.2 (decrease)	Step/0.2 Hz/< 10 per pulse
Sawtooth	≤ 0.05	≤ 0.05 (decrease)	Sawtooth: 0.1-0.01 Hz

ELM	≤ 0.05	≤ 0.05 (decrease)	Sawtooth: 2-0.2 Hz
L- to H-mode	~ 0.1	~0.2 (increase)	Ramp (5 s)/once per pulse

8.2.1.3. ITER magnetic control requirements

Magnetic and PF control in ITER will rely wholely on a set of ten-independently-powered PF coils located outside of the Toroidal Field coil set (see Fig. 8.2.1-2 below). Changing the currents in these coils changes the poloidal flux distribution around the plasma periphery and thus alters the plasma current, shape and position. The aim of PF control in ITER and of the corresponding control system is to co-ordinate these PF current modifications to satisfy the various operational requirements. Since the nominal ITER shape is significantly elongated, a vacuum quadrupole field is required, and this field renders the vertical position of the plasma current unstable. The presence of passive conducting structures (the torus vacuum vessel and the nucelar-shield module support backplate) around the plasma slows this unstable movement down to the time scale of the dissipation of the image currents induced in these passive structures by the plasma movement. In ITER this timescale is of the order of one second.

The first role of the PF control system is to provide controlling actions which counteract the positional instability. The second role of the PF control system is to establish the PF coil currents to control the plasma configuration to obtain the desired evolution of the plasma shape and current throughout the plasma operation scenario and to control divertor geometry and plasama shape (or alternately, gaps g_1-g_6 as defined above) during the quasi-stationary fusion ignition and burn phase of the scenario. The third role of the PF control system is to correct disturbances to this otherwise steady-state equilibrium that result from transient plasma phenomena, such as minor disruptions, sawtooth cycles or ELMs.

In order to perform these functions, the PF control system has to have adequate information on the parameters to be controlled in real time. In ITER, this information will be provided primarily by in-vessel magnetic diagnostics measuring magnetic fields and magnetic fluxes. There will also be measurements of the PF coil currents. This ‘magnetics’ information can be supplemented, if required, by non-magnetic measurements, such as infra-red thermography to indicate areas of contact of the plasma with the divertor plates and the first wall, or microwave reflectometry to supplement the estimation of the plasma-to-first-wall separation. The essential magnetic control requirements can be expressed in terms of control of the plasma current, control of the plasma to first-wall spacing (gaps) and control of the intersection between the diverted plasma separatrix and the divertor plates (strike-points).

8.1.2.4. Magnetic control in present tokamaks

PF control similar to ITER requirements has already been successfully implemented on all presently-operating tokamaks with shaped plasma cross sections and independently-controlled PF coils, as in JET [8.2.4], JT-60U [8.2.5], DIII-D [8.2.6], ASDEX-Upgrade [8.2.7], Alcator C-MOD [8.2.8] and TCV [8.2.9]. While none of these experiments have PF coil configurations that are fully 'ITER-like' in terms of the exact coil number, position and relative coil-to-plasma-surface location, there are many ITER-like features in the PF coil designs and control approaches and all of these experiments are able to successfully control 'ITER-like' single-null divertor plasmas with elongations at the separatrix of about 1.8. Figure 8.2.1-2 shows a comparison of the plasma cross-sections and PF coil geometries of ITER and ASDEX-Upgrade, which is arguably, except for the presence of an independent set of vertical position control coils, highly 'ITER-like' with regard to PF coil and plasma configuration geometry, PF coil number and location and the number and configuration of controlled plasma shape attributes (fiducial shape control points). Apart from the obvious difference in size and magnitude of the stored poloidal field energy, there are no fundamental differences in the control of ASDEX-Upgrade and ITER, and in fact many of the ITER plasma control attributes are separately less challanging than those that are achieved in ASDEX-Upgrade and/or the other experiments cited above.

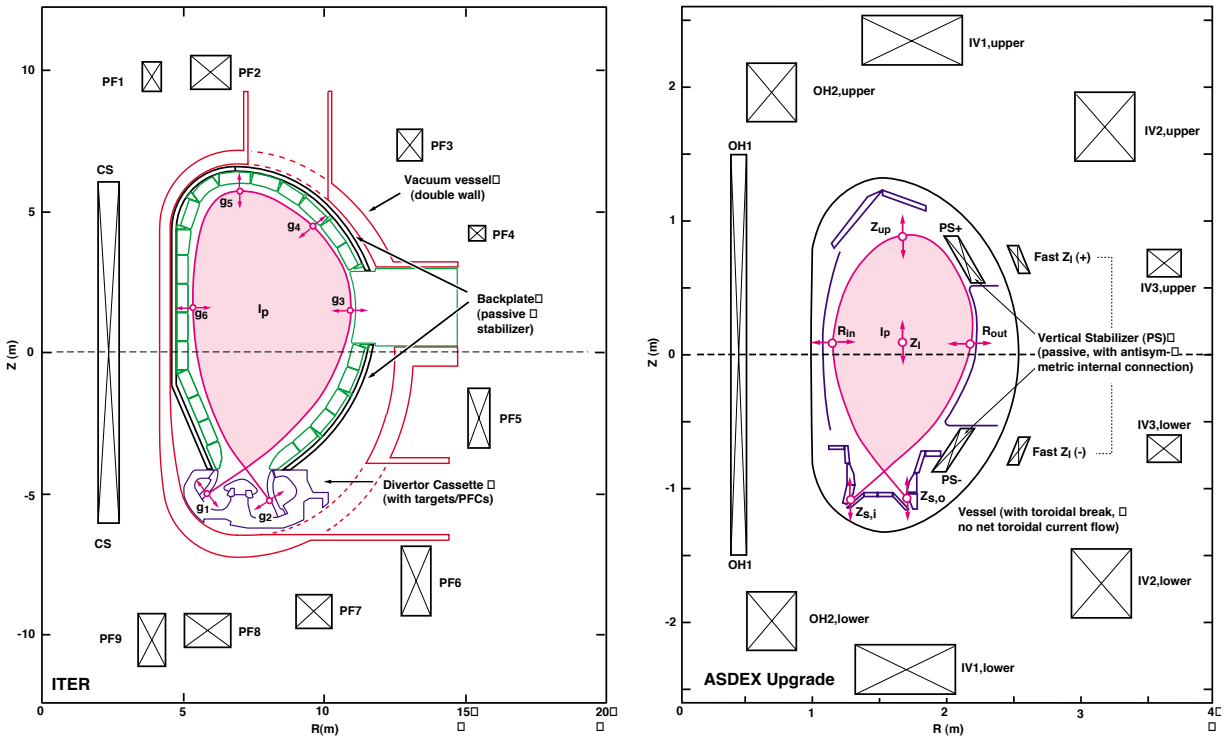

FIG. 8.2.1-2. ITER and ASDEX-Upgrade plasma and PF coil cross-sections compared. Plasma shape control fiducial points are indicated by the small circular symbols with bidirectional arrows. The orientation of the arrows indicates how the respective fiducial point is controlled. Waveform data for the dynamic control response for ASDEX-Upgrade and ITER are respectively shown below in Figs. 8.2.1.3 and 8.2.1.6.

The elongation of ITER (κ_{95} = 1.6, $\kappa_X \cong 1.8$) is comparable to the elongation used for routine plasma operation in ASDEX-Upgrade, C-MOD, COMPASS-D, JET and JT-60U and is significantly less than the maximum elongation obtained in DIII-D and TCV, which can reach κ_X = 2.5. The vertical control stability margin, the ratio between the vertical stabilising and destabilising forces, is 1.7 in ITER. This stability margin is much larger than in existing devices: DIII-D, ASDEX-U and TCV can operate with stability margins within a few percent of unity. The vertical instability growth rate in ITER (1.4 s^{-1}) is significantly lower than in current devices (up to 2500 s^{-1} for COMPASS-D and TCV). The plasma triangularity in ITER (δ = 0.23) is less extreme than other tokamaks ($\delta \geq 0.8$ is routinely achieved for DIII-D and TCV). The precise control of the X-point or target strikepoints in a closed divertor configuration has been achieved in many tokamaks (JT-60, JET, ASDEX-Upgrade and C-MOD) and both ASDEX Upgrade and C-MOD achieve this precise divertor control with PF coils that are relatively far removed from the X-point and strikepoints. Relative control precison for the various shape and position parameters involve is

comparable to ITER requirements (for example $\delta R/R = 0.05$ m/8.1 m = 6×10^{-3} is required in ITER; $\delta R/R = 0.005$ m/1.7 m $\leq 3 \times 10^{-3}$ is obtained in ASDEX-Upgrade, see Fig. 8.1.2.-3 below). Finally, the complexity of the ITER PF coil system (10 independently-powered coils) is similar to that of existing tokamaks (18 for TCV, 16 for DIII-D and 9 for JET). This means that the multiple-input/multiple-output aspects of ITER PF coil control algorithm design will not be materially different from what has been already been achieved.

ITER magnetics control will, however, differ from magnetics control in present tokamaks in two important regards: in the area of the relative availability of power for plasma control and in the similarity of the shape and vertical position control time scales. The plasma control power limitation comes about in ITER (and a reactor) owing to the need to obtain the power for plasma shape corrections from the local utility grid. While the grid power capability for ITER or a reactor is a site-dependent consideration and can, if necessary, be supplemented with on-site pulsed power (rotating machines or magnetic storage), the present allocation of grid power for ITER magnetic control is specified to be 250 MW. Limitations are also specified as to the rate at which line power demand can change. The ITER line power allocation is not greatly larger than the peak control power capabilities of present experiments and the rate-of-change specification is more restrictive than in present experiments. Given the inherently much larger plasma magnetic energy of ITER relative to present tokamaks, the relative power available for plasma control is more limited, and hence restriction of the peak control power demand and rate of change of demand become significant control design constraints. This makes development of a power-efficient control system concept and control algorithm more essential for ITER than for present experiments.

The similarity of the time scales for vertical position instability and more general shape perturbation instabilities in ITER and the lack of a well-decoupled set of vertical position control coils (mandated in ITER by the technical difficulties of providing in-vessel control coils decated to vertical control) make design of an efficient control algorithm less straight-forward than in present experiments, where the ‘fast’ vertical control function and ‘slow’ equilibrium control functions are more separated in terms of both PF coil function and control action time scale. Again, for ITER there is no fundumental physics basis difference relative to present tokamak control practice, but the similarity of time scales makes the controller design task more challenging and less intuitive than for present experiments. However, as will be addressed below, there are ’modern’ controller design methods and plasma response modelling methods that are capable of dealing with the complexities inherent in a reactor/ITER PF control system design and which can also make power demand optimization an explicit part for the overall control design procedure.

8.2.1.5. Intelligent or adaptive magnetics control

Magnetic (and also kinetic) control of a an elongated-cross-section tokamak plasma is inherently dynamic in the sense that during the plasma startup and shutdown phases of a given discharge, the basic parameters of the plasma—size, position, current and shape—change significantly. This means that magnetic control procedures must follow the evolution of the various plasma states and control objectives that correspond to the progression of states—initiation, current rampup, current flattop, auxiliary heating and ultimately current termination—that comprise the normal plasma operation sequence (see §8.2.3). Past and present tokamak control practice has focused on providing a sequence of *a priori* determined control procedures and algorithms that address the control needs for the various phases of the plasma operation sequence. Present tokamaks are also having some degree of success in implementing what can be termed 'intelligent' or adaptive magnetics control procedures. Such control allows the control system itself to be able recognize plasma states and state transitions in real time and to take appropriate control actions. Adpative control can also recognize that there are additional practical operational considerations—power demand, coil current and force limits, etc.) beyond the fundumental requirements for plasma magnetics control, and that the PF coil control algorithm can—owing in part to the over-determined nature of the equilibrium control problem (there are more controllable parameters than controlled plasma attributes)—be optimized to address such considerations while still mantain acceptable magnetic control performance. Here it is envisioned that in ITER that the plasma current, position and shape control will be embedded in a higher layer of more intelligent control. This supervisory layer will act to adjust the reference inputs to the PF controller in such a way as to keep the PF currents away from their maximum values and to adjust the current, shape and position control algorithms in a manner that will individually optimize the control in the respective operational scenario phases or plasma operation states (ohmic, L-mode, H-mode, steady-state,.....). A certain degree of this type of on-line 'intelligent' or adaptive optimisation is already incorporated within the capabilities of existing tokamak control systems, and work on implementing higher-level intelligent optimizers that are not totally dependent on *a priori* design is showing encouraging progress.

Intelligent/adaptive optimisation becomes more important for the ITER/reactor generation of tokamaks for a number of reasons. First, the size and cost of the ITER device are such that careful attention must be given to not over-designing any of the component sub-systems. Here the available swing of coil voltages, coil currents and total PF power demand have limits which are relatively somewhat more restrictive than in presently operating tokamaks. These 'non-physics' limitations mean that more attention is required when designing the ITER PF controller, but these voltage, current and power limitations do not of themselves introduce any new physics issues.

Second, in ITER the precision of the separatrix positioning will be more crucial to optimizing the divertor operation, since departure from the nominal discharge position and shape may increase the plasma-wall interaction to the point of compromising divertor power handling and/or particle exhaust efficacy. This could require terminating the burn if tolerable heat loads of the divertor or first wall are exceeded, or the resulting excessive impurity product could lead to disruption. The required positional accuracy for divertor magnetic configuration control (≤ 10 cm separatrix deviation in the divertor channels) imposes requirements on diagnostic and feedback control precision that are somewhat more challanging than in present tolkamaks. Again, this means more attention to magnetic diagnostic accuracy and PF controller design, but no new physics issues.

Third, ITER will operate with very long (or even steady-state) duration pulses with superconducting PF and TF coils. The need for a corresponding set of dc 'non-magnetic' plasma current, shape and position diagnostic data has already been noted. However, in addition to these diagnostic requirements, the use of superconducting coils introduces the further consideration of limiting the 'ac losses' that arise from plasma system control action. Here the continuous quasi-random displacement ('dithering') of the controlled plasma parameters around a stable operating point owing to variations in the plasma parameters themselves and to repetitive plasma disturbances lead to heating of the superconducting coils and to the cyrogenic-temperature structure in the magnet systems. The heating resulting from these effects is grouped together under the heading of 'ac losses'. Estimates of these losses for typical ITER operation indicate that they may become important during long discharges, and in certain disturbance scenarios could become a significant factor in the long-term thermal balance of the coil systems. Accordingly, design of the ITER controller to limit cummulative ac losses owing to repetative disturbances and noise to acceptable levels will be required: present non-superconducting tokamaks are not impacted by this requirement and present controller designs are sometimes not optimized to minimize dither levels.

Fourth, the presence of a massive passive structure combined with a larger relative distance between the magnetic diagnostics and the plasma surface will make the reconstruction of the plasma-wall gaps somehwat more delicate than in some present tokamaks. Again, this puts some constraints on the reconstruction algorithm design and possibly on the controller transient response compensation, but is not a new physics issue.

8.2.1.6. Magnetics controller experience

All presently-operating tokamaks employ feedback controllers to effect the desired quasi-static equilibrium control, control the plasma radial position and current and to stabilize the vertical position instability during elongated cross-section operation. As a result of the adequate

performance of existing feedback controller designs, the basis for tokamak magnetics control has remained with so-called PID (proportional/integral/derivative) controllers. These controllers counteract errors in the waveforms to be tracked (controlled to follow a pre-determined 'reference waveform') by applying voltages to the PF coils that are derived from the waveform errors, their time derivatives and their time integrals. For the case of tokamaks with separated-function coil sets (separate plasma currrent/ohmic heating, elongation, radial and vertical position control coil groups), the usual design solution is to provide an individual PID controller for each function. For tokamaks without separately-identified coil sets for particular shape parameters, it has been possible to apply physical models (equilibrium codes) to identify combinations of the individual control variables (PF coil voltages or currents) that adequately decouple the current, shape and position control functions. These functions are then controlled by individual PID controllers that are dedicated to the respective plasma control function. This is the case for JET, DIII-D, JT-60, ASDEX-Upgrade, C-MOD and TCV and can also be the case for ITER.

There are however, certain difficulties that arise in designing an efficient multi-PID-based controller for ITER. For present tokamaks, a fairly primitve plasma response model is adequate to identify the decoupled function control sets. All of the plasma models used to date include the dominant vertical positional instability, but the model of this instability can be quite elementary, and in some cases it is possible to obtain a workable controller design even with use of a 'plasmaless' model. The dynamics of the controllers that are developed with such elementary plasma response models must then generally be empirically tuned (wherein the weighting and frequency characteristics of the P, D and I feedback circuits of the controller are separately adjusted to optimize control error, dynamic response and transient stability) during tokamak operation. In present tokamaks this empirical tuning is facilitated by the fact that shape control takes place on a longer time scale than the time scale of control of vertical stabilisation, and because it is possible to ignore the effect of passive structure currents on shape control, except implicitly for the vertical control. As an example of control of an ITER-like plasma shape with a decoupled-function coil set, Figure 8.2.1-3 shows the variation of the position and shape parameters during the application of additional heating on ASDEX-U.

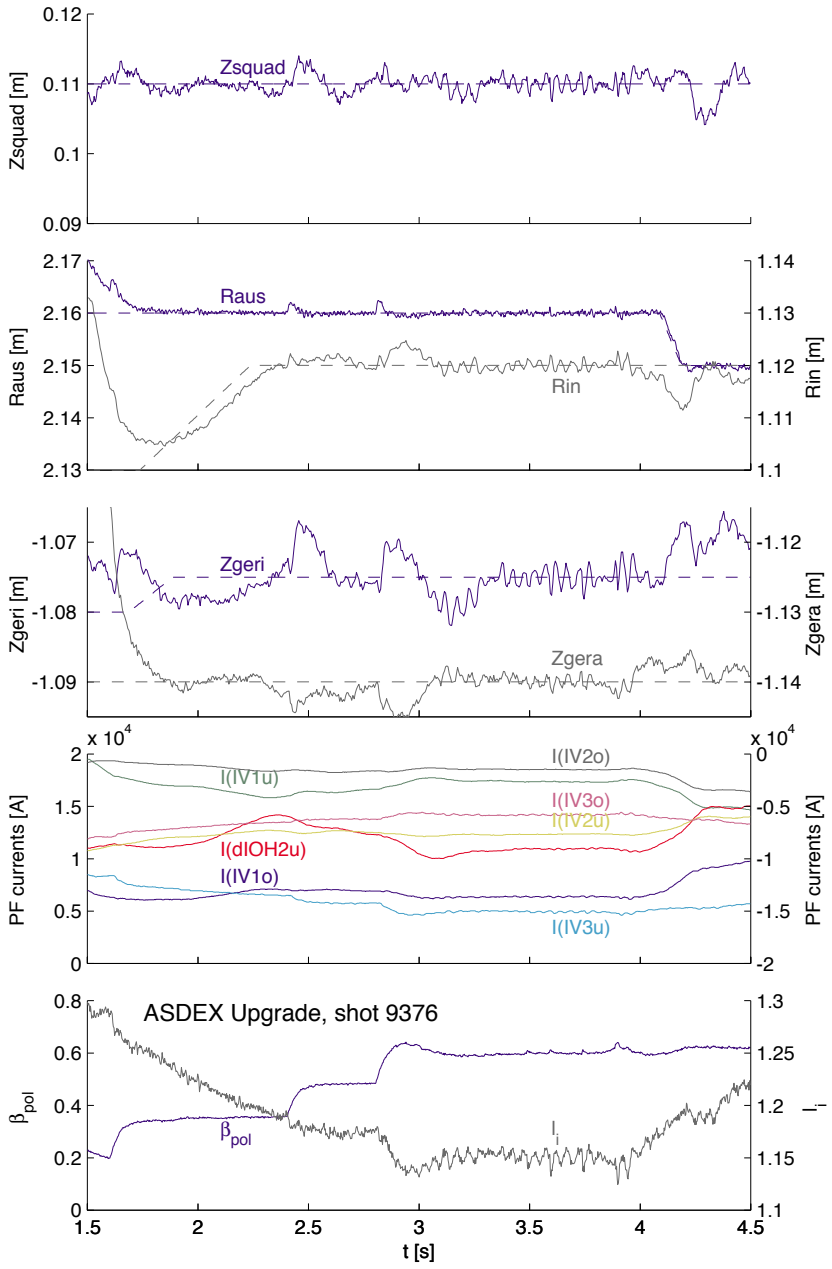

FIG. 8.2.1-3. Plasma shape control in ASDEX-Upgrade during NBI heating with an 'ITER-like' plasma boundary shape control algorithm (fiducial points as illustrated in Fig. 8.2.1-2). Dashed lines show the control programs (reference waveforms). Height of the current centroid (Z_{squad}), inner and outer major radius (Rin and R_{aus}) and divertor target strikepoint heights (Z_{geri} and Z_{grea}) are sucessfully controlled with transient variations $\leq \pm 5$ mm ($\delta R/R \leq 3 \times 10^{-3}$). Control 'noise' during the quasi-stationary β_p 'flattop' is ~ 1 mm rms ($\delta R/R \sim 0.6 \times 10^{-4}$).

While an ITER plasma magnetics control system based upon the same type of plasma-model-determined 'separation-of-function/multi-PID' controller is certainly workable, it is likely that such a controller will not be fully optimal with regard to some of the 'non-physics' considerations noted above. For example, studies of candidate controllers of this type have shown that they can produce transient peak power demands well in excess of ITER allocations. These high demands, which are usually of very short duration, arise from competing interactions among the individual controllers that attempt to control different attributes of the plasma on similar time scales. These interaction difficulties can be minimized by suitable adjustment ('tuning') of the various control responses involved. For ITER, this controller tuning can, with availability of a suitable 'system model' (see below), be done before operation with simulations, or could also be done 'on-line' once ITER plasma operation commenses. However, if this tuning is to be done on-line for ITER, it will be time-consuming (and hence expensive) at best and may also cause an undue frequency of disruption. Both of these considerations and the related consideration that development of the ITER plasma magnetics control system should not be the dominant aspect the initial plasma operation commissioning period argue for applying more sophisticated *a priori* control design methodologies.

Fortunately, in this regard, there are now a variety of 'modern' control optimiztion techniques—*e.g.*, linear quadratric gaussian (LQG) optimization [8.2.1.10] or 'H-infinity (H_∞) optimization [8.2.1.11]—available to develop the design and characteristics of feedback controllers which optimize the response of the multiple-input/multiple-output (MIMO) control system needed for ITER PF control. These 'advanced' or 'modern' control design methods make it possible to optimize the basic control characteristics with constraints on additional performance characteristics such as reducing the ac losses or reducing the required total power. Given definition of a 'cost' function (plasma shape control, power limitation, ac loss limitation), development of an optimized controller is then mathematically straight-forward.

However, the higher degree of optimization capability of these modern control design methods carries with it a corresponding requirement for greater accuracy and detail in the model of the system that is being controlled. For ITER, such a model describes the interaction between the PF control coils, the conducting structures surrounding the plasma and the plasma itself. Modelling of the first two parts of the system is in principle straight-forward (electrical engineering design practice), but questions arise as to the degree of plasma modelling accuracy required. To answer this 'physics' question, considerable research effort has gone into deriving and comparing plasma models which are either non-linear, containing the full information of the plasma equilibrium and including different physics assumptions, or locally linearised versions of the non-linear models around particular operating points.

For ITER PF control design, a linearized model system that combines a full 2-D model of the ITER conducting structures and PF coils with a linearized 2-D plasma equilibrium model has been developed and applied to explore the design of candidate ITER controllers optimized in a variety of manners. The resulting generic model is termed the ‘CREATE-L’ model. A version of the model for the TCV tokamak has also been been developed. Systematic benchmarking tests of this model against the TCV tokamak has provided encouraging agreement with the experimental closed-loop and open-loop responses, implying that the underlying physics assumptions of this linearised model are valid and adequate [8.2.1.12]. Figure 8.2.1-4 shows an example of the response of several plasma parameters of an SND TCV plasma to square-wave voltage stimulation of particular PF coils, compared with the CREATE-L model responses.

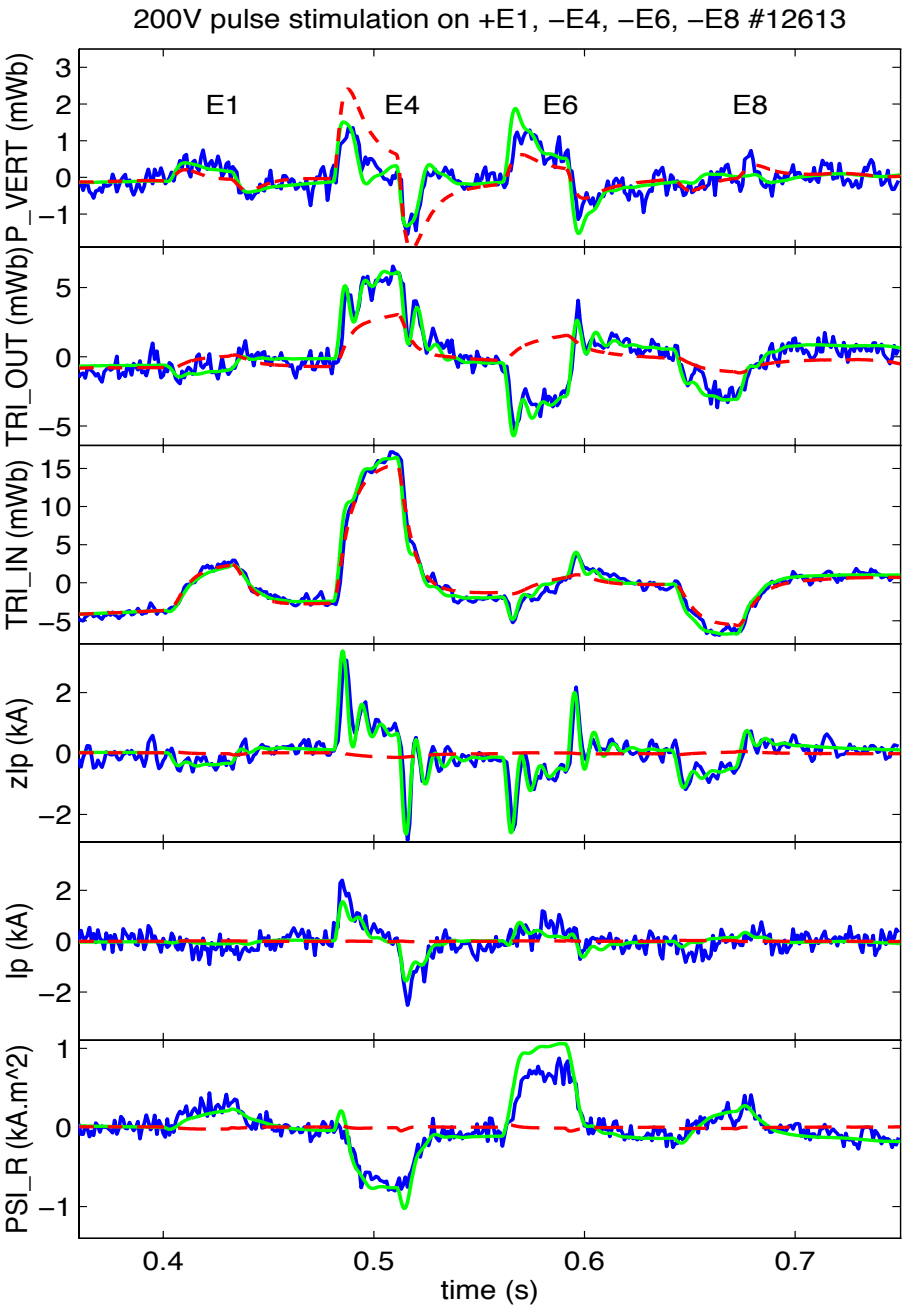

FIG. 8.2.1-4. The closed loop evolution of TCV shape parameters during square-pulse voltage stimulation of inboard coils (dark solid and noisy line). This response shows good agreement with the nominal CREATE-L linearised model (solid grey noise-free line). A model excluding the plasma response (dashed line) shows inadequate agreement, illustrating the importance of the plasma content of the PF system model.

The TSC code [8.2.1.2] is widely used for full plasma simulations, including transport of energy, particles and magnetic flux and has shown good agreement with experimental measurements during both slowly-evolving quasi-stationary plasmas [8.2.1.13] and disruptive and vertically-unstable plasmas [8.2.1.14], [8.2.1.15], [8.2.1.16]. The plasma model embodied in TSC has become the *de facto* standard non-linear plasma model against which other non-linear plasma models, linearized or other more-approximate plasma models and/or control response models can be compared. Work to design a feedback controller using modern control theory and subsequently test it in a non-linear simulation is presently in progress. This testing will confirm that the physics basis of the linearised model is adequate for designing a highly-tuned high-order feedback controller which will give the required performance in ITER or a reactor tokamak. Preliminary results of one such test for an ITER controller design are described below.

8.2.1.7. ITER controller design simulations and predicted response

The effects on ITER PF/plasma control of controller design methodogy, plasma model accuracy, PF control strategies (number of controlled plasma-wall gaps), PF coil current and voltage limitations and the effects of passive structure configuration and conductivity have been examined in an extensive set of studies with various modelling methods. For these studies, specific performance criteria against which the controller can be judged are required and we have chosen as a figure-of-merit the controller's ability to limit variances —within power demand constraints) in the divertor strikepoint gaps (g_1, g_2) and in the plasma-to-first-wall gaps (g_3-g_6) to 'allowable' magnitudes. Here 'allowable' includes consideration of the fact that the pre-disturbance values of gaps g_3-g_6 contain an allowance for uncontrolled (or uncontrollable) plasma boundary deviation following onset of a disturbance, and for the additional fact that for gaps 3-6, an increase in the plasma-to-wall gap does no immediate harm, while decreases beyond the allowed clearance result in an increasing degree of plasma-wall interaction. A similar 'allowable variance' criterion applies for the divertor strikepoint control gaps g_1 and g_2, again with preference for deviations that move the strikepoint 'up' rather than 'down' the inclined portion of the target. In essence, an adequate controller is one in which 'control' of a given disturbance (avoidance of appreciable wall interaction and of excessive divertor strikepoint deviation) is obtained with otherwise minimum power demand.

Specification of the type and details of candidate disturbances are critical to this kind of assessment. Since we cannot predict the exact details of a sawtooth crash or an ELM or a minor disruption in ITER, we consider a set of canonical disturbances which cover the likely disturbances during ITER operation. Since from the physics of the plasma equilibrium the first order

disturbances are changes to β_p and l_i, these are the disturbances considered during the key phases of the 21 MA reference scenario.

Studies of the performance of ITER controllers have focused on two classes of disturbance: Firstly, we have consider a repetitive disturbance, similar to Type I ELMs, considered to be more demanding on the control system than the sawtooth crashes, and characterised by a rapid β_p drop of 0.03 followed by a 0.2-s linear recovery, at a frequency of 1 Hz. These 'ELM-like' self-healing disturbances do not present a serious challenge to the PF control and are barely above the noise level of β_p changes seen in currently-operating tokamaks. However, during long pulses in ITER, they could, depending on the AC loss characteristics of the ITER superconducting magnet systems, lead to an accumulation of AC losses in the superconducting PF coils and thus prove to be a limiting factor for extremely long discharges.

Secondly, we consider two large-scale isolated recoverable disturbances. The first is typical of a 'compound ELM' (see §3) and is characterised by an instantaneous l_i drop of 0.05, followed by a 1-s linear recovery, that is simultaneous with a β_p drop of 0.03 followed by a 0.2-s linear recovery. The second large-scale disturbance is typical of a 'worst-case' minor disruption (see §3.4.1) and is characterised by an instantaneous l_i drop of 0.1 without recovery that is simultaneous with drop of β_p of 0.2 followed by a 5-s linear recovery. These disturbance parameters apply during the burn phase of the discharge ($\beta_p = 0.9$, $l_i = 0.9$). The corresponding plasma energy loss is about 0.2 GJ. Transport simulations show that thermal recovery of the pre-disruption plasma energy is only marginally possible at this energy loss level, so there is good basis for believing that this type of minor disruption is in fact a worst-case limit to a recoverable disturbance in ITER.

Figure 8.2.1-5 shows a simulation of the ability of the ITER PF system and a candidate H_∞ controller design [8.2.1.] to control this rather severe disturbance. The plasma and controller response is simulated with a TSC non-linear model. The separatrix-to-first-wall gap responses shown in Fig. 8.2.1-5 demonstrate that the immediate response of the separatrix is to shrink away from the wall. The maximum excursion of the gap between the separatrix and the first wall or the position of the divertor leg strike point is +17 cm. The power required to bring the plasma back to the nominal separatrix location is ~80 MW, well within the ITER line-power demand and rate-of-demand-variation specifications. There is no plasma (separatrix) contact with the wall. The rf antenna-separatrix separation (gap g_3) does not decrease by more than 5 cm. All nominal PF control requirements are therefore met.

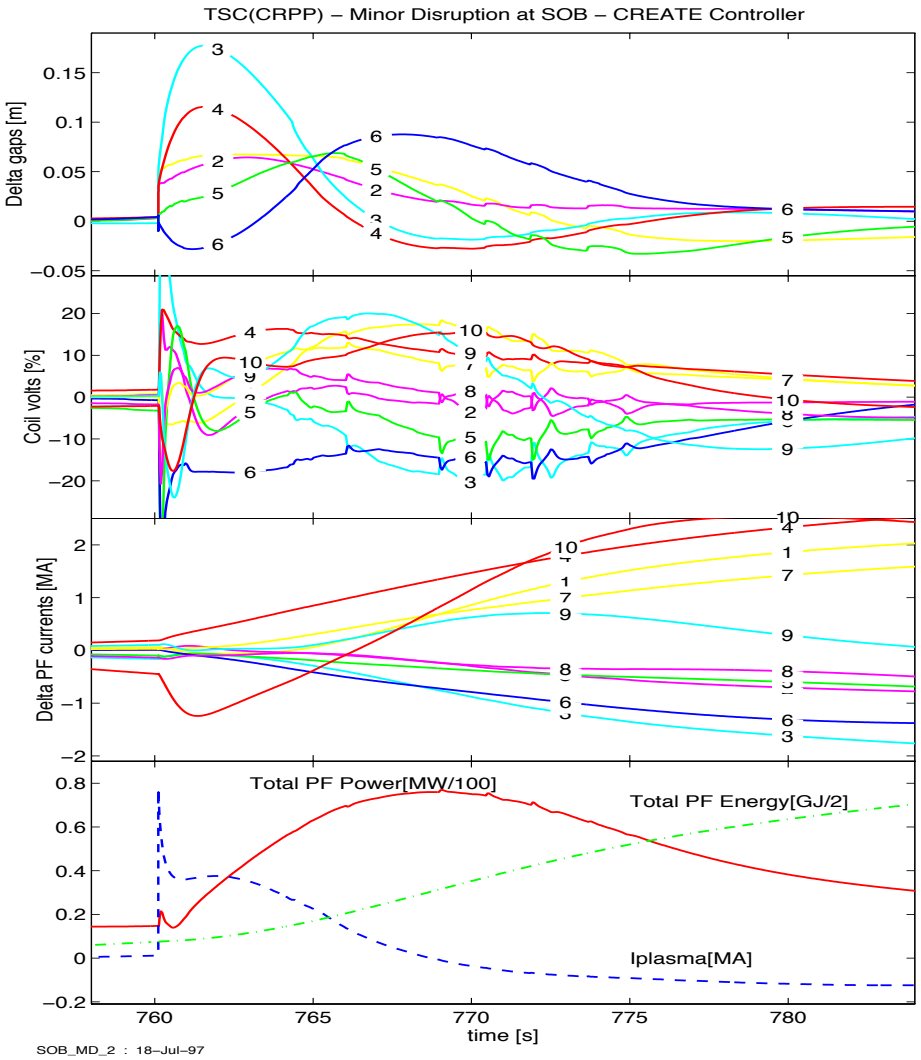

FIG. 8.2.1-5. The modelled evolution of the separatrix gaps (numbered 1-6; positive denotes separatrix motion away from the first wall), the PF coil voltages as a percentage of the nominal design, the PF coil current changes, the plasma current variation, the total PF control power and energy.

Simulations of the type shown in Fig. 8.2.1.-5 have been developed for a variety of candidate controller designs, linear and non-linear plasma response models and a number of controller design optimization methodologies. The effect of disturbances that occur at various critical points in the PF scenario (where the currents in the various PF coils and the resulting control power demands differ) and the effects of credible variations in the distrurbance modeling parameters and disturbance repetation rate have been explored. While definitive exploration of the many cases possible among these disturbance, scenario, controller and modelling basis parameters remains to be completed, we have concluded from our understanding of the ITER magnetic control problem that the physics basis for ITER PF control is conventional and that the ITER PF control

system will be able to handle the likely range of recoverable plasma disturbances expected during all phases of ITER operation.

8.2.1.8. Summary and implications for ITER

The physics basis for magnetic control and magnetics data interpretation in tokamaks is fully understood. There are no fundumental uncertainties in the extrapolation of this physics basis to ITER or a similar reactor-regime tokamak, and a number of present tokamaks have demonstrated sucessful plasma magnetics control with plasma and control system attributes that are very similar to those envisioned to be used for ITER. However, with regard to the design of the ITER plasma control system, there are a number of practical design considerations—power efficiency, minimization of unnecessary ac losses, and before-operation demonstration of nearly-optimal control response—that argue for the application of 'modern' control optimization methods. The availability of a relatively accurate plasma response model is identified to be a key factor for the application of such control optimization methods. In this regard, studies of the application of non-linear and locally-linearized Grad-Shafranov plasma equilibrium models for candidate ITER control design have demonstrated that either class of plasma response model can be applied for ITER design purposes. In addtion, comparison of locally-linearized models with expeimental data and control system response in present tokamaks shows that such locally-linearized models (and also non-linear models) can describe the plasma and plasma control system response to a high degree of accuracy. It thus appears that all of the design basis knowledge—physics, plasma response and control design methodology—needed to produce a reliable and efficient ITER plasma magnetic contrller design are in hand.

References to Section 8.2.1

[8.2.1.1] Lao, L. L., H. St. John, R. D. Stambaugh, *Separation of β_p and l_i in tokamaks of non-circular cross-section*, Nucl;. Fusion **25** (1985) 1421-1436.

[8.2.1.2] Jardin, S. C., N. Pomphrey, J. Delucia, *Dynamical modeling and position control of tokamaks*, J. Comput. Physics **66** (1986) 481-507.

[8.2.1.3] Wesley, J., H.-W. Bartels, D. Boucher, A. Costley, L. DeKock, Yu. Gribov, M. Huguet, G. Janeschitz, P-L. Mondino, V. Mukhovatov, A. Portone, M. Sugihara and I. Yonekawa, *Plasma Control Requirements and Concepts for ITER*, Fusion Technology **32** (1997) 495-525.

[8.2.1.4] Puppin, S. et al., Proc 19th Symp on Fusion Technology, Lisbon,1996 Vol. I (1997) 949.

[8.2.1.5] K. Toyoaki. K. Kurihara, Y. Kawamata, K. Akiba, M. Takahashi, T. Terakado, R. Yoshino, *JT-60U Plasma Control System*, Fusion Technology **32** (1997) 404-415.

[8.2.1.6] DIII-D Team (presented by R. Stambaugh), *DIII-D Program Overview*, in *Plasma Physics and Controlled Nuclear Fusion Research 1994* (Proceedings 15th IAEA Conference, Seville 1994), IAEA Vienna (1995) **1** 83-101.

[8.2.1.7] Köppendörfer, W., F. Ryter, H. Zohm, M. Alexander et al, The H-mode in ASDEX Upgrade: physics and operating regimes, in *Plasma Physics and Controlled Nuclear Fusion Research 1994* (Proceedings 15th IAEA Conference, Seville 1994), IAEA Vienna (1995) **1** 241-254.

[8.2.1.8] Horne, S. *et al*., 15th IEEE Symp. on Fusion Engineering, Hyannis, USA, 1993 **Vol 1** (1995) 242.

[8.2.1.9] Lister, J.B. et al., Fusion Technology **31** (1997) in press.

[8.2.1.10] Doyle, J. C., G. Stein, IEEE Trans. Autom. Control **AC-26** (1981) 4-xx.

[8.2.1.11] Maciejowski, J. M., *Multivariable Feedback Design*, Addison-Wesley, Reading MA (1989).

[8.2.1.12] R. Albanese, F. Villone, *The linearized CREATE-L plasma response model for the control of current, position and shape in tokamaks*, Nucl. Fusion **38** (1998) 723-738.

[8.2.1.13] Jardin, S.C., M. G. Bell, N. Pomphrey, *TSC simulation of Ohmic discharges in TFTR*, Nucl. Fusion **33**, (1993) 371-382.

[8.2.1.14] Jardin, S.C., J. Delucia, M. Okabayashi, N. Pomphrey, M. Reusch, S. Kaye, H. Takahasi, *Modelling of the post-disruptive plasma loss in the Princeton Beta Experiment [PBX]*, Nucl. Fusion **27** (1987) 569-582.

[8.2.1.15] Merrill, B. J., S. C. Jardin, M. Ulrickson, M. Bell, *Dynamics and energy flow in a disrupting tokamak plasma*, Fusion Engineering and Design **15** (1991) 163-180.

[8.2.1.16] R. O. Sayer, Y.-K. M. Peng, S. C. Jardin, A. G. Kellman, J. C. Wesley, *TSC Plasma Halo Simulation of a DIII-D Vertical Displacement Event*, Nucl. Fusion **33** (1993) 969-978.

[8.2.1.17] Ambrosino, G. et al., Proc 19th Symp on Fusion Technology, Lisbon,1996 **Vol. I** (1997) 735.

8.2.2. Kinetics Control and Divertor Control

Kinetics control comprises the establishment and sustainment of the kinetic attributes of the core and divertor plasma regions of the tokamak discharge. At the most elementary level, the key kinetic attributes of the core are density, temperature, impurity content and, in the case of a DT plasma, fusion power. At the same elementary level, the key attributes of the divertor region plasma are temperature, density, impurity content and ionization state and the corresponding levels of radiated power and power conducted and convected to the material plasma-facing-surfaces (divertor targets). The physics basis considerations that apply to the core and edge/divertor plasma region attributes are respectively described in Chapter 2 and Chapter 4. The subject of this Section is how these attributes are manipulated and controlled by external means (actuators) and procedures (control algorithms) during the course of a tokamak discharge. Such kinetics control now plays an increasing important role in modern tokamaks, especially when they are operated so as to obtain maximum plasma performance ($nT\tau$ or fusion energy gain $Q = P_{fus}/P_{in}$). In fact, it is common for kinetics control to be described as 'performance control'. In ITER, control of the plasma kinetic attributes to obtain sustained DT fusion burn at pre-determined fusion power is a central and arguably first-priority plasma operation objective.

8.2.2.1. Introduction and background

Tokamak plasma control encompasses both magnetics control (magnetic equilibrium and plasma configuration control, see §8.2.1) and kinetics control. The overall integration of magnetics and kinetics control results in the plasma operation sequence or scenario that comprises a complete tokamak discharge pulse (see §8.2.3). In most present cases of tokamak control, there is a clear distinction between magnetics control and kinetics control functions, both in terms of the actuators used (the PF coil system for magnetics control versus fueling, heating and pumping systems for kinetics control), the plasma diagnostic sensors used for enabling the respective feedback control loops (magnetic probes and flux loops versus density, temperature, radiation and fusion power measurements) and in the respective control algorithms are implemented. In terms of control system hardware, magnetics control is usually implemented independently from kinetics control: one set of control procedures and hardware is responsible for magnetic control of the discharge and PF power supplies; a second set is responsible for kinetics control and the respective kinetics control actuators. In divertor tokamaks, further subdivision of the kinetics control into core and divertor subsystems is common if divertor attributes are to be explicitly controlled.

The kinetic properties of the plasma—especially the electrical conductivity, pressure and current profile, or $V_{\Omega,}$ β_p and l_i—of course ultimately affect magnetic control. However,

traditionally these parameters are not directly manipulated for magnetic configuration control purposes: instead, the PF control system is designed to control the plasma position, shape and rate of surface flux variation ($d\Psi_{surf}/dt$) in a manner that endeavors to maintain acceptable magnetic control despite variation in the plasma kinetic parameters. In contrast, some degree of direct or 'active' kinetics control (e.g. keeping plasma density a range that is neither too high or too low, see §8.2.3) to avoid disruption is required for successful tokamak operation. In this sense, kinetics control is ultimately the *active* or dominant aspect of plasma scenario control; PF/magnetics control is *reactive* or subordinate aspect. In operation scenarios in which active current drive and pressure profile control means are used to modify the naturally-occurring positive-shear safety-factor profile (see §3.2.7), the same action/reaction basis applies, with the important distinction that active control of the current profile via non-inductive current drive and pressure control (and hence bootstrap current control) becomes the primary kinetic control consideration. The physics basis for such 'advanced performance control' is addressed in §2 and §3.2.7. Implementation of control of 'modified-shear' and other plasmas in which the plasma current or pressure profiles are actively modified is addressed separately below in §8.2.4. However, for such plasmas the underlying *reactive* basis for PF control—maintenance of the equilibrium fields required to sustain an acceptable plasma surface magnetic configuration and maintenance of fixed plasma surface flux variation (e.g., $d\Psi_{surf}/dt = 0$) is identical to the basis that applies for control of positive-shear inductively-driven plasmas.

The introduction above focuses on the organization and linear control aspects of kinetics control. However, as is now well known, there are also dynamic considerations that apply to the overall conduct of the plasma operation scenario, and plasma kinetic performance is state-dependent and non-linear (L-mode to H-mode transition, internal transport barrier formation, etc.; see §2 ,§3 and §4), wherein the achievable kinetic parameters of a tokamak plasma can be affected (improved) in a sustainable manner by judicious dynamic manipulation of the plasma magnetic and kinetic states at some initial point in the operation scenario. The attainment of quasi-stationary H-mode discharges following the application of sufficient auxiliary heating [1] is a now-classic example of this non-linear aspect of kinetics control and plasma performance optimization and the attainment of H-mode and other types of optimized plasma performance by such dynamic means is now sometimes described in terms of 'control' of the underlying transport and MHD stability attributes of the optimized plasma. However, the converse to this positive dynamic aspect of 'control' can also apply: as is well known, the onset of certain types of MHD instability in an optimized plasma—triggered by evolution of the underlying plasma kinetic attributes—can lead to a irreversible degradation of kinetic performance that does not always immediately terminate the plasma discharge, but which never-the-less precludes subsequent recovery of before-onset performance.

Historically, kinetics control in tokamaks has lagged in sophistication and directness somewhat behind magnetics control: this lag reflects the fact that directly-controllable kinetics control actuators (e.g., fuelling, pumping, and heating systems and well-controlled wall conditioning) have usually been provided at a latter point in a given tokamak's development cycle than the corresponding controllable PF system needed for effecting basic discharge operation and magnetic control. More recently, however, this lag is being reduced with the provision of diverse and separately-controllable heating systems, H/D/T and impurity fuelling systems, controllable divertor pumping and neutral particle exhaust systems, between-pulse and in-pulse wall conditioning, and, most recently, heating and current-drive systems with controllable radial and temporal localization capabilities and sufficient power to locally modify the inherent plasma current and temperature profiles. The availability these increasingly-capable and agile kinetics control actuators, when combined with a corresponding availability of key plasma kinetic diagnostics (*e.g.*, real-time data on the temperature, density and radiated power profiles), has lead to an increasing ability to effect more-direct control of the kinetic attributes of the core and divertor plasma. This control has lead to both improved plasma performance and sustainment—as opposed to only transient attainment—of near-optimal performance. The same control ability, combined with comprehensive plasma diagnostic data can also provide a basis for taking before-onset action to avoid the occurrence of deleterious MHD activity or to limit the amplitude of such activity to acceptable levels. In this sense, modern kinetics control has begun to be pro-active rather than just reactive and there has been recent progress in using kinetic control to avoid the onset of disruption or the onset of a fully-developed MARFE. Specific examples of this type of progression in sophistication in present tokamak control practice are presented below in §8.2.2.3.

8.2.2.2. Kinetics control requirements for ITER

Achievement of sustainable and simultaneous control of the plasma core, edge and divertor kinetics attributes in ITER discharges will be mandatory for achieving controlled ignition and sustained fusion burn at high performance. As is described in Chapters 2, 3 and 4, it will be necessary to obtain a plasma that simultaneously provides *i*) adequate energy confinement, *ii*) adequate MHD stability and operating density and *iii*) adequate divertor particle exhaust and benign (target power densities within engineering limits) divertor power exhaust. To meet these requirements, stationary discharges will have to be obtained with a prescribed evolution of plasma parameters and their profiles (pressure, density) and plasma regimes (H-mode, low impurity content, adequate He removal and partial divertor detachment). Target parameter ranges and access trajectories for such discharges in ITER are—on the basis of physics understanding embodied in Chapters 2-6 of this Article—already established and control procedures for their attainment and

dynamic control have been developed [2]. But we anticipate that modifications of these target parameters and trajectories and to the corresponding control procedures will be needed depending on precisely how the physics of this burning plasma regime actually develops. And ability to quasi-statically and dynamically control the burning plasma operation point (density, temperature, thermal He and other impurity content, edge and divertor power flow) will be needed to conduct scientific studies and to ascertain the plasma conditions and operation procedures that result in optimal performance and plasma operation reliability.

The basic concepts for ITER plasma control are already well defined. Simulation studies of the dynamic control of DT-burning plasmas predicated upon ELMy H-mode (or similar) energy/particle confinement show that thermally-stable fusion burn will be obtained and that the fusion power can be controlled by control of the core plasma density and/or the D/T mixture. Control of the DT fueling rate is the most direct 'actuator' for fusion power control, and simple 0-D particle balance and fusion burnup models and also similar 1- or 1.5-D transport simulation models that take profile and particle transport effects into account readily demonstrate that fueling rate control is always sufficient to effect long-term fusion power control in ignited or driven burn plasmas where the operating point has positive to neutral thermal stability [3]. In ITER, such plasmas typically have volume-average temperatures of 10-15 keV and densities of about 1×10^{20} m^{-3}. Figure 8.2.2-1 shows a representative POPCON (Plasma Operation Contour) diagram for ITER: for 'standard' ITER ELMy-Hode confinement modelling assumptions, a thermally-stable high-temperature sustained-ignition operation point with 1.5 GW fusion power exists at a volume-average density $\langle n_e \rangle$ of approximately 1×10^{20} m^{-3} and a volume-average temperature $\langle T \rangle$ of approximately 12 keV. This operation point is also consistent with maintaining plasma pressure below the nominal ITER design-basis beta limit ($\beta_N = 2.5$) and being able to sustain H-mode (i.e., $P_{sep} > P_{L\text{-}H}$ in Fig. 8.2.2-1, where P_{sep} is the power crossing the separatrix and $P_{L\text{-}H}$ is the separatrix-crossing power for an L- to H-mode transition; see §2). In this high-temperature regime, fueling/density control provides direct control of fusion power. As the Figure shows, there is a modest-sized domain in $\{n,T,P_{fus}\}$ space where sustained ignition at $1 \leq P_{fus} \leq 1.5$ GW without encountering either the beta limit or loss-of-H-mode limit is possible.

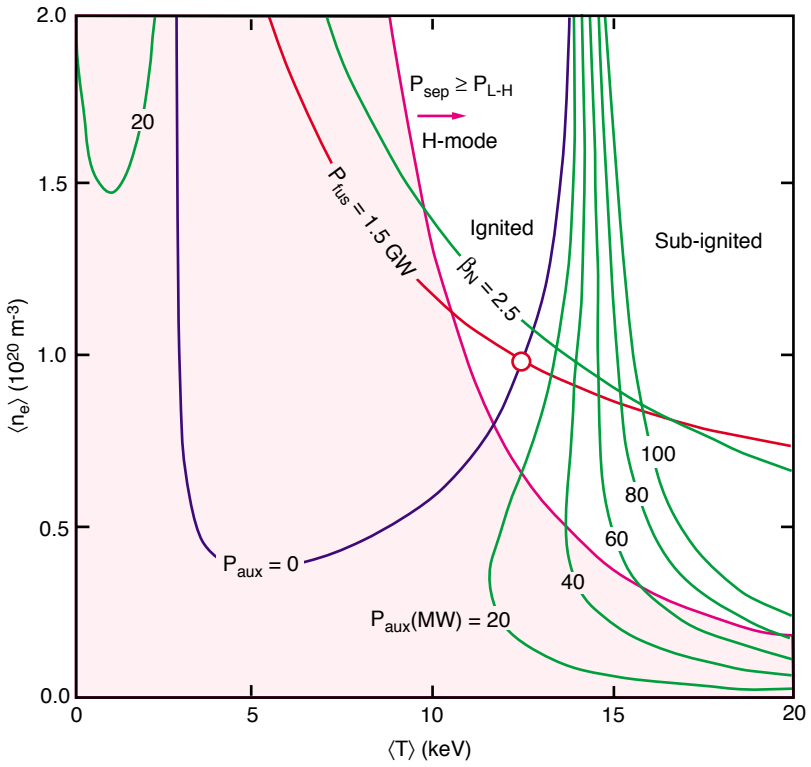

FIG. 8.2.2-1. Plasma operation contour diagram for ITER (21 MA). Standard ELMy H-mode energy confinement applies and equilibrium thermal He levels are calculated self-consistently everywhere in the domain. However the ignition ($P_{aux} = 0$) and finite-Q ($P_{aux} > 0$) contours are meaningful only in the H-mode domain ($P_{sep} \geq P_{L-H}$), which is the unshaded region in the Figure.

With finite auxiliary power, thermally-stable sub-ignited driven burn in this high-temperature regime is also possible. Plasma temperatures for driven burn lie in the 13-17 keV range. In this regime, control of auxiliary heating power can also be used to supplement fueling/density control. However, fueling/density control is still the primary burn control actuator.

Sub-ignited auxiliary-power-controlled operation in ITER at low-temperature/high-density plasma operation point is also possible in so far as the ELMy H-mode confinement scaling (plus bremsstrahlung) power balance is concerned [3]. Such plasmas have low temperature (5 keV) and high density (3×10^{20} m^{-3}) and are thermally unstable when ignited. With active feedback control of the auxiliary power, stable sub-ignited operation is theoretically feasible, but the required plasma densities lie far above the Greenwald density limit (~10^{20} m^{-3}, see §3.3) and the available edge power flow is well below the H-mode power threshold (see §2). These 'operation point' considerations appear to preclude ITER operation in a sub-ignited low-temperature/high-density regime. Accordingly, the strategy for ITER plasma operation and burn control will be operation at a thermally-stable high-temperature/low-density (10^{20} m^{-3}) static operation point with DT fueling

rate control that is supplemented with auxiliary power burn control. The utilization of auxiliary power control (which can include sustained addition of auxiliary power) leads to a control strategy where the transition from ignited to high-Q driven burn occurs seamlessly without modification of the control algorithm [3]. The corresponding accessible domain of operation for up to 100 MW auxiliary power lies to the right of the $P_{sep} \geq P_{L\text{-}H}$ contour in Fig. 8.2.2-2 and corresponds (for 1.5 GW power) to plasma temperatures in the range $12 \leq \langle T \rangle \leq 17$ keV and densities in the range $0.8 \leq \langle n_e \rangle \leq 1.0 \times 10^{20}$ m^{-3}. For 1 GW, the corresponding densities are slightly lower and the overall density range for 1-1.5 GW (i.e., 'full-power') operation is $0.7 \leq \langle n_e \rangle \leq 1.0 \times 10^{20}$ m^{-3}.

In most present tokamaks and plasma operation regimes, explicit control of the plasma edge and divertor characteristics (target power and degree of plasma-to-target attachment) is optional owing to the ability of inertially-cooled divertor targets to adequately handle the moderate power loadings and pulse durations typically encountered. In ITER, where divertor target power loadings (proportional to P/R, see §4) are inherently higher and where continuous (actively-cooled) heat removal is required, it will be necessary to separately control the plasma edge and divertor plasma characteristics so as to keep divertor power and transient energy (ELM) loadings within engineering limits. At the plasma edge, the power flow across the separatrix, edge density and ELM type and frequency are key attributes where control is needed or will be desirable. In the divertor, the target heat flux must be limited to acceptable values and the neutral gas pressure and exhaust will have to be adjusted to maintain constant fuel, helium and impurity densities in both the plasma core and the edge/divertor. Impurity seeding both in the main chamber and in the divertor is envisioned to be the main tool to control divertor power fluxes.

Maintenance of the power flow at the plasma edge above the level necessary for sustainment of H-mode is also required (see §2). The requirement for some minimum power at or near the separatrix to sustain H-mode (estimated to be ~100 MW for ITER) combined with a limit on maximum power conducted to the divertor targets (the ITER specification is ≤ 50 MW, although the targets can handle up to 100 MW on a routine sustained basis) in turn implies that significant (~ 50 MW) radiative power dispersal between the plasma edge/separatrix and the divertor targets is required. Modelling of the plasma edge and divertor region radiation and power conduction/convection characteristics indicate that the required edge-to-target radiative power dispersal can in fact be obtained (see §4), and that the resulting contamination/dilution of the core plasma by the added impurities is small enough that ignition or driven burn with adequate fusion power can still be obtained (see§2).

Representative specifications for ITER kinetics control are summarized in Table 8.2.2-I. For ignited/driven burn plasmas, there are three primary parameters to be controlled: fusion power, edge/separatrix power and divertor target power. There is also a limit—for density limit disruption or performance-degradation avoidance—on maximum plasma density, specified for illustrative

purposes in Table 8.2.2-I as 1.5 times the Greenwald density $n_{GW}(10^{20}\ m^{-3}) = I(MA)/(\pi a^2)$. The factor of 1.5 is provisional and subject to future modification depending upon better understanding of what the effective 'density limit' for H-mode operation with adequate confinement proves to be in ITER (see §3.3). Finally there is a limit—imposed by installed heating/CD capacity—of 100 MW of auxiliary power input.

TABLE 8.2.2-I: ITER Plasma Kinetics Control Specifications[a]

Plasma kinetic attribute	Nominal (for ignited or high-Q burn)	Control accuracy (%) (variance during normal operation)	Maximum or minimum
Density ($10^{20}\ m^{-3}$)	0.7–1.0	±10%	≤ 1.3 (≅1.5 n_{GW})
Fusion power (GW)	1.0–1.5	±10%	≤ 1.8 (for 10 s)
Edge/separatrix power (MW)	≥ 120 (= 1.2 P_{L-H})	± 20% (?)	≥ 120 (?)
Divertor power (to target) (MW)	≤ 50	± 20% (?)	≤ 100 (steady-state) ≤ 200 (for ~3 s)
Auxiliary power (MW)	0 (ignited); 0–100 (high-Q driven burn); e.g. 100 MW at Q = 15	0-100 MW as required (dynamic P_{fus} control in ignited plasmas or supplemental P_{fus} control in driven-burn plasmas)	≤ 100

[a] Representative parameters for B = 5.7 T, I = 21 MA, ELMy H-mode energy confinement, ~9% thermal He, 0.2% Ar, 'most-likely' L-H power threshold (α = 0, see §2.4.3)

The use of three independent 'actuators'—DT fueling rate, impurity injection rate and P_{aux}—to independently control three key attributes—fusion power, edge conducted power and divertor target power—leads naturally to a 'modular' kinetics control scheme like that shown in Fig. 8.2.2-2, wherein three PID (proportional/integral/derivative) feedback control loops with additional logic control ('modules') serve to effect control of the respective actuators [4,5]. The DT module controls either plasma density or fusion power. Density control overrides power control if the requested density exceeds an allowable maximum (limit) density. The Ar module limits the divertor target power to less than a specified allowable power. The P_{aux} module controls the amount of auxiliary heating, in order of decreasing priority, to *i)* maintain the plasma in H-mode, *ii)* maintain the plasma density below a maximum value, and *iii)* assist in the control of the fusion power.

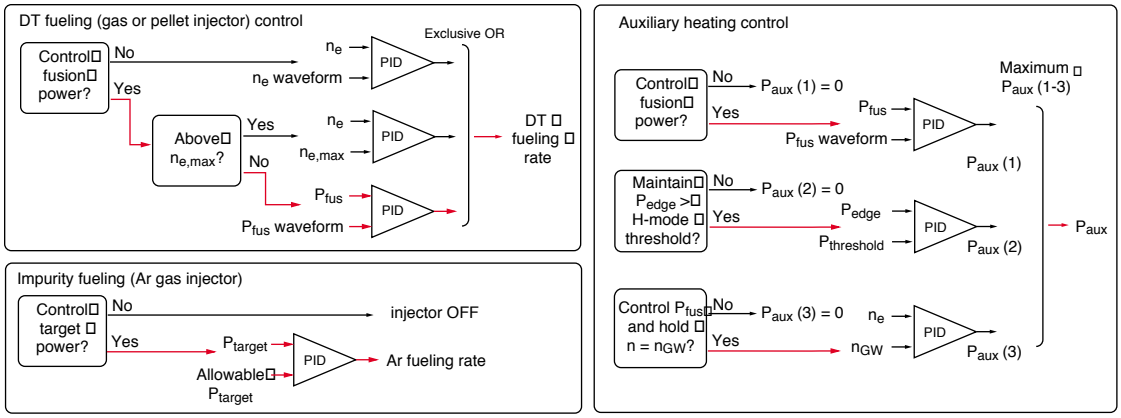

FIG. 8.2.2-2. Schematic concept for the ITER plasma kinetics control system (fusion and divertor target power control).

Whether it will be possible meet all these requirements simultaneously and reliably in ITER raises a number of physics and control implementation issues. The physics considerations of plasma energy and particle confinement, H-mode maintenance, DT and impurity injection, transport and exhaust, auxiliary heating and radiative dispersal of energy in the plasma boundary and divertor are reasonably well defined (see §2-6), and so it is possible to evaluate the efficacy of the control concept embodied in Fig. 8.2.2-2 with plasma simulations. These simulations (an example is presented in §8.2.2.4) show that the control system shown in Fig. 8.2.2-2 is capable [4] of providing effective burn and divertor power control for ELMy H-mode plasmas with operational conditions set by the 'reference ITER physics basis' summarized in Chapters 2-6 of this Article. These simulations also show that burn and divertor control is reasonably robust with regard to tolerance of credible plasma disturbances, variation in modelling assumptions and variations in the feedback loop gain parameters. Furthermore, as will be documented in §8.2.2.3 below, all of the basic control techniques embodied in Fig. 8.2.2-2 (actuator utilization, feedback implementation and demonstration of ITER-equivalent {diagnostic → actuator → plasma} closed-loop control) have taken or are taking place in present tokamaks. So there is a reasonable basis for expecting that the type of control approach embodied in Fig. 8.2.2-2 will be successful in ITER and fully adequate for the conduct of initial DT burn and ignition experiments.

Despite this positive outlook about ITER kinetics control, there is still a clear need for better and more-precise data on the fundamental considerations that underlie Fig. 8.2.2-2, and there is also a need for continued exploration of kinetic control methods and optimization methodology in present tokamaks. The ITER kinetics control design can also benefit from the application of modern control techniques which are starting to be applied to present-day tokamak experiments. Within the kinetic control "matrix" (actuator → plasma effect), there are both strong and weak elements involving the coupling of the core, edge and divertor kinetics to the respective actuators.

There are also indirect couplings between the core, edge and divertor plasma elements: the plasma characteristics in each of these regions is affected to so degree by the plasma characteristics in the other regions. This makes kinetic control a multivariable problem, requiring multiple diagnostic input signals to ultimately control separate actuators for fueling, heating, current drive and neutral particle exhaust. Consequently, a basic requirement of the control method is to simultaneously control weakly-coupled quantities and to perform multivariable control of strongly-coupled quantities, such as fusion power, radiated power, divertor target plate power and the main chamber and divertor neutral pressures.

While the has been good success to date in present experiments in sorting out these couplings and in designing control systems by heuristic or empirical methods (see §8.2.2.2 below), for future reactor and ITER designs in which certain coupling factors are stronger or more critical, the application of modern control design methodologies (H-infinity or Linear Quadratic Gaussian optimization) will be beneficial. These type of control design methods require a relatively accurate plasma response model plus a comprehensive model of plasma-control-related features of the plant/facility systems. These modelling and simulation aspects are further discussed in §8.2.2.3 and §8.2.2.4. These discussions are preceded by a presentation of the status and growing sophistication of kinetics control in present tokamaks.

8.2.2.3. Present experience and accomplishments

All present major tokamak experiments employ some degree of kinetics control—typically control of gas fueling input to effect density control—and a number of experiments have implemented more-elaborate methods for kinetic control that play a key role in achieving specialized or optimal plasma performance. As Table 8.2.2-II below shows, these kinetic control features tend to be specific to each tokamak and reflect in part the plasma diagnostics and plasma control actuators available and the associated objectives of the experimental program. The common theme of this type of kinetics control is improvement of experimental reproducibility: thus enables experiments to run with more precisely-controlled quantities and ultimately, with more reproducible and usually improved performance. Quantities which will be relevant to ITER and have already been controlled in experiments are listed in Table 8.2.2-II. The intent of the Table is to provide representative examples: citations of specific experiments and references on control methods are not necessarily intended to be exhaustive.

TABLE 8.2.2-II: Plasma Kinetics Control Experience in Present Tokamaks

Control category or controlled plasma attribute	**Control method and/or procedure: sensor/parameter → actuator**	**Example/reference**
CORE KINETICS		
Electron density (n_e or $\bar{n}_e (= \int n_e dl / l)$	Interferometry or bremsstrahlung → fuel gas (H, D or T) injection valve	All major experiments
ditto	Bremsstrahlung → bang-bang controller → pellet centrifuge	ASDEX-Upgrade [6]
DD fusion power (via D-D neutron yield)	DD rate (neutron counter) → number of NBI sources	JT-60U [7]
Species mix	Global Alfvén eigenmodes → 2 gas feeds	TCA [8]
W_{th} or β_N (= aBβ/I)	W_{mhd} (diamag.) NBI duty cycle β_N (diamag.) → number NBI sources	DIII-D [9] TFTR [10]
core radiation fraction	P_{rad}(core)/P_{heat} → impurity gas injection	ASDEX-Upgrade [11]
ditto	*ditto*	TEXTOR [12]
current profile j(r) or moments	MSE or polarimetry → ECH	DIII-D [13]
ditto	l_i → phasing of LH launcher modules (changes $n_{\|\|}$ and current drive profile)	Tore Supra [14]
Axial safety factor (q_0) or j(r)	MSE → P_{aux}(heat)	DIII-D [13]
neoclassical modes (q=2)	SXR, ECE or Mirnov island detection → ECCD	ASDEX-Upgrade [15], DIII-D (planned)
EDGE KINETICS AND DIVERTOR		
n_e(edge)	n_0 (midplane or div.) → gas injection (div.)	DIII-D [13]
neutral pressure (n_0)	n_0 (div.) → gas injection (div.)	ASDEX-Upgrade [11]
ditto	Langmuir probe div. → gas injection (div)	JET [16]
Edge radiation	Bolometer (core) → gas imjection (midplane)	ASDEX-Upgrade [11]
In-divertor radiation	Bolometer (core) → gas injection (div)	JT-60U [17]
ditto	Bolometer (core) → gas injection (div)	DIII-D [13]
Wall and limiter temperature	IR camera set → plasma control system, also protection interlock	Tore Supra [18] (planned)
MARFE level	MARFE detection (localized bremsstr.) → NBI.duty cycle	ASDEX-Upgrade
FAST PLASMA SHUTDOWN		

W_{th} and/or I_p shutdown	trigger → massive He injection	JT-60U, DIII-D
W_{th} and I_p shutdown without VDE	trigger → massive He injection	JT-60U
W_{th} and/or I_p shutdown (typically with VDE in elongated plasmas, but with reduced halo current)	trigger → impurity pellet (Ne, Ar, D_2+Kr, D_2+Au or Ag)	JT-60U, ASDEX-Upgrade, DIII-D, TFTR, Alcator C-Mod [19]
SIMULTANEOUS CORE AND DIVERTOR		
Simultaneous control	core radiation fraction + divertor neutral pressure	ASDEX-Upgrade [11]
ditto	n_{edge} + in-divertor radiation	DIII-D [13]
REGIME DETECTION AND SCENARIO SEQUENCING		
plasma regime detection	P_{aux}, P_{rad}, P_{OH}, bolo, β, l_i, → regime (plasma state)	ASDEX-Upgrade [20]
event dependent sequencing	'phase shifting'	JT-60U [21]
ditto	Tokamak + plasma status, scenario phase → scenario phase	ASDEX-Upgrade [22]
ditto	Scenario phase, event → scenario phase]	DIII-D [23]
control method selection	Plasma regime → scenario phase and control mode	ASDEX-Upgrade [24]

Recently, there have been significant experimental advances in simultaneous core and divertor control in 'ITER-like' plasmas and in the implementation of autonomous control to replace human shot-to-shot direction of the plasma operation scenario. These latter 'autonomous' aspects of kinetics control are presented in the final "Regime Detection and Scenario Sequencing" segment of the Table. The concept here is to combine a plasma operation regime (or plasma state) recognition capability with a control algorithm selection capability so as to make the algorithm selection state-dependent. This gives the control system an autonomous capability to react to state transitions in the operation scenario sequence and (with proper choice of algorithms) to take corrective action if a state transition fails to take place as desired or if an operational anomaly causes a recoverable loss of the desired plasma operation state. For example, in ASDEX-Upgrade, an autonomous control procedure has been successfully implemented for the control of ITER-relevant high-radiation H-mode (HRH) discharges (Fig. 8.2.2-3) [20], [22], [24]. In these discharges, precisely-controlled edge/divertor radiation (effected by Ne injection) is used to produce an H-mode discharge with a detached divertor plasma. To achieve this HRH (also called CDH, for completely detached H-mode) regime, simultaneous control of the neutral gas flux in the divertor by hydrogen puffing and of the radiative fraction P_{rad}/P_h in the main chamber by Ne seeding is used. Precise dynamic control of the Ne flux is necessary: excessive Ne or edge

radiation results in a high-radiation L-mode (HRL) rather than HRH discharge. Figure 8.2.2.-3 shows the operation of the ASDEX-Upgrade control system in which the various plasma states that lead up to initial achievement are identified by the control system and in which a reversion from the HRH mode to HRL mode is autonomously detected and corrected by control of the Ne injection rate. A plasma-regime recognition algorithm and a connected scenario sequencing procedure is used, and the pre-divertor radiated power fraction is calculated from the bolometer signals depending on the discharge state. Measurements of the plasma internal inductance also enter into the regime-recognition algorithm.

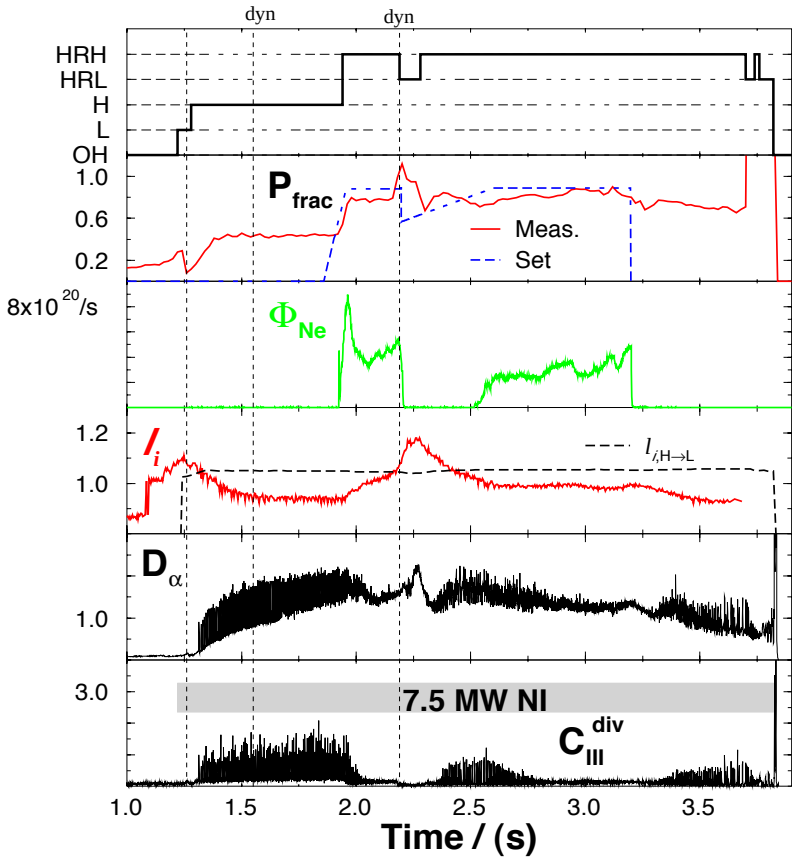

FIG. 8.2.2-3. Supervisor autonomy and plasma regime-driven kinetics control during a ASDEX-Upgrade discharge.

The kinetics control system can also be made responsible for maintaining the plasma operation in a safe 'operational limits' region, particularly in view of disruptions at high β_N, close to $q_{95} = 2$ or near the density limit. To accomplish this type of disruption avoidance, the control system needs a model of the dangerous regions and a procedure for how to "back off" from them without causing a disruption or thermal collapse. An example of this type of multi-parameter operational domain DIII-D is during high-β, high-density, high-elongation and low-q operation. The zone

with maximum performance is in an acute region of operational space and backing away from any single limit is likely to exacerbate another limit. In DIII-D, automation is already implemented for a single parameter, namely the approach to the high-β limit and similar auxiliary-heating-control method for β-limit disruption avoidance are now being used in all major tokamaks.

In the DIII-D disruption avoidance study [25], a parametrisation of the β limit was obtained from a neural network description of the disruption boundary based on experimental data (see §3.4.6 for a further presentation of this result and also presentation of simulated β-limit-based disruption avoidance in TFTR). This neural-net estimate of the β-limit was subsequently used as the basis for disruption avoidance and non-disruptive operation close to the limit was obtained. The study showed that neural network description of the β limit was appreciably more accurate than the modified Troyon limit $\beta_N = 4l_i$ (see §3.2.1 and 3.4.6) in predicting onset of disruption. This finding demonstrates the advantage of using the neural net to provide a *posteriori* control or disruption proximity estimator. Additionally, the neural-net-based control system was able to adapt to negative central shear discharges once they had been included into the control system database.

The content of Table 8.2.2-II and the brief descriptions of the regime-recognition-based control and disruption-avoidance control presented above show that kinetic control is being actively investigated and appropriate control methods are being developed as part of the general research process for tokamak control. Simultaneous control of several variables and plasma state-dependent switching between control algorithms have been demonstrated: both of these demonstrations are useful for ITER. The experience gained so far allows us to address the reactor-oriented goals of kinetic control. To make this a physics/engineering task rather than rely on a heuristic approach a number of modelling-related problems still must be addressed. These modelling and simulation aspects of extrapolating present control experience to ITER are discussed below.

8.2.2.4. Kinetic control modelling, simulation and model validation

The design of kinetic control loops and their conceptual improvement typically requires a system model that relates the effect of available actuators to the controlled plasma variable(s). In the case of magnetic control, such system models are available and can be regarded as definitive for control system design (i.e., there is no question about the validity of the plasma response model), but for kinetic control the understanding of the underlying plasma physics basis is not as complete or computationally tractable and further understanding of the interacting core, edge and divertor regions and wall behavior is required before a fully-definitive plasma model can be provided to control system designers (control engineers) for kinetic ‘control system design’. There are, however, a number of presently-available plasma simulation models, typically embodied in the

form of 1.5-D transport codes, that are capable of simulating most aspects of plasma core kinetic behavior as seen in positive-shear L-mode and H-mode plasmas (see §2). These transport codes are capable of following (simulating) the dynamics of the core plasma evolution on time scales that are appreciably longer that the Alfvén time but still a small fraction of the energy confinement time (say ≥ 1 ms in ITER). There are also 2-D plasma edge and divertor simulation codes that can give details of the edge/divertor plasma behavior, albeit not as readily on a 'fast' dynamic time-scale (see §4), so one typically uses quasi-static 'survey' data from such 2-D models to construct more-dynamic simplified 0-D or 1-D edge and divertor 'modules' that can then be appended to a 1.5-D transport code. Using this type of procedure, simulation codes starting either from a core modelling basis or from edge/divertor modelling basis have been modified to include the other plasma zone and 'fast' (ms) dynamic capabilities. The resulting 'coupled' plasma system model [3,4] is then capable, given adequate validation of the simplified edge and divertor modules, or core modules, of dynamically examining the dynamics of proposed reactor plasma operation scenarios (i.e., initial ignition in a DT-plasma) and the dynamics of the control of such scenarios.

The broad outline of plasma kinetics control for a future tokamak can be ascertained with an idealized dynamic model in which time- and space-response characteristic of plasma diagnostics are not explicitly taken into account, and in which the actual finite rise time and finite rate-of-change (e.g., dP_{aux}/dt) limitations of candidate kinetics control actuators are similarly suppressed. However, at some latter point the control design process, the effect of these 'real-world' limitations on sensors and actuators must also be assessed and if necessary incorporated into the control system model. Accordingly, descriptions of diagnostics and actuator response are being added both for core transport, divertor and wall physics. The intent of these developing 'system models'—which can eventually encompass the whole tokamak/reactor facility—is to enable model-based computation of control-loop parameters rather than empirical tuning. These models can also be used for exploration of plasma and plant/facility operation anomalies.

Obtaining an estimator of the plasma quantities to be controlled is an important aspect of the kinetics control problem and is closely related to diagnostic availability and utilization. In addition to the fundamental problem of being able to measure the controlled quantity (or a plasma attribute that is more-or-less linearly related to the controlled quantity), for reliable control, there are also considerations of the effects of imperfect measurements, selection of optimal observation channels and selection/utilization of additional/alternative diagnostics to improve control reliability and redundancy. These latter considerations become particularly important for an ITER/reactor-class tokamak, where plasma energy levels are high and where plasma kinetic control system anomalies can put certain in-vessel systems at risk. Given that the unexpected discovery of plasma control system 'surprises' during the course of ITER operation will be at very least expensive in terms of the operation time that is wasted, there are strong economic and operational efficiency arguments

for conducting comprehensive simulations of ITER kinetics control—in both normal and off-normal situations—before the corresponding plasma operation is attempted.

The analogy of present use of an aircraft flight simulator for crew training and for mission planning can be invoked here: it seems likely that before an operational procedure or experiment is to be implemented in ITER, it will be prudent (or mandatory) to 'test' the procedure or experiment using an ITER facility operation simulator that incorporates a well-validated plasma operation simulation model. The intent here goes beyond just the plasma simulation itself: it will also be necessary to simulate the diagnostic/plant/facility response to the proposed experiment and to test the effects of credible variations and anomalies in all of the systems involved. This testing will presumably include consideration of plant/facility failures and on the corresponding effect on plasma operation and continuing function of the ITER tokamak and its ancillary systems. Validating a prototype ITER 'simulator' of this comprehensive nature against presently operation experiments will be required prior to qualifying the simulator for ITER use, and the continuing refinement of the validation of this type of simulator can anticipated to remain a task for presently operating tokamaks up to and beyond the time when ITER operation commences.

8.2.2.5. ITER kinetics control simulations

The feasibility of ITER kinetics control has been explored with a variety of quasi-static and fully-dynamic simulation models, including with the PRETOR 1.5-D transport code with a coupled divertor model and self-consistent modelling of noble-gas impurity (Ar) injection divertor power control [4]. Since the coupled-plasma/divertor model is dynamic and not inherently stable, it is necessary to incorporate elementary PID controllers for DT fueling and Ar fueling into the overall simulation so as to be able to obtain a stable modelling result. These controllers, which are implemented in the configuration illustrated in Fig. 8.2.2-2 are in effect a representation (based on idealized plasma data and actuator response) of ITER control.

Figure 8.2.2-4 illustrates how the ITER kinetics control system illustrated in Fig. 8.2.2-2 can maintain control of fusion and divertor power during a severe plasma power balance transient (100 MW power added) [4]. The simulation demonstrates that fusion and divertor target power control during power ramp up and rampdown are also maintained. The high-frequency power transients are likely modelling artifacts and in any case are within the transient capabilities of the divertor targets and first wall components). Refinements of this type of simulation in which control of the Ar injection rate with a divertor temperature infrared-emission monitoring system is explicitly simulated (including the non-linear emission versus temperature characteristic and

instrumental noise) show the overall divertor power control system is stable and has adequate transient response and noise level characteristics [26].

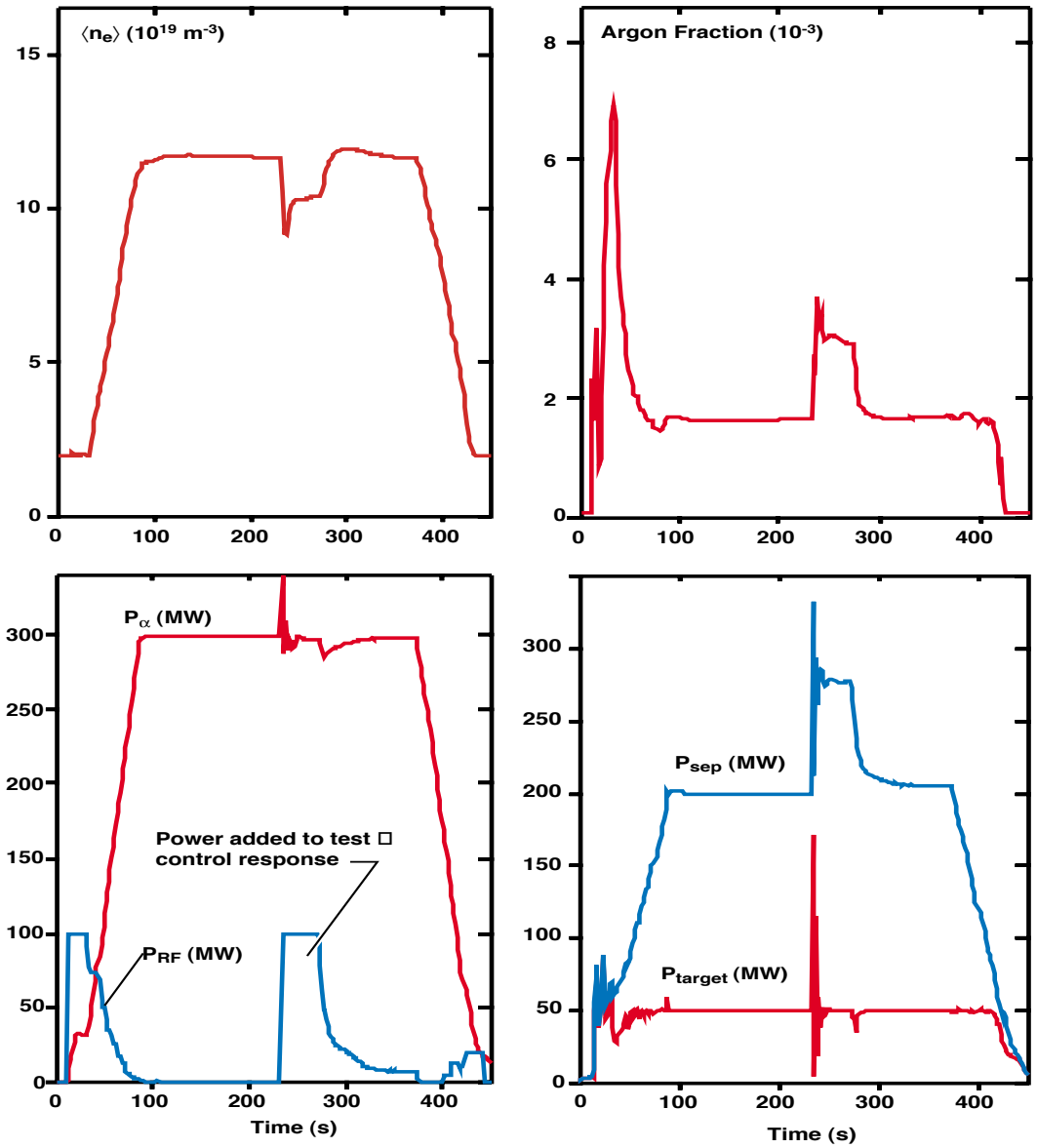

FIG. 8.2.2-3. Simulation of burn and divertor power control during a 'reference case' ITER plasma operation scenario pulse (fusion burn duration intentionally limited to 400 s) that includes a 100-MW auxiliary power input transient. The kinetics control system shown in Fig. 8.2.2-2 successfully controls plasma and divertor power during both burn initiation and termination and also during burn power flattop despite the addition of 100 MW of auxiliary power.

Control of the kinetic properties of ITER plasmas is of course contingent on having a corresponding set of plasma diagnostic data with adequate temporal and spatial resolution. Here the

planned ITER diagnostics set for DT operation (Table 8.2.2-III) [27] is arguably equal to or more complete than the diagnostic sets available on the present generation of well-instrumented medium- and large-size tokamaks. As the Table illustrates, present plans for the ITER plasma diagnostics divide the diagnostics into three categories: those to be used for 'basic' control and tokamak protection (Group 1a), those to be used for 'advanced' control (including profile control) (Group 1b) and those to be used 'off-line' for plasma performance evaluation and physics analysis (Group 2). While this division is useful for planning purposes, given the planned reliance of ITER control on plasma-state or operation-regime recognition (which can benefit from using a wide range of diagnostics) and given the likely progression in sophistication of the diagnostics inputs that will ultimately enter into such control, we anticipate that both Group 1a and 1b data and even Group 2 data will contribute to real-time plasma-regime identification and hence will important (essential) for the operation and kinetics control of ITER plasmas. Comprehensive diagnostics data will also be necessary for implementation of pro-active 'before-incident' protection of the ITER plasma-facing-components that are at risk during plasma operation. In this sense, the distinction between the utilization of plasma diagnostic data for plasma control, machine protection and the acquisition of scientific data will, like the partitioning of the plasma control and machine protection functions among the ITER control system units, become increasing blurred as the final design of the ITER plasma control system is fully defined.

TABLE 8.2.2-III: ITER Plasma and Tokamak Diagnostics

GROUP 1a Machine Protection and Basic Control		GROUP 1b Advanced Control		GROUP 2 Evaluation & Physics	
Parameter	**Diagnostic**	**Parameter**	**Diagnostic**	**Parameter**	**Diagnostic**
Shape / Position Locked Modes q(a), q(95%) Plasma Current Beta m=2 Mode 'Halo' Currents Loop Voltage	Magnetics	MHD Activity	Magnetics ECE Reflectometry	Fishbones, TAE Modes	Magnetics
Impurity Influx (main plasma & divertor)	Impurity Monitors	Shape / Position (very long pulse)	Reflectometry (plasma posit.)	Confined α-Particles	Collect. Scatt., Knock-on Tail Neutr. Spectr., Gamma Spectr.
Runaway Electrons	Hard X-Rays, Synchrotron Radiation	Neutron Profile, α-Source Profile	Rad. Neut. Cam., Vert. Neut. Cam.	$n_T/n_D/n_H$ (edge)	NPA, H_α Spec., Two-Photon Ly-a Fluoresc.
Line-averaged Density	Interf. / Polarim.	n_{He} Profile	CHERS	$n_T/n_D/n_H$ (div)	H_α Spectrosc.
J_{sat} (divertor)	Tile Shunts	Plasma Rot., T_i Profile, Impurity Profile	CHERS, X-Ray Crystal Spectroscopy	T_e Profile (edge)	Thomson Scatt. (edge)
Surf. Temp. (divertor plates & first wall)	IR Cameras	T_e Prof. (core), n_e Prof.(core)	LIDAR (main), ECE	n_e, T_e Profiles (X-point)	Thomson Scatt. (X-point)
Rad. Power from Core, X-point and Divertor	Bolom. Array (main pl. & div.)	T_i Profile (core)	Radial Neutron Spectrometer	n_e, T_e (plate)	Langmuir Probes
Neutron Flux	Neutron Flux Monitors	n_e Profile (edge)	Reflectom. (main)	T_i in Divertor	Imp. Monitor. (div)
n_T/n_D in Plasma Core	NPA, Fast wave Reflectometry	q Profile	MSE, Polarim. System	Plasma Flow (div)	Imp. Monitor. (div)
Z_{eff} Line-Aver.	Vis. Continuum (single channel)	P_{rad} Profile	Bolom. Arrays (main pl.& div.)	Pellet Ablation	H_α Spectrosc.
H / L Mode Indicator	H_α Spectrosc. (typ. channel)	Z_{eff} Profile	Visible Cont. Array	T_e Fluctuations	ECE, Soft X-Ray Array
ELMs	ECE, Refl.(main)	n_{He} (divertor)	RGA, Laser Induced Fluoresce. (LIF)	n_e Fluctuations	Reflectometry, Microw. Scatt.
Gas Pressure (div. & duct)	Pressure Gauges	Heat Deposition Profile in Div.	IR Camera	Radial E Field and E Fluctuat.	CHERS (plasma rot.)
Gas Composit. (div. & duct)	RGAs	Div. Ionization Front Position	Vis . Spectrom., Bolometry	Edge Turbulen.	Reflectometry
Toroidal Magnetic Field	Current Shunts	Neutral Density (near wall), Particle Source	H_α Spectrosc. (many chann.)	MHD Activity in Plasma Core	ECE, Soft X-Ray Array
		n_e, T_e (divertor)	Reflect. (div) ECA (div.)		

8.2.2.6 Summary and implications for ITER

Plasma kinetics control in the present generation of auxiliary-heated tokamaks has reached a state of sophistication in which all of the basic kinetics control requirements projected to be needed for ITER—DT fueling rate control, impurity-injection divertor target power and attachment control, auxiliary power control and kinetics control-based disruption avoidance—have been successfully demonstrated. The successes in present experiments and the inherent similarity between density control in present tokamaks and burn control in a DT-burning tokamak give confidence that the methods used in present tokamaks for kinetics control of present H-mode plasmas are applicable and adequate for similarly robust control of 'high-temperature/low-density' ignited- and driven-burn ITER DT plasmas. Simulations of ITER kinetics control demonstrate that simultaneous control of fusion power and limit of divertor power to acceptable levels will be possible. The incorporation of regime-identification and control reaction capabilities—already demonstrated in several present tokamaks—into the ITER plasma kinetics control system is anticipated to make ITER plasma control more reliable and robust. A comprehensive suite of plasma diagnostics will be available to support such regime- and event-guided kinetics control. Finally, the use of modern control system design methodologies combined with the planned availability of a detailed ITER plasma and facility operation simulator can be expected to further enhance the present expectation that plasma kinetics control in ITER will meet design objectives and demonstrate of the potential for tokamak reactors to provide a predictable and well-controlled source of magnetic fusion energy.

References to Section 8.2.2

[1] Wagner, F, G. Becker, K. Behringer *et al*., Phys. Rev. Lett. **49** (1982) 1408-1411.

[2] Wesley, J., H-W. Bartels, D. Boucher, A. Costley, L. DeKock, Yu. Gribov, M. Huguet, G. Janeschitz, P-L. Mondino, V. Mukhovatov, A. Portone, M. Sugihara, and I. Yonekawa, *Plasma Control Requirements and Concepts for ITER*, Fusion Technology **32** (1997) 495-525.

[3] Boucher, D., J. Wesley, *Modelling of ITER Operation*, in *Controlled Fusion and Plasma Physics* (Proceedings 22nd European Physical Society Conference, Montpellier 1994, Europhysics Conference Abstracts, Geneva ,1994) **18B Part II** 524-527.

[4] D. Boucher, F. Louche, N. Karulin, ITER Joint Central Team, ITER Home Teams, *ITER Fusion Performance Projections*, in *Controlled Fusion and Plasma Physics* (Proceedings 24th European Physical Society Conference, Berchtesgarten 1997, Europhysics Conference Abstracts, Geneva ,1997) **21A Part III** 953-957.

[5] Wesley, J., *Operation and Control of ITER Plasmas*, to be published in *Proceedings 17th IAEA Fusion Energy Conference (Yokohama 1998)* .

[6] Lang, P., H. Zohm, K. Büchl, J. Fuchs, O. Gehre, O. Gruber, V. Mertens, H. Moller, J. Neuhauser, ASDEX Upgrade Team, NBI Team: *Pellet Fuelling of ELMY H Mode Discharges on ASDEX Upgrade*, Nuc. Fusion **36**, 1996, p. 72.

[7] Neyatani, Y. *et al*.: *Feedback Control of neutron emission Rate in JT-60U*, to be published Fus. Technology, 1997.

[8] TCA Alfven species mix control:

[9] DIII-D Wth control (to NBI).

[10] Lawson, J. E., M. G. Bell, R. J. Marsala, D. Mueller: *Beta Normal Control of TFTR using Fuzzy Logic*, in Proceedings18th Symposium on Fusion Technology, Karlsruhe, 1994, p.739.

[11] Kallenbach *et al*.: hi radiative H regime (??? where).

[12] J. Wienbeck, J. Rapp: *Automated Real-Time Control of Radiation Cooling at TEXTOR*, SOFT 1996, p. ??.

[13] M. Walker, J. Ferron, B. Penaflor,. D. Humphreys, J. Leuer, A. Hyatt, C. Forest, J. Scoville, B. Rice, E. Lazarus, T. Petrie, S. Allen, G. Jackson, R. Maingi: *Status of DIII-D Plasma Control*, Proc. 16th Symp. on Fusion Engineering, 1995, Illinois (USA), p. 885.

[14] van Houtte, D. and Equipe Tore Supra: *Tore Supra: Advances towards Long Pulse Steady State Operation*, Proc. 16th Symp. on Fusion Engineering, Illinois (USA), 1995, p. 730; also G. Martin, Equipe Tore Supra, *Enhanced Performances for Long Pulses on Tora Supra*, in 17th IEEE/NPSS Symposium on Fusion Engineering, (Proceedings 17th SOFE, San Diego 1997), IEEE, Piscataway New Jersey (1998), **Vol. 1** 92-95.

[15] Zohm, H., G. Gantenbein, S. Günter, F. Leuterer, M. Maraschek, J. P. Meskat, A. G. Peeters, W. Suttrop, D. Wagner, Q. Yu, ASDEX Upgrade Team, *First experiments on neoclassical tearing mode stabilisation by ECCD in ASDEX-Upgrade*, to be published in *Proceedings 17th IAEA Fusion Energy Conference (Yokohama 1998)* .

[16] M. Gadeberg, P. Andrew, T. Budd, T. Hartrampf, J. How, H. S. Jensen, A. Peacock: *A Combined Divertor and Bulk Plasma Density Control System*, in Proceedings18th Symposium on Fusion Technology, Karlsruhe, 1994.

[17] H. Tarnai et al.: *Feedback Control of Radiation Region in Radiative Divertor Plasma on JT-60U Tokamak*, 4th lnt. Symp. on Fus. Nuc. Technology, Tokyo, 1997.

[18] M. Lipa, Ph. Chappuis, P. Garin, G. Martin, R. Mitteau, J. Schlosser, G. F. Tonon, *Towards long pulse high performance discharges in TORE SUPRA: upgrading of inner vessel components (CIEL PROJECT)*, in 17th IEEE/NPSS Symposium on Fusion Engineering, (Proceedings 17th SOFE, San Diego 1997), IEEE, Piscataway New Jersey (1998), **Vol. 1** 353-355.

[19] Granetz R., *et al*., *Disruptions and Halo Currents in Alcator C-Mod*, Nuc. Fusion **36** (1996) 545-569.

[20] P. Franzen, V. Mertens, G. Neu, T. Zehetbauer and ASDEX Upgrade Team: *Online Confinement Regime Identification for the Discharge Control System at ASDEX Upgrade*; 23rd Europ. Conf. on Fusion and Plasma Physics, Kiev, (Ukraine), 1996.

[21] N. Hosogane, R. Yoshino, K. Kurihara, T. Kimura, A. Ogata, I. Yonekawa, H. Aikawa, 1. Kondo, Y. Suzuki: *Design Concept for Real-Time Plasma Control for JT-60*, 9th Symp. on Eng. Prob. Fusion Res., 1981, p. 904.

[22] G. Raupp, H. Bruhns, K. Förster, F. Hertweck, R. Huber, A. Juelich, G. Neu, H. Richter, U. Schneider, B. Streibl, W. Woyke, D. Zasche, T. Zehetbauer: *ASDEX Upgrade Discharge Control and Shot Managemen*t, Proc. 17th Symposium on Fusion Technology, Roma (1), 1992, p. 1072 and *Discharge Supervision Control on ASDEX Upgrade*; Fusion Technology **32** (1997) 444-458.

[23] Ferron, J., B. Penaflor, M. Walker, J. Moller, D. Butner: *A Flexible Software Architecture for Tokamak Discharge Control Systems*, Proc. 16th Symp. on Fusion Engineering, 1995, Illinois (USA), p. 870.

[24] Zehetbauer, T., P. Franzen, G. Neu, V. Mertens, G. Raupp, W. Treutterer, D. Zasche and ASDEX Upgrade Team: *Plasma Regime Guided Discharge Control At ASDEX Upgrade, Proc. 19th Symposium on Fusion Technology*, Lisboa, 1996; also T. Zehetbauer, C. Aubanel, V. Mertens, G. Neu, G. Raupp, H. Richter, W. Treutterer, D. Zasche: *Management of RT Processes for Plasma Parameter Optimization at ASDEX Upgrade* ; Proc. 9th Conference on Real-Time Computer Applications in Nuclear, Particle and Plasma Physics, Chicago, (USA), 1995.

[25] Wroblewski, D., et al., "*Tokamak disruption alarm based on a neural network model of the high-β limit*", Nuclear Fusion **37** (1997) 725.

[26] Boucher, D., *et al, Assessment and Modeling of Inductive and Non-Inductive Scenarios for ITER*, to be published in *Proceedings 17th IAEA Fusion Energy Conference (Yokohama 1998)* .

[27] Costley, A. et al., *Overview of the ITER Diagnostic System*, Diagnostics for Experimental Thermonuclear Fusion Reactors Vol. 2, Plenum Press, New York (1998) 41-56.

8.2.3. Plasma Operation Scenario and Related Considerations

In this Section, specialized aspects of the plasma/PF system operation scenario and plasma control are addressed. These aspects occur during the plasma initiation, current ramp-up and current shutdown phases. Plasma operation and magnetic and kinetic control during current and/or heating/burn flattop phase are treated separately in Sections 8.2.1 and 8.2.2. Options for fast plasma energy/current shutdown—potentially needed at any time during the scenario—are also summarized herein, with further reference to Section 3.2.5 for details. A brief discussion of the requirements—and possibilities—for plasma-control-related machine protection follows. The Section concludes with a presentation of scenario simulations for ITER and with a discussion of still-open physics and plasma operation scenario integration issues.

8.2.3.1. Plasma initiation

ITER will, like all presently-operating tokamaks, depend on ohmic (or inductive) plasma initiation effected by using voltages applied to the poloidal field (PF) coil system to produce a Townsend avalanche breakdown in a low-pressure (10^{-5} torr $\cong 10^{-3}$ Pa) filling gas, either deuterium (or hydrogen or tritium) or helium. In ITER, the parameters for ohmic initiation are constrained by two reactor-tokamak-design related considerations: a somewhat limited one-turn voltage and in-vessel electric field capability, about 20 V/turn and 0.3 V/m, imposed by terminal voltage limitations on the multi-turn superconducting PF coil system, and by the substantial in-vessel poloidal fields (error fields) that arise from induced and resistive toroidal currents that develop in the toroidally-conducting nuclear shield module support backplate and torus vacuum vessel [1]. High error fields compromise the effectiveness of Townsend avalanche breakdown, and so must be reduced to low-enough levels (~10^{-3} T) such that Townsend breakdown of the filling gas can be obtained. Analysis (see e.g. [9]) of the Townsend avalanche and error-field reduction capabilities of ITER shows that ohmic plasma initiation should be possible, albeit with relatively small margins and the need for careful error field and filling pressure control. Since these calculations demonstrate that avalanche margins are small and also that ohmic heating alone may fail to provide sufficient power for full ionization of low-Z impurities (‘impurity burn-through’), following initial D or He ionization, present ITER plans are to provide 3 MW of electron cyclotron EC assist during the breakdown and burn-though phases of plasma initiation [1]. If necessary, this assist power can be increased to up to 10 MW.

The maximum in-vessel electric field available for the plasma initiation in ITER will be about 0.3 V/m (≅ 15 V/turn). This limitation comes about primarily owing to terminal voltage limitations—set by insulation technology—at the central solenoid (CS) and at the outboard PF

coils, of 15 V/turn for the CS (~3000 turns) to 60 V/turn for the largest PF coils (~1000 turns) [1]. There are also economic constraints set by the cost of the PF power supply interrupters (opening switches) that generate the high voltages needed for plasma initiation. Finally, the presence of the resistive torus vacuum vessel and shield module backplate (R ~5 μΩ) results in delay of the in-vessel voltage rise and hence some loss of usable in-vessel voltage: the applied ex-vessel voltage for ITER is actually about 20 V/turn. Similar or perhaps even more restrictive startup E-field constraints are expected to apply to future tokamak reactors. The fact that the ITER coil conductors are superconducting is of only limited importance in constraining startup parameters: *ac* losses (related to dB/dt in the superconducting windings) are themselves not a major voltage-limiting constraint.

Elementary analysis of the neutral gas breakdown characteristics (Townsend avalanche) shows that reliable plasma initiation in hydrogen or deuterium will be possible in ITER at this electric field. In fact, Townsend breakdown at lower E-fields and much lower one-turn voltages has been demonstrated in smaller tokamaks (e.g., 0.25 V/m and 3 V/turn in DIII-D [2]). However, the resulting initial buildup of ionization under these low E-field conditions is relatively slow (30 ms) and careful adjustment of the filling gas pressure and field null geometry are required. The addition of modest amounts of electron cyclotron power (EC assist) with a resonance positioned near the center of breakdown location (multi-pole field null) results in faster (< 3 ms) and more reliable breakdown with greatly increased tolerance to field null quality [2]. This latter advantage is significant, since it allows the breakdown field configuration to be adjusted to favor optimal radial equilibrium of the initial plasma (which requires a weak vertical field) rather than the high-order multi-pole null that is optimal for initial breakdown.

Reduction of the breakdown loop voltage using ECH pre-ionization has been investigated in many tokamaks (FT-1, WT-1, ISX-B, Tokapole II, CLEO, WT-2, JFT-2, and DIII-D, see Ref. [2] and further References therein), and reliable breakdown a minimum electric field of 0.15 V/m (1.6 V/turn) was achieved in DIII-D with 700 kW of 60 GHz EC assist power [2]. Alternatively plasma current startup without a primary voltage was demonstrated in PLT [3] by injecting Lower-Hybrid (LH) waves. In these experiments, pre-ionization by RF heating played an essential role in reducing the loop voltage, with hydrogen gas used as the prefill gas. In JT-60U stable plasma current startup with 0.08 V/m was obtained with helium prefill gas and LHRF heating (1.7-2.4 GHz, 1.5 MW) [4]. Helium gas was also used in TEXTOR-94 for low voltage startup assisted by ICRF (350-500 kW, 32 MHz, second-harmonic frequency regime) [5]. As is shown below, the use of helium rather than hydrogen or deuterium facilitates initiation at low voltage.

There are three principal considerations for achieving successful plasma startup: *i)* Townsend avalanche characteristics (set essentially by the ratio of the applied E-field to the gas pressure), *ii*) magnetic connection length (set by the ratio poloidal error field to toroidal field) and

iii) impurity ionization radiation 'burn-through'. Considerations *i)* and *ii*) determine whether initial breakdown occurs; consideration *iii*) determines whether the initial ionization-produced plasma current can be sustained and increased by application of a finite plasma loop voltage. All of these considerations are well-known and we find that there are no unknown physics issues related to achieving plasma initiation in an ITER-class tokamak. However, careful design of the startup strategy based upon the three considerations above is required. A fourth consideration—that of producing runaway electrons during low-E-field/low-density startup—has also been identified [2]. However, experimental results to date show little indication for low-E-field/low-density startup to produce significant runaways.

In what follows, the four physics design considerations for plasma initiation are further developed below and the resulting implications for ITER evaluated.

1) Electric Field and Prefill Gas Pressure. According to Townsend avalanche theory, the ionization growth rate α (ionizations per unit length) is $\alpha = \mathrm{A}\, p \exp(-\mathrm{B}pE)$, where p is the neutral gas pressure (traditionally measured in torr; 1 torr = 1/760 atmosphere ≅ 131 Pa), E is the electric field, and A and B are coefficients that depend on the gas species: A = 510 m^{-1} $torr^{-1}$, B = 1.25×10^4 V m^{-1} $torr^{-1}$ for hydrogen or deuterium (and presumably for tritium); A = 300 m^{-1} $torr^{-1}$, B = 1.25×10^4 V m^{-1} $torr^{-1}$ for helium. Setting $\alpha^{-1} = L$, where L is an effective connection length (average length of a magnetic field line between intersections with material surfaces; what constitutes 'effective' is addressed below) gives a minimum electric field $E_{\min}(p,L)$ for breakdown

$$E_{\min}\,(\mathrm{V/m}) = \frac{1.25\times10^4\, p(torr)}{\ln\left[510\;\; p(\mathrm{torr})\, L(\mathrm{m})\right]} \qquad (1a)$$

for hydrogen, deuterium or tritium and

$$E_{\min}\,(\mathrm{V/m}) = \frac{3.4\times10^4\, p(torr)}{\ln\left[300\;\; p(\mathrm{torr})\, L(\mathrm{m})\right]} \qquad (1b)$$

for helium. Figure 1 shows plots of Eqs 1a and 1b versus p for effective connection lengths $200 \le L(\mathrm{m}) \le 2000$. This range is representative ofconnection lengths achieved in present medium to large-size tokamaks and projected for ITER (see below). The minimum value of $E_{\min}$, i.e., the lowest field at which breakdown is possible at a given L, typically occurs for $5 \times 10^{-6} \le p(\mathrm{torr}) \le 5 \times 10^{-5}$. For deuterium and $200 \le L(\mathrm{m}) \le 2000$, the corresponding range of minimum E-field is

$0.04 \leq E_{\min}(\mathrm{V/m}) \leq 0.4$. For reliable breakdown and burn-through, $E \geq \sim 2E_{\min}(p,L)$ is desirable.

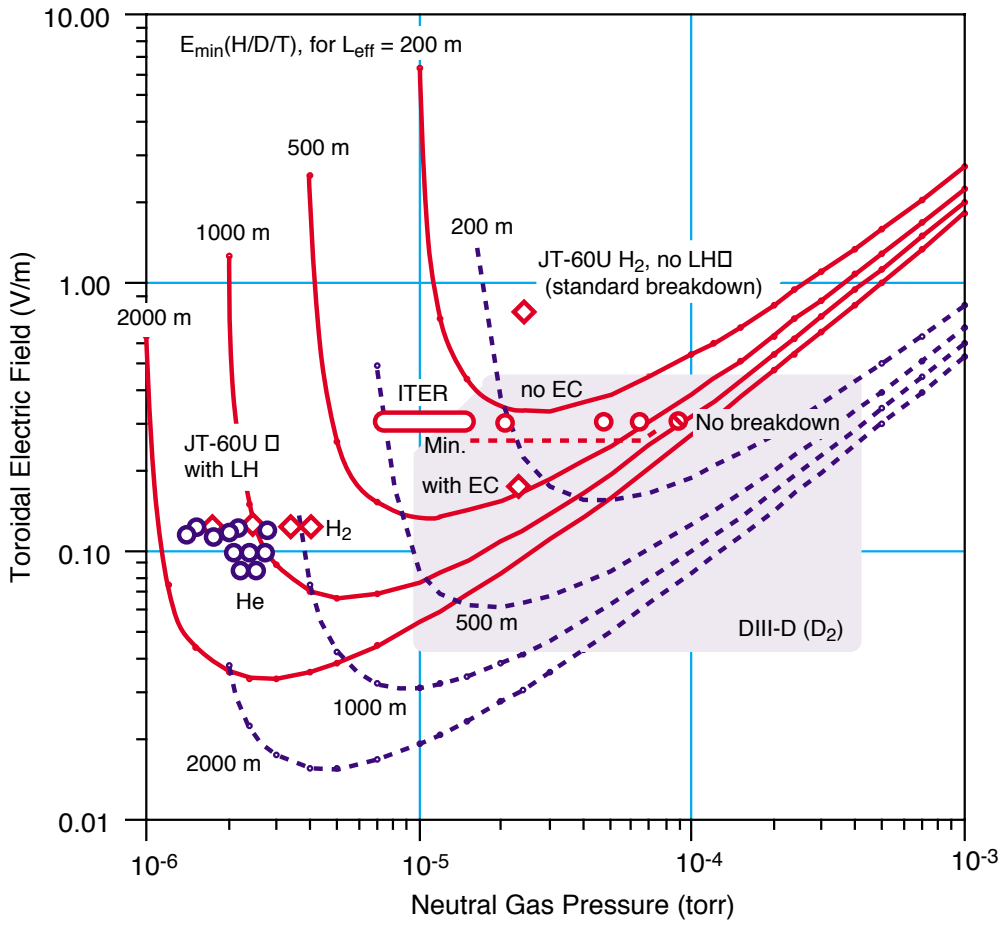

FIG. 1. Minimum electric fields for Townsend avalanche breakdown in hydrogen, deuterium or tritium and in helium (dashed lines), for various connection lengths L_{eff}. Data for unassisted (ohmic) and rf-assisted plasma initiation in JT-60U [4] and DIII-D [2] are superposed. Proposed startup parameters for ITER are also shown. The shaded domain encompassing the DIII-D data is to facilitate identification of the data: it has no scientific significance. The dashed line labeled "Min." shows the lowest E-field at which unassisted breakdown in DIII-D is possible.

Figure 1 demonstrates that at minimum $E_{\min}$ (i.e., for $p \sim 10^{-5}$ torr), helium should theoretically reduce the breakdown electric field by a factor of 2.5 relative to the field for hydrogen. Figure 1 also shows selected experimental data for ohmic and rf-assisted breakdown experiments in DIII-D [2] and JT-60U [4]. In the DIII-D experiments with D_2 [2], the minimum E-field for breakdown was 0.25 V/m and the effective connection length inferred from the high-pressure limit

for breakdown was 500 m ($\cong 50 \times 2\pi R$). With the addition of EC assist (700 kW, 60 GHz), breakdown at 0.15 V/m was possible. In JT-60U with LH assist (up to 1.5 MW at 1.7-2.4 GHz), the minimum E-field for plasma initiation was 0.12 V/m for H_2; 0.08 V/m for He, both achieved at prefill pressures of 2-3 x 10^{-6} torr. Normal unassisted breakdown in JT-60U takes place at higher pressures (2×10^{-5} torr) that are more typical of standard tokamak practice, with E-fields of about 0.8 V/m. The proposed pressure range for ITER startup is $0.7–2.0 \times 10^{-5}$ torr (see e.g. [9]). As Figure 1 demonstrates, this range should yield reliable Townsend breakdown in D_2 for $L \geq$ ~300 m. Overall, the ITER startup parameters are rather similar to those demonstrated in DIII-D.

Helium prefill offers two additional advantages for low E-field plasma initiation: *i*) better controllability of the prefill gas pressure compared to hydrogen (especially at low pressure), because wall absorption of helium is much lower, and *ii*) charge exchange energy losses are lower for helium, which improves the power balance after the initial ionization phase of the breakdown (see below).

2) Connection Length and Allowable Stray Field. The effective length L that enters into the Townsend avalanche growth [$n_e \propto \exp(\alpha L)$] is set by the ratio of poloidal (perpendicular) and toroidal fields. In tokamaks with toroidally-conductive vacuum vessels, poloidal 'error' fields at startup arise primarily from the eddy currents that application of the one-turn voltage produces. There may also be error fields produced by a non-ideal Ohmic heating coil (e.g., a finite-length central solenoid). Application of a simple 'free-drift' model shows that the length L for an electron staring at the center of a toroidal region with minor radius a_{eff} to drift to the wall is

$$L = a_{eff}\, B_T / B_\perp \qquad (2)$$

where B_T is the toroidal magnetic field, and a_{eff} is the distance to the wall along the direction of $B_\perp$. For avalanche growth, $\alpha L \geq 1$ is required. This is for an simple '0-D' drift model: comparisons of magnetic connection lengths with the connection lengths inferred from observations of the avalanche growth time (see [2]) and recent re-investigations of data from DIII-D and JET [7] show that

$$L_{eff} \cong 0.25 \cdot a_{eff}\, B_T / B_\perp \qquad (3)$$

gives a better estimate of the effective connection length for avalanche growth. The factor of 0.25 can be understood from the facts that not all electrons start from the initiation region center and that $B_\perp$ obtained in a typical multi-pole null increases more rapidly than r/a_{eff}. This means that the

effective radius of the startup region is somewhat smaller than the actual radius of the low-field 'breakdown' region.

For ITER startup with a 0.5-m radius null region positioned near the outboard limiter, the estimated $B_\perp$ is 0.002 T and the effective connection length from Eq (3) is ≥ 300 m. The E_{min} data for D_2 plotted in Fig. 1 shows that reliable ohmic initiation should be possible for pressures of about 10^{-5} torr, albeit with little additional margin beyond the experimental 'safety' factor of 4 (1/0.25) that is incorporated in Eq (3).

Since error fields arising from induced vessel currents tend to increase linearly with applied voltage, and since higher error fields (lower L) lead to a higher E_{min} (Fig. 1), a E $B_T/B_\perp$ requirement also arises. The empirical scaling for the allowable error field for reliable Ohmic breakdown in JET [8] is

$$E\ B_T/B_\perp \geq 1000\ V/m \qquad (4)$$

This requirement is marginally satisfied in ITER (see [9]). Startup assist relaxes the requirement significantly: the DIII-D EC-assist plasmas described in [2] obtain reliable startup at E $B_T/B_\perp$ ~ 150 V/m. In JT-60U E $B_T/B_\perp$ of ~300 V/m is obtained for plasma initiation with helium and LHRF heating [4].

3) Impurity Burn-through. It is well known that the survival of the plasma produced following initial breakdown and hydrogen ionization depends critically upon achieving subsequent ionization of low-Z impurities such as carbon or oxygen. Until these impurities (which can easily constitute 10% of the initial plasma ion density) become nearly fully ionized, they radiate strongly and hence prevent the plasma from heating to temperatures >100 eV where it is possible to sustain (and raise) the plasma current with reasonable applied voltages. The resulting (successful) transition to a nearly fully-ionized impurity state is termed 'impurity burn-though': failure to achieve full burn- through results in being unable to maintain the initial plasma current, and the discharge fails.

Reduction of the initial influx of wall-released low-Z impurities, especially oxygen, by wall-conditioning (see §8.1) is a primary consideration for startup optimization. Given that low-Z contamination is reduced to acceptable levels, the secondary requirement is to have enough plasma power input such that a favorable global power balance ($P_{in} > P_{ion} + P_{rad}$) is obtained following initial Townsend ionization. For ohmic startup, this requires sufficient loop voltage and in present tokamaks it is usually the 'ohmic burn-through' requirement that determines the applied startup voltage rather than the Townsend avalanche initiation voltage requirement. In ITER and reactor tokamaks, the option to apply enough voltage to attain ohmic burn-through is not available. In

addition, even when marginal ohmic burn-through is possible, the prolonged plasma current dwell period that follows Townsend avalanche initiation—during which the plasma temperature remains below 100 eV — results in resistive flux-consumption (resistive V-s loss) that can be avoided if higher input power can be provided (see e.g., [2] and [4]).

Simulations of ITER breakdown and impurity burn-through with a 0-D model [9] show that with a post-avalanche electron density of $n_e \approx 3 \times 10^{18}$ m^{-3} and no impurities, discharge survival without EC assist is marginal. With $n_e \approx 1.5 \times 10^{18}$ $m^{-3,}$ a beryllium impurity level of about 2% is tolerable without EC start-up assist. In contrast, with 2 MW of externally added power (e.g., EC), $n_e \approx 5 \times 10^{18}$ m^{-3} with up to 5% Be is tolerable. For 5% C,5 MW of absorbed power provides reliable startup. This calculations lead to an ITER requirement for 3 MW EC power for plasma startup assist. A 3-s pulse duration and two frequencies, ~90 GHz and ~110 GHz are specified to ensure that the EC power absorption radius falls within the cross-section of startup plasmas positioned on the outboard limiter for on-axis toroidal fields of 4.0-5.7 T [1]. In this regard, the DIII-D and JT-60U experiments show that for burn-through assist, it is (not surprisingly) essential to have the rf absorption region fall within the startup plasma boundary. In contrast, having an rf absorption resonance or absorption region anywhere within the torus volume is usually sufficient to facilitate Townsend breakdown assist.

4) Suppression of Runway Electron Generation: Runaway electron generation is possible during low voltage plasma initiation because low prefill gas pressure is required. High electron temperature at low prefill pressure is claimed to generate runaway electrons [2] because the cross-section for collisions between electrons and hydrogen becomes small at T_e > 4-5 eV and high energy electrons can gain energy from the applied electric field between collisions. The threshold condition of runaway electron generation is proposed as [4]:

$$E/p > (2\text{-}2.5) \times 10^4 \ \mathrm{Vm^{-1}torr^{-1}} \qquad (5)$$

However runaway electron generation was not observed for E/p of ~8 x 10^4 $Vm^{-1}torr^{-1}$ in JT-60U even in the presence of super-thermal electrons (at the energy range of 80~200 keV) during LH heating [4]. The possible causes are: *i*) lower resistive electric field than the Dreicer field at a high electron temperature of ~100 eV, ii) not enough time for the super-thermal electrons to be accelerated to runaway energies and *iii*) magnetic fluctuations during plasma initiation (see §3.4.4).

In summary, the physics design considerations embodied in categories 1) - 4) above have been evaluated for ITER and ohmic/inductive plasma initiation by Townsend avalanche in 10^{-5} torr D_2 gas with an applied electric field of 0.3 V/m is found to be feasible. Acceptably low error fields, ~0.002 T, for such startup can be achieved in a 0.5-m radius multi-pole field null positioned near

the outboard limiter. The planned addition of 3 MW of EC assist power that is resonant in the startup plasma will both facilitate reliable breakdown over a wider range of error field and pressure conditions and also reliable impurity ionization following initial Townsend+EC assisted breakdown. Substitution of He for D_2 as the initial filling gas is also projected to provide a further margin for reliable plasma initiation.

8.2.3.2 Plasma current ramp-up

Initial breakdown and impurity burn-through in present medium- and large-size tokamaks typically results in an initial plasma current of 20-100 kA. The corresponding initial current in ITER at 1 s after initiation will be about 0.5 MA [9]. In all cases, a further increase of the current is required to obtain the 'flattop' current (21 MA in ITER) needed for full plasma performance. This increase is typically accomplished by a more-or-less linear (versus time) ramping up of the plasma current. In addition, in elongated cross-section tokamaks with divertors, and in ITER, the current ramp-up phase is accompanied by a plasma elongation increase and/or cross-section expansion that includes a transition from an initial limiter-defined low-current startup plasma to a final full-current/full-cross-section divertor-defined plasma. Figure 2 illustrates the current ramp-up and plasma cross-section expansion sequence proposed for ITER.

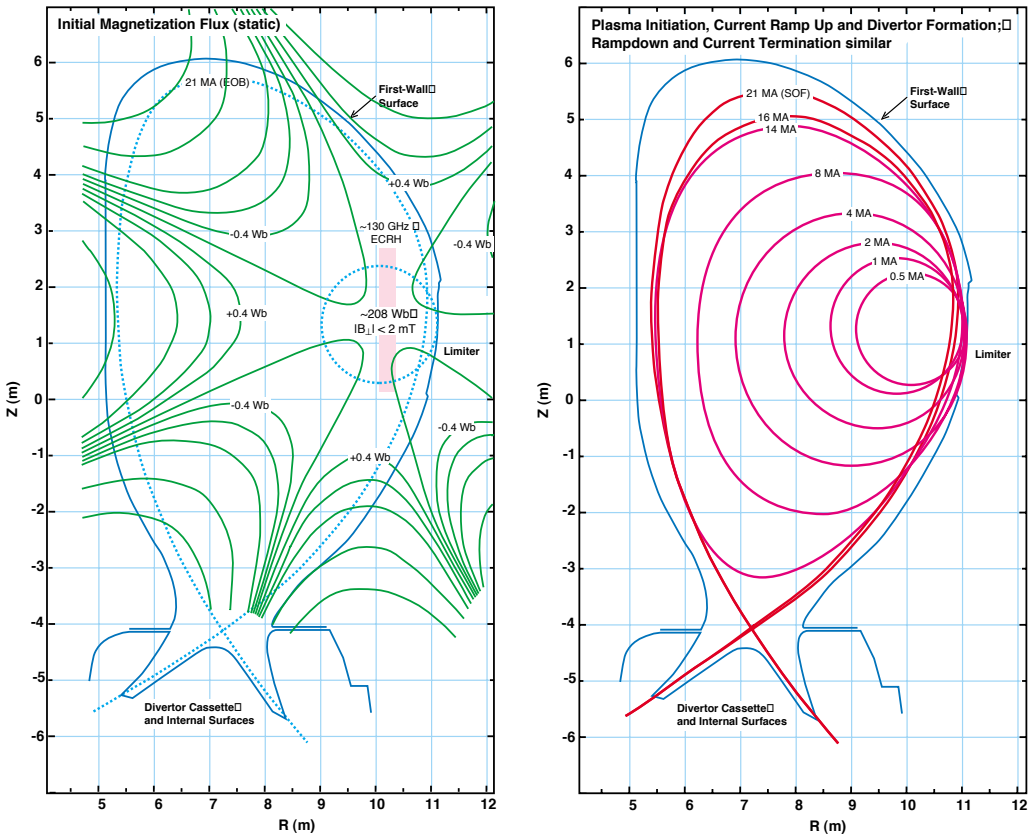

FIG. 2. Plasma inititation and current ramp-up configurations in ITER [1].

There is usually some increase of plasma density—typically effected by gas injection, see §8.2.2—during the current rise. While this portion of the plasma scenario is typically described as the 'current ramp-up' phase, in present divertor tokamaks it actually involves a rather carefully coordinated sequence of plasma current increase, magnetic configuration development and plasma densification that ensures that the various MHD and kinetic/power balance operational limits that govern plasma stability, confinement and power and particle exhaust are successfully skirted. During this process, it is also usually necessary to implement a ramp-up strategy that avoids unnecessary plasma resistive loss (resistive volt-second consumption) and thus arrive at the final flattop current state with a PF flux variation reserve for inductively sustaining the plasma current through the balance of the scenario.

The principal physics and plasma operation considerations that enter into the design of the current ramp-up phase of the scenario are 1) MHD stability, 2) plasma densification, and 3) resistive flux (resistive V-s) consumption . In addition, is of course necessary for the PF coil system to provide 1) the one-turn voltage needed to raise the current, 2) 'slow' quasi-static equilibrium control to achieve the desired plasma configuration evolution and 3) 'fast' dynamic equilibrium control to stabilize the plasma vertical position and compensate for the effects of

plasma disturbances (minor disruptions, ELMs, etc.) that occurr during the current ramp-up. These plasma magnetic control matters are addressed using the same PF system design procedures and control methods described in Section 8.2.1. There implementation is a matter of engineering design and suitable dynamic control of the PF power supplies: there are no true physics issues in this implementation. For ITER, there are, however, important practical and cost issues for the PF system that arise from having to meet physics requirements and hence the final ITER current ramp-up scenario design represents a careful optimization among consideartions of meeting fundumental physics requirements, providing operational flexibility (current ramp rate and shape evolution variation) and minimizing PF system costs (total coil ampere-turn capability and installed power). Similar 'non-physics' considerations apply in at least some degree to scenario designs and capabilities in present tokamaks. Discussion of these design-specific considations is largely beyond the scope of this Section. Presentation of some of the 'non-physics' design considerations for ITER will be found in Ref. [1].

The more generic physics issues that apply to the design of the current ramp-up phase in present tokamaks and ITER are addressed below.

MHD Stability and Operation Limits During Current Ramp-up. The immediate requirement is to achieve current ramp-up without encountering a major disruption. As is presented in Chapter 3, there are two causes of major disruption, *i*) growing internal MHD instability, and *ii*) density limit/plasma-edge radiation power balance initiated current profile peaking. During plasma current ramp-up, resistive tearing mode instability (double tearing modes) that produces transient magnetic reconnection localized at the q = m/n rational surface is the principal potential category *i*) trigger for major disruption. This type of instability develops if the plasma current density profile becomes too broad and is thus associated with low values of the dimensionless plasma internal inductance l_i. In contrast, too-high values of the plasma density, which lead to excessive plasma edge cooling, current profile shrinkage and hence high values of l_i result in category *ii*) 'density limit' disruption.

The experimental manisfestation of these two constraints on plasma operation is embodied in the well-known l_i-q operation space diagram, as illustrated for JET in Fig. 3. As the Figure shows, sucessful ramp-up requires negotiating a trajectory in the l_i-q domain that avoids the lower 'sawtooth-like' tearing mode internal instability boundary and the upper density-limit edge power balance boundary. The essential requirement is to maintain the internal inductance between about 0.8 to 1.2, with a final refinement to 0.9-1.0 near q = 3. The principal experimetal means to control the inductance are current ramp rate (higher dI/dt reduces inductance; lower dI/dt raises inductance) and gas injection, which both directly controls the density and also cools the edge, thus raising the inductance. These 'control means' lead to the well-known strategy for successful ramp-up that combines a gradually decreasing rate of current rise with carefully-controlled gas injection that suppresses edge current without unduly raising the plasma density. Greater precision in

controlling the startup trajectory is needed near rational q values, especially q = 3, where the range of allowable l_i is relatively small.

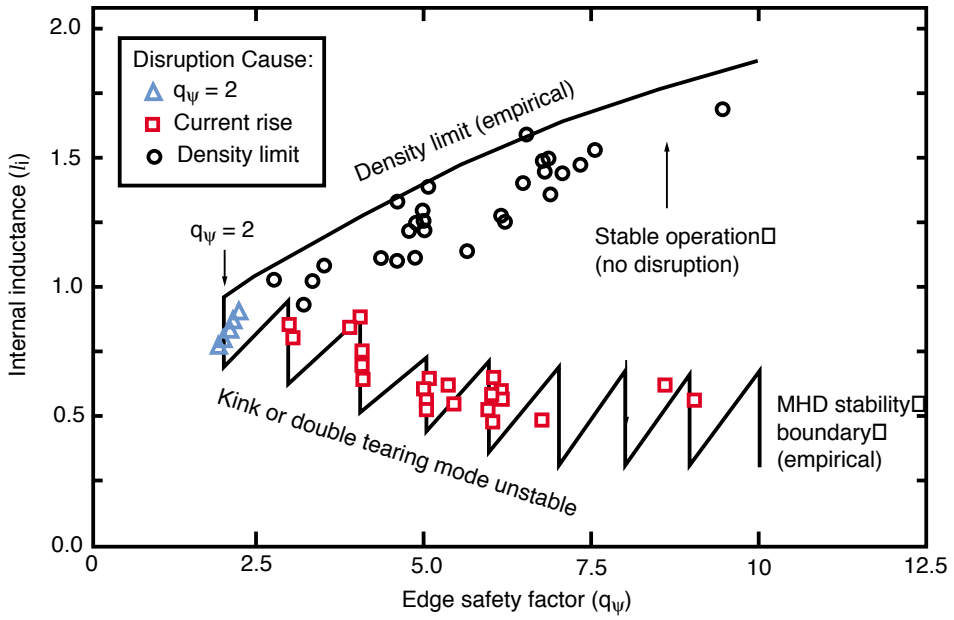

FIG. 3. Empirical stability diagram for JET, with cause of MHD activity or disruption indicated. Data and empirical limit boundaries reproduced from [10].

Double tearing mode instabilities occur during current ramp-up at low l_i when the ramp rate is excessive. When q_a passes a rational value, strong growth of a tearing mode with $m/n=q_a$ is observed. The mode growth rate is sufficently fast that it can lock toroidally, often with a toroidal phase determined by error fields (see §3.2.5) and be preserved during the rest of discharge, where it can ultimately produce a disruptive termination. Increase in l_i is essential to avoid this type of problem. As has been noted above, inductance control by gas-puffing has been demonstrated in many tokamaks, and current profile control by LHCD, and by the use of an ergodic divertor has been demonstrated in Tore Supra [11]. The use of NBI—which provides toroidal rotation drive—to avoid mode locking has been demonstrated in JT-60 [12] and other tokamaks.

The tearing mode stability boundaries plotted in Fig. 3 are semi-empirical and hence provide an indictative rather than definitive characterization of the actual stability boundary, which must ultimately be determined during experimental operation. However, data presentations like that shown in Fig. 3 can provide useful guidence in ascertaining an optimal start-up strategy and also serve as a basis for an ‘intelligent’ startup plasma kinetics control system (see §8.2.2) and for a disruption proximity indication and avoidance system (see §3.4.6).

Tearing mode instabilities can also lead to minor rather that major disruption and hence are not always fatal with regards to obtaining successful plasma current ramp-up. Occurance of one or more minor disruptions during current ramp-up is common and usually permissible, although it tends to increase resistive V-s consumption (see below). It is, of course, essential that the plasma control system be able maintain equilibrium control during the temporary drop of plasma energy and pressure that minor disruption produces (see §8.2.1).

The rate of current rise that can be obtained in a large-minor-radius plasma with appreciable edge temperature is limited by the tendency of current to concentrate at the plasma edge and lower l_i excessively. However, this difficulty can be minimized by using a [nearly]-constant-q ramp-up scenario wherein the minor plasma radius is gradually increased, adding a new current-carrying layer around the original high-temeprature plasma core without decreasing l_i. This type of expanding cross-section scenario is illustrated in Fig. 2. Current ramp-up rates of up to 2 MA/s have been obtained in JT-60U with this method [13]. This rate can be contrasted with the rate of ~0.5 MA/s that is more typically used in 'full radius' JT-60U or JET plasma current rampup.

Figure 4 illustrates a simulation of the ITER plasma current rise phase implemented with the expanding radius/increasing elongation configuration expansion sequence illustrated in Fig. 2. The initial dI/dt is 0.2 MA/s. Current ramp rate decreases as the ramp-up continues, ultimately falling to 0.05 MA/s prior to attainment of current flattop. An instability-free trajectory through l_i-q space is achieved at start-of-current-flattop (SOF) and maintained during the DT burn phase (SOB to EOB). Following end of burn, the internal inductance rises but remains within acceptable limits (to avoid density limit disruption) during the plasma current rampdown (see §8.2.3.3 below).

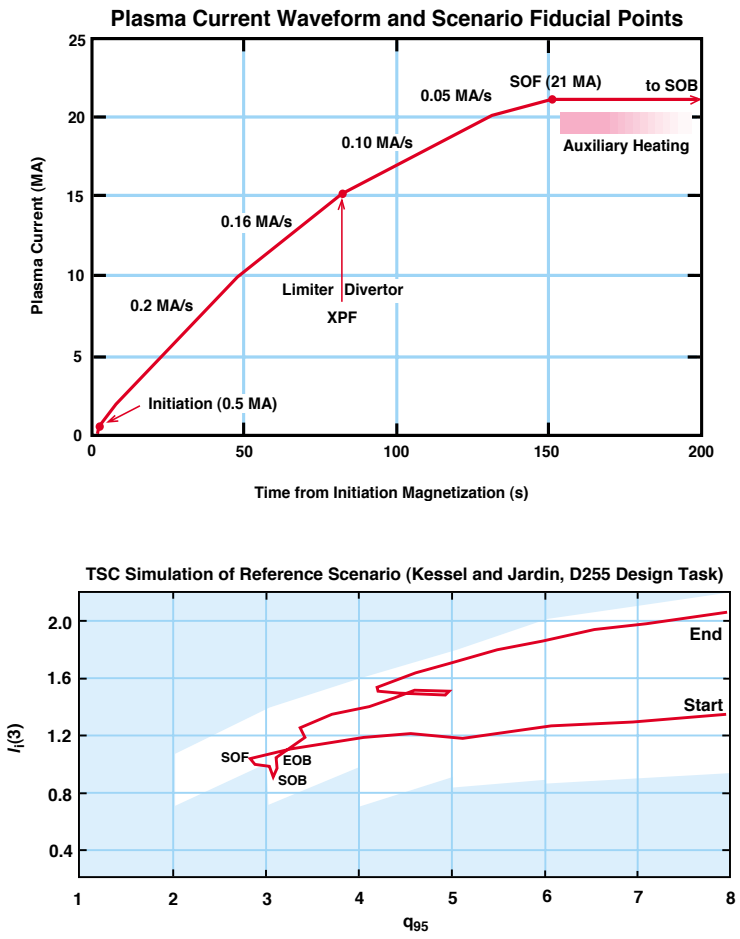

FIG. 4. Waveform for ITER plasma current rampup to start-of-flattop (SOF) and simulation with a Tokamak Simulation Code plasma scenario model of the resulting trajectory in l_i-q space. The simulation also shows the l_i-q variation during the ignition, burn and current rampdown phase. TSC Simulation by C. Kessel and S. Jardin for the ITER Joint Central Team [1].

In a given tokamak there is an optimal current rampup time asnd/or current rise waveform that results in reaching a fully-penetrated quasi-stationary equilibrium current profile at the end of the rampup with near-minimum resistive V-s consumption (see following). Slower current ramps increase resistive losses and hence are undesirable; faster ramps can achieve current 'flattop', albeit with a broadened non-equilibrium profile, with decreased inductive and resistive flux consumption. However, the 'flux savings' produced by this strategy are ultimately expended when the current profile finally equilibriates, and the use of auxilary heating during current rampup serves only to delay rather than reduce ultimate resistive V-s consumption. In contrast, non-inductive current drive during rampup can reduce net volt-second consumption and also relax the requirement for fast plasma current ramp-up. In JT-60U the plasma-current start-up from the

plasma breakdown to 1 MA plasma current with a rate of ~0.2 MA/s has been demonstrated using a low electric field of ~0.1 V/m [4].

Resistive Flux Consumption. The plasma resistive flux consumption ($\Delta\Psi_{res}$) during the current ramp-up phase is an important scenario design basis consideration. Here the underlying physics basis is well understood: there is a irreducible minimum resistive (Poynting formalism) flux consumption that is described by empirical "Ejima" formula:

$$\Delta\Psi_{res}=C_{Ejima}\mu_0 R_0 I_p \qquad (6)$$

where C_{Ejima} is a coeficient depends weakly on the precise details of the evolution of the plasma profile quantities such as the impurities and the electron temperature, and R_0 is the plasma major radius. The theoretical minimum value of C_{Ejima} is about 0.4 for a q = 3 plasma and for design purposes, C_{Ejima} = 0.45 constitutes a practical estimate of the minimum flux consumption. Figure 5 shows the data that support this basis: flux consumption for q = 3 plasmas typically falls in the range $0.4 \le C_{Ejima} \le 0.5$.

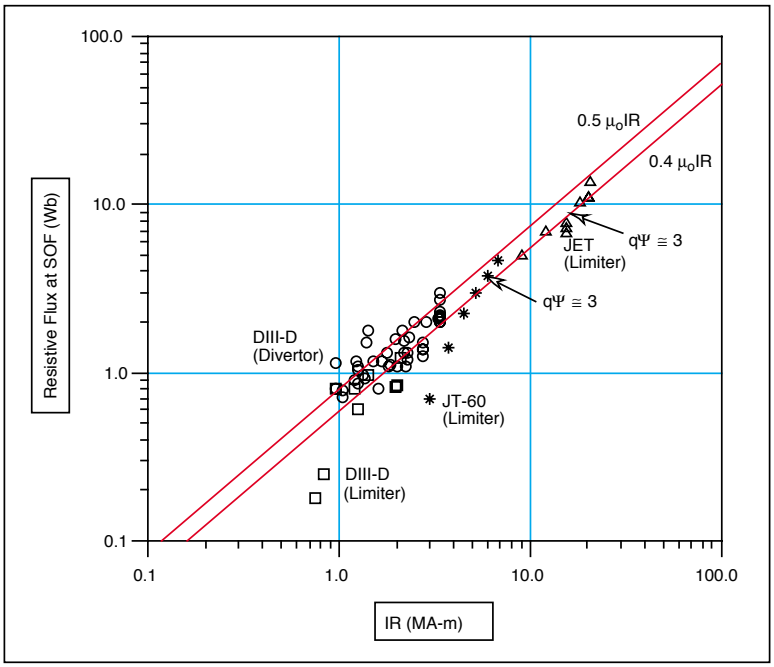

FIG. 5. Resistive flux consumption in various limiter and divertor tokamaks at start of current flattop.

Greater-than-minimum flux consumption can occur in situations where the current ramp rate is too slow and excessive resistive losses accumulate. Greater-than-minimum resistive loss (C_{Ejima} > 0.45) can also occur in large tokamaks (ITER) in startup situations with a non-optimal minor

radius expansion. Finally, it is worth noting that adding auxiliary heating during current ramp-up does *not* reduce the total resistive loss that is accrued when a fully-penetrated current profile (i.e., l_i ≅ 0.9 for a q = 3 plasma) is achieved. Heating does delay the accrual of full resistive loss and of course the time to achieve full current profile equilibration.

8.2.3.3 Plasma current ramp-down

Two types of disruptions are observed during the plasma current ramp-down and they can be presented in the Hugill diagram in Fig.3 [14]. One is the disruption which is seen to occur close to or even above the Greenwald density

$$n_{GW} = I_p/\pi a^2 \ [10^{20}, \text{MA, m}].$$

The other disruption occurs at very low density and is observed at high l_i (see Fig.1) and occurs at densities below 0.2 n_{GW}. Thus there is a wide density window of 0.2 to 1.0 n_{GW} to get a stable plasma ramp-down for hydrogen plasmas. These two types of disruption are caused by the same tearing instability due to the peaking of the current profile. The following three methods have been demonstrated for obtaining stable ramp-down:

- The plasma minor radius is decreased to suppress the increase in l_i during the plasma current ramp-down. This is the method that is used conventionally on non-circular tokamaks, together with a small ramp-down rate;

- MHD instability is excited by external helical fields to reduce the increase in l_i during ramp-down, which has avoided high l_i disruption [15];

- The density window can be expanded by further heating and/or an intense helium puffing. The density limit of the helium plasma during the plasma current ramp-down is about two times higher than that of the hydrogenic plasma (see Fig.3), and the maximum ramp-down rate of -6 MA/s was obtained from 2 MA to 0 MA [16]. The reduction of the charge exchange loss is considered to be a possible cause of the higher density limit for helium plasmas. This method relies on fast positional control of the plasma at the neutral point.

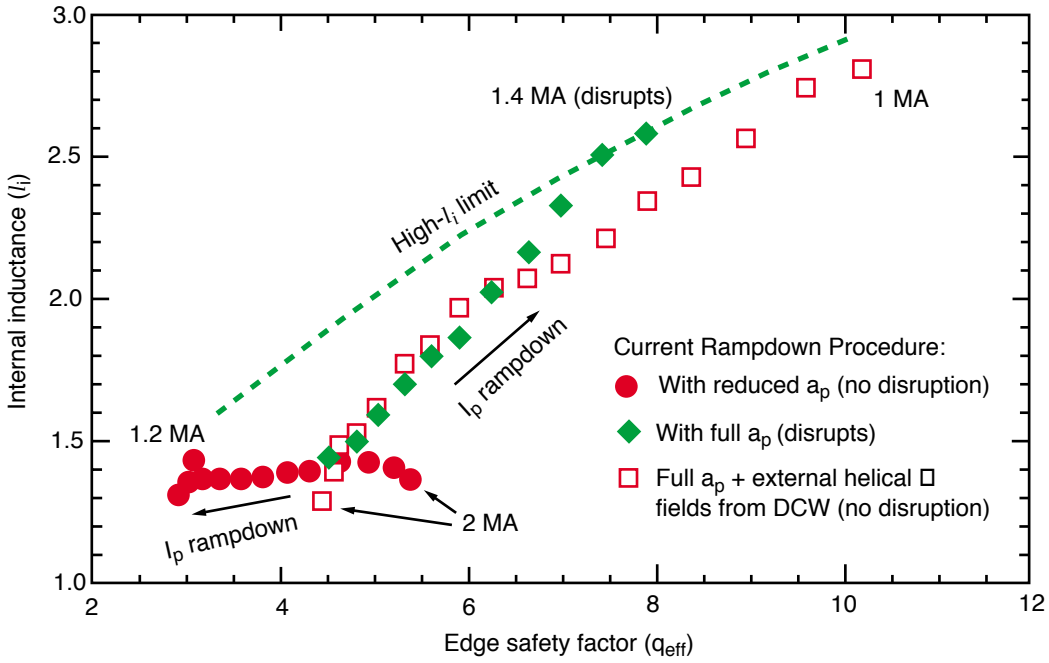

FIG. 6. Comparison of plasma current shutdown trajectories in l_i-q space *(cf.* Figs. 3 and 4) in JT-60U with 'standard' full-minor-radius current rampdown down procedure (disrupts owing to high l_i), with minor radius contraction (disruption avoided), and with standard rampdown with external helical fields added (l_i decreased, disruption avoided).

8.2.3.4. Fast plasma shutdown: requirements and options

Normal plasma shutdown in ITER from a current of 21 MA requires approximately 200 s to complete: this shutdown time is set by both the current rampdown rate limitations necessary to avoid a high-l_i disruption and by the time required to exhaust the plasma particle inventory in a well-controlled manner. Current shutdown in shorter times is projected to lead to disruption and the voltage capabilities of the ITER PF system limit more-rapid current shutdown to about 50 s. Fast shutdown for purposes of machine protection or other plasma operation need will require some form of impurity injection to enhance plasma radiation cooling and current rampdown. Massive deuterium or helium gas injection, liquid-hydrogen-jet injection or solid low-Z pellet injection (D_2, Li, Be....) are proposed as candidates for fast plasma energy and current shutdown in ITER (see §3.4.5). All of these means appear to be capable of rapidly terminating a full-performance ITER plasma in a few seconds or less. However, to what extent such shutdown can be radiative rather than disruptive, to what extent vertical instabilities and halo currents during

shutdown can be avoided and to what extent significant runaway electron current conversion during shutdown can be avoided are all matters of on-going study for reactor-scale tokamaks and ITER. These matters, especially the concerns about runaway conversion, are more-fully discussed in §3.4.5.

8.2.3.5. ITER scenario concept and simulations

Plasma operation in ITER will be conducted within the framework of an inductively-driven and controlled plasma operation scenario. The scenario concept is identical to that employed in the present generation of shaped-cross-section divertor tokamaks. Figures 7 and 8 illustrate the overall scenario concept and show a summary of the plasma current/shape/configuration evolution that the scenario will incorporate.

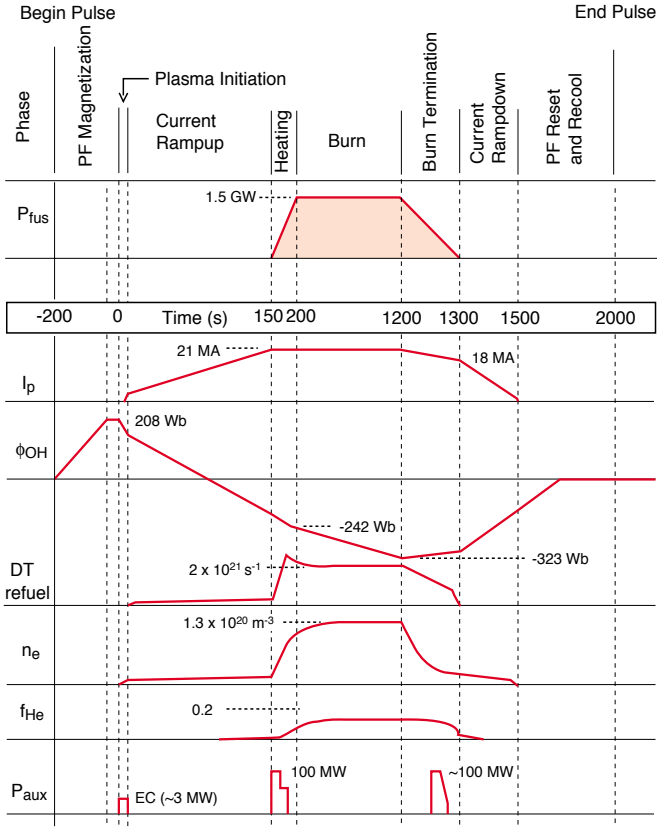

FIG. 7. Plasma operation scenario waveforms for 1.5-GW inductively-sustained ignited burn in ITER.

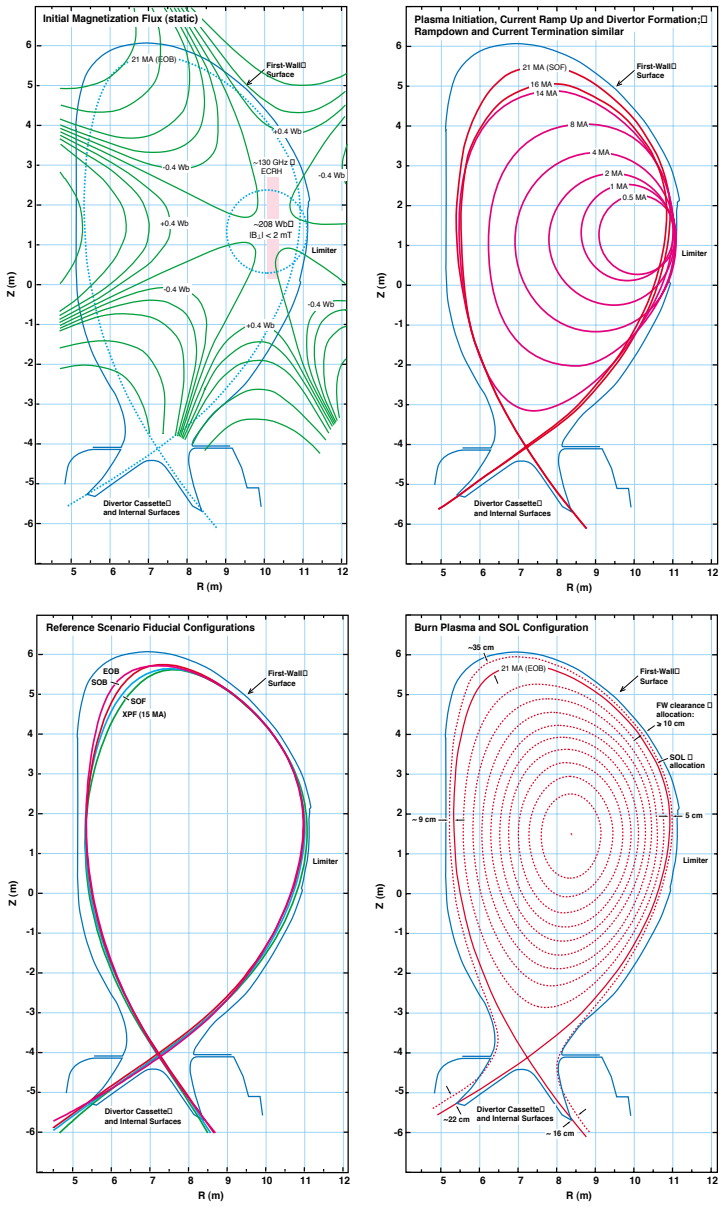

FIG. 8. Plasma configurations and configuration evolution for the 21-MA sustained-ignition scneario shown in Fig. 7.

Features of the scenario include *i)* a 530 Wb PF system flux swing, *ii)* inductive plasma initiation (Townsend avalanche breakdown with EC assist) in a high-order multipole field null positioned near the outboard port-mounted limiter, *iii)* minor radius and elongation expansion of the startup plasma on the limiter prior to divertor formation at I_p ~15 MA, and *iv*) maintenance of a well-controlled single-null divertor configuration during the heating/burn/burn-termination phases. Burn terminastion occurs in a diverted configuration to allow the plasma particle inventory to be exhausted by the divertor pumping. Current termination is effected following burn termination with

a minor radius and elongation contraction on the limiter. The configuration evolution sequence during current ramp-down is the reverse of the ramp-up evolution. Final current termination occurs in a circular plasma on the outboard limiter.

Simulations of the plasma startup and shutdown dynamics show that MHD stability (trajectory in the q-l_i domain) and the edge plasma power balance needed to avoid a density-limit disruption are satisfied with acceptable margins (Fig. 4). The resistive flux (volt-second) consumption during the startup and current rampup phase falls within the physics design basis of $0.45\mu_0 R_o I_p$ ($\cong$ 100 Wb) and $\geq$ 80 Wb of PF system flux swing will be available for sustaining the 21-MA plasma current during fusion burn. For the estimated burn-phase plasma resistive voltage, this flux swing will provide a 1300-s burn.

The scenario design basis is predicated upon a 'reference case' plasma with I_p = 21 MA, β_p = 0.9 and $l_i(3)$ = 0.9. The sizing of the PF coils and power supplies allows equilibrium control and in most cases $\geq$1000-s inductively-sustained burn to be obtained for 21-MA plasmas with $0.7 \leq \beta_p \leq 1.2$ and $0.7 \leq l_i \leq 1.1$. Operation at 24 MA ($q_{95} \cong 2.6$) with $\beta_p \cong 0.8$ and $l_i \cong 0.8$ (1.5 GW fusion power) is also feasible. Inductively-sustained burn at 24 MA is about 500 s. The scenario will also support operation with ohmic and auxiliary-heated DD plasmas during initial plasma commissioning, and extended-pulse inductively sustained driven-burn operation with reduced plasma current (e.g., 6000 s burn at ~1 GW with I_p = 17 MA and 100 MW H/CD power). True steady-state operation may also be possible with a reversed-shear plasma at I_p ~12 MA (see §3.2.7 and §8.2.4). The trade-off that exists among plasma current, scenario basis (ignited, driven-burn, non-inductive steady-state) and burn duration is summarized in Fig. 9. As the Figure demonsotrates, the scenario capbilities span a range of plasma currents from 12-24 MA and burn durations from 500 s to steady-state. There is also a general tendency for the longer-duration driven and steasdy-state scenarios to require 'enhanced' confinement ($H_{H>1}$) and beta limit ($\beta_N > 2.2$) performance relative to the performance required for nominal 21-MA igntion in ELMy H-mode.

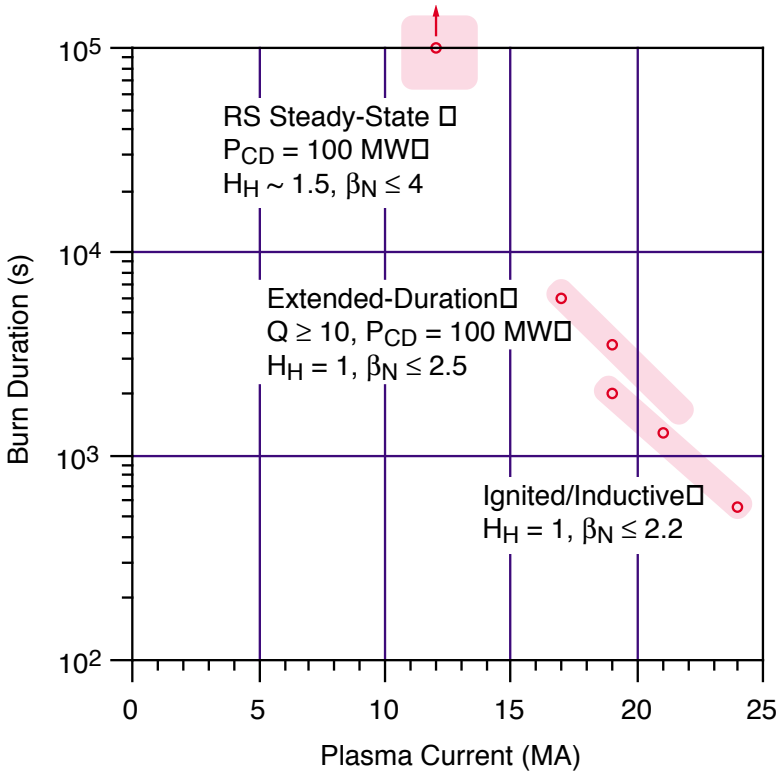

FIG. 9. ITER plasma operation scenario capabilities.

References to Section 8.2.3

[1] ITER-JCT, Technical Basis for the ITER Final Design Report, Cost Review and Safety Analysis (FDR), to be published by the IAEA (1998).

[9] Lloyd, B. P. G. Carolan, C. D. Warwick, ECRH-Assisted Startup in ITER, Plasma Physics and Contr. Fusion **38** (1996) 1627-1643.

[2] Lloyd, B. , G. L. Jackson, T. S. Taylor, E. A. Lazarus, T. C. Luce, R. Prater, Low voltage ohmic and electron cyclotron heating assisted startup in DIII-D, Nucl. Fusion **31** (1991) 2031-2053.

[3] Jobes, F. et al., Phy. Rev. Lett. **52** (1984) 1005.

[4] Yoshino, R., M. Seki, Low electric field (0.8 Vm^{-1}) plasma-current start-up in JT-60U, Plasma Phys. Control. Fusion **39** (1997) 205-222.

[5] Koch, R., et al., 16th IAEA Fusion Energy Conf., Montreal, (1996) IAEA-CN-64/AP1-6.

[6] Engel, A. Von., Ionized Gases (2nd edn) (1965) Clarendon Press, Oxford.

[7] Lloyd, B., Breakdown in ITER, ITER-EDA Technical Meeting, Naka, April (1993).

[8] Tanga, A., et al., in Tokamak Start-up (Knoepfel, U., Ed.) Plenum Press, New York (1986) 159.

[9] Lloyd, B. et al., Plasma Physics and Contr. Fusion **38** (1996) 1627.

[10] Wesson, J., R. D. Gill, H. Hugon F. C. Schüller, et al., Disruptions in JET, Nucl. Fusion **29** (1989) 641-666.

[11] Edery, D., et al., Proc. 14th Int. Conf. on Plasma Phys. and Contr. Nucl. Fus. Res., Würzburg, **1** (1993) 279.

[12] Ninomiya, H., et al., Nucl. Fusion **28** (1988) 1275.

[13] Schüller, F. C., A. A. M. Oomens, Fusion Engineering and Design **22** (1993) 35.

[14] Yoshino, R., et al., J. of Plasma and Fusion Research **70** (1994) 1081.

[15] Yoshino, R., et al., Proc. 14th Int. Conf. on Plasma Phys. and Contr. Nucl. Fus. Res., Würzburg, **1** (1994) 685.

[15.1] Yoshino, R., N. Hosogane, Y. Neyatani, S. W. Wolfe, S. Miura, A. Tanga, Y. Kamada, H. Ninomiya, D. J. Campbell, K. Ushigusa, T. S. Taylor, M. Matukawa, H. Shari, JT-60 Team, Disruptions and stable plasma shutdown in JT-60U, in Plasma Physics and Controlled Nuclerar Fusion Research 1992 (Proceedings 14th IAEA Conference Würzburg), IAEA Vienna (1995) **Vol. 3** 405-414.

[16] Yoshino, R., et al., Nuclear Fusion **33** (1993) 599.

8.2.4. Control of the Current and Pressure Profiles

This Section deals with the control issues of the current- and pressure-profile-modification plasma operation regimes described in §3.2.7, wherein modification of the current density profile is an enabling basis for the subsequent formation and sustainment of a radially-localized heat transport barrier, usually described as an internal transport barrier or ITB. The resulting reduction in overall transport in the plasma core gives such regimes enhanced energy confinement relative to otherwise-similar plasmas lacking the transport barrier, and because of such enhancement, such regimes are frequently described in terms of the achievement of 'advanced performance' or 'advanced tokamak' operation [1]. Present examples this type of plasma operation are the transient regimes with optimized magnetic shear as obtained in DIII-D [2], TFTR [3], JET [4] and JT-60U [5], and the steady-state lower hybrid current drive (LHCD) sustained hot-electron LHEP mode in Tore Supra [6] and similar steady-state LHCD-sustained optimized-shear plasmas in JT-60U [7].

These 'advanced-performance' regimes in present tokamaks are characterized by formation of a transport barrier at a radius between 1/3 and 2/3 of the discharge minor radius. This transport barrier sustains a large pressure gradient and provides the confinement enhancement. In some cases 'enhanced' MHD stability—as manifested by values of normalized beta [$\beta_N = \langle\beta\rangle$(%)a(m)B(T)/I(MA)] that exceed the corresponding 'wall-at-infinity' ideal MHD stability limit $\beta_N = 4l_i$, where l_i is dimensionless internal inductance (see §3.2.1)—are also obtained. The confinement and MHD stability enhancement aspects of such modified-shear and barrier-enhanced operation regimes are addressed respectively in §2.3.4 and §3.2.7. This Section deals with the operational means how the shear reversal and transport barrier is established and controlled. As a prelude to the control discussion that follows, it is important to understand that this type of plasma operation constitutes an 'emerging subject' both in terms of physics understanding and in terms of experimental implementation, particularly implementation of control in the formal sense, wherein shear profile and/or barrier characteristics are actively controlled by non-inductive means rather than passively established on a transient basis by inductive means.

8.2.4.1. Candidate parameters for 'Advanced Performance' operation in ITER

Two distinct applications for 'advanced performance' operation in ITER can be foreseen, and these applications parallel the two ways in which advanced performance is being implemented in present tokamaks. The first application is the achievement of 'advanced performance' operation on a transient basis by inductive means (current ramping) to provide enhanced confinement to facilitate the attainment (in ITER) of ignition or high-Q driven burn, perhaps at lower-than-normal plasma current. Here transient denotes operation that can be sustained for at least several plasma

energy confinement times (typically > 10 s in ITER) and ideally, for times that are comparable to the thermal He equilibration time (typically about 100 s in ITER). Here the size and temperature of an ignited or near-ignited plasma in ITER are such that the magnetic relaxation time (the time for current profile equilibration) will be about 500 s, so even 'transient' advanced performance established by current ramping will make it possible to achieve quasi-stationary ignition or driven burn operation and allow study of energy and particle transport effects on a quasi-stationary basis and meaningful investigation of He build-up and removal.

The second application of 'advanced performance' operation for ITER lies in the achievement of true steady-state plasma operation, wherein the plasma current is sustained wholly by non-inductive means (non-inductive current drive plus bootstrap current). Here, as is summarized in Table 8.2.4-I, self-consistent reverse-shear plasma operation scenario analysis that includes generic consideration of likely plasma temperature and density profiles and achievable current-drive efficiencies shows the *possibility* (in a parametric sense) of obtaining non-inductively-sustained steady-state operation in ITER with a plasma current of approximately 12 MA and a bootstrap current fraction (I_{BS}/I_p) that is typically ≥ 80% (i.e., I_{bs} ≥10 MA) [8].

TABLE 8.2.4-I: Advanced Steady State Operating Modes in ITER

Parameter	Fully Optimized	H-Mode-Like Density Profile	Low Density Reversed-Shear
P_{fusion} | P_{CD} (MW)	1500 | 100	1500 | 100	1000 | 100
Q_{CD}	15	15	10
Ip (MA) | q_{95}	12 | 4.95	12 | 4.95	12 | 4.95
R_0 | a (m)	8.66 | 2.32	8.66 | 2.32	8.66 | 2.32
$\kappa_{95\%}/\delta_{95\%}$	2.00 | 0.44	2.00 | 0.44	2.00 | 0.44
f_{BS}	94%	79%	71%
γ_{cd} (10^{20} A/W-m^2)	0.06	0.21	0.21
β_N | $\beta_{toroidal}$	2.9 | 2.8%	3.8 | 3.7%	3.6 | 3.5%
$\langle T_e \rangle_n$ | T_{eo} (keV)	10.2 | 18.1	12.5 | 25.9	15.8 | 32.9
$\langle n_e \rangle$|n_{eo} (10^{20} m^{-3})	1.0 | 1.7	1.0 | 1.1	0.71 | 0.78
$\langle n_e \rangle/n_{GW}$	1.4	1.4	1.0
τ_E (s)	2.35	2.46	2.84
$\tau_E/\tau_{ITER93\text{-}H}$	1.05	1.22	1.26
$\tau_E/\tau_{ITER89\text{-}P}$	2.0	2.26	2.38

The parameters given in Table 8.2.4-I are predicated on a reduced-minor radius reverse-shear plasma configuration with increased elongation and triangularity (e.g., Fig. 8.2.4-1). Such plasmas can be produced in ITER by shifting the plasma radially outwards relative to the normal full-sized ITER plasma equilibrium (*c.f.* Fig 8.2.1-1) and are well matched in terms of separatrix configuration to the ITER divertor geometry. Poloidal field system and fast-alpha-particle toroidal-ripple-loss calculations show that such plasmas have acceptable vertical position control and ripple-loss characteristics. The plasma shown in the Figure is not ideally suited for operation scenarios in which a gap-sensitive rf launcher is involved, but are variants of the configuration illustrated in Fig. 8.2.4-1 that also have acceptable plasma-to-first-wall conformity in the outboard midplane region. Such conformity will be needed if a gap-sensitive rf current-drive scheme (ion-cyclotron or lower hybrid) is to be used.

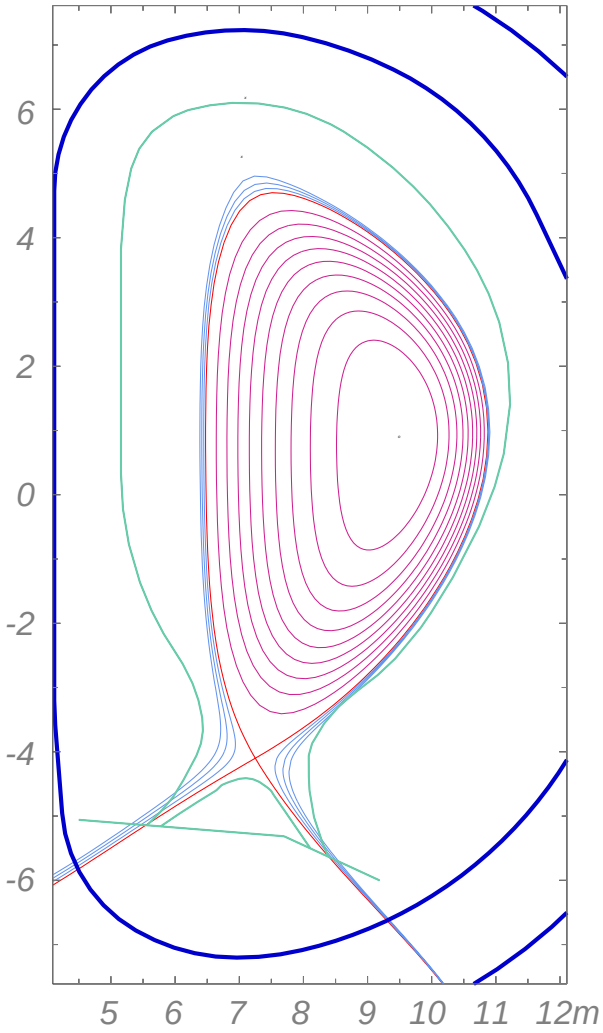

FIG. 8.2.4-1. A 12 MA ITER reversed-shear equilibrium which is feasible from the point-of-view of both fast-alpha ripple losses and vertical control.

The results summarized in Table 8.2.4-I are based upon assumed plasma density and temperature (and hence pressure) profiles. Both fully-optimized profiles and 'H-mode-like' density and temperature profile cases are examined. Figure 8.2.4-2 shows the respective profiles: the optimized profiles are L-mode-like in the edge region; the H-mode profiles have nearly flat density and an edge temperature pedestal.

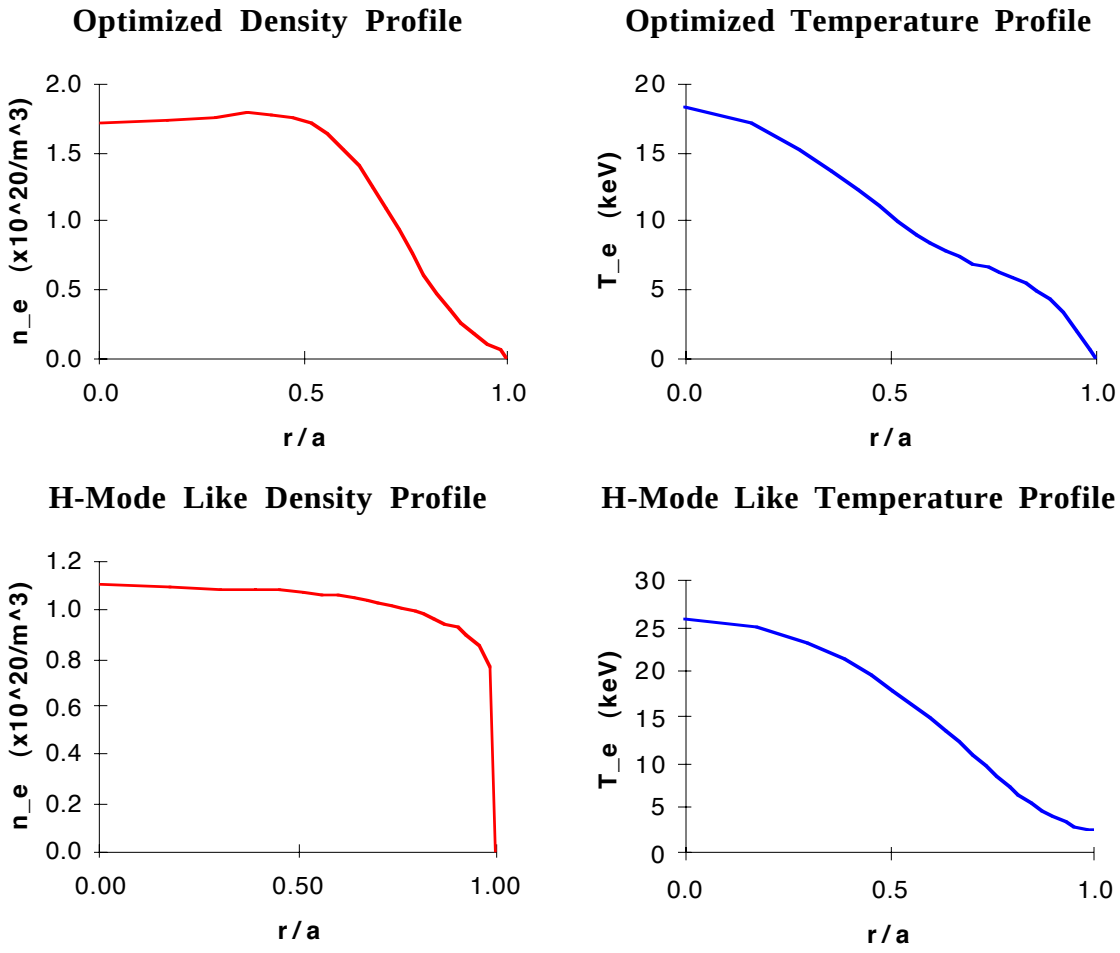

FIG. 8.2.4-2. Density and temperature profiles assumed for the optimized-profile and H-mode-like profile cases in Table 8.2.4-I.

The different profile assumptions lead to substantially different bootstrap current profiles and corresponding differences in the non-inductive current drive requirements (Fig. 8.2.4-3). The optimized profiles lead to excellent bootstrap current alignment (radial match to the total current profile): the H-mode profiles require more off-axis current drive and also some reverse current

drive at the plasma edge. Bootstrap current alignment is not as favorable as the optimal-profile case and the current-drive efficiency requirement is about 3 times higher than for the optimal profile case.

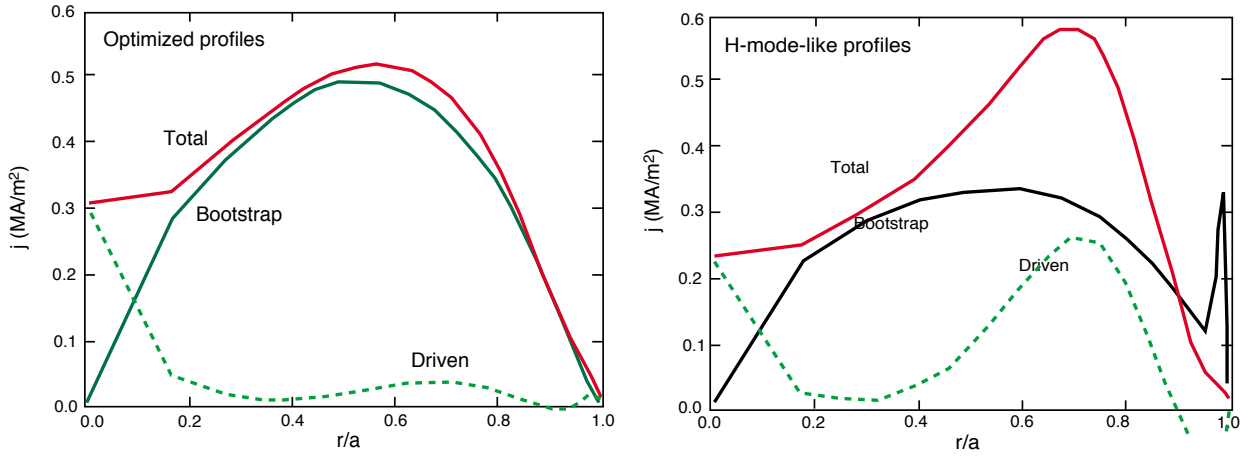

FIG. 8.2.4-3. Current density profiles for the optimized and H-mode-like density/temperature profiles in Fig. 8.2.4-2. Note the higher off-axis current drive requirement and the negative edge current drive needed for the H-mode-like case.

In Table 8.2.4-I, a total of 100 MW of auxiliary power is assumed be available to both heat and drive current. The required current-drive figure-of-merit, γ_{CD} is computed for each case using the formula

$$\gamma_{CD} \equiv \langle n_e \rangle I_{CD} R_0 / P_{CD} \ ,$$

where $<\langle n_e \rangle$ is the volume-averaged electron density, I_{CD} is the current which must be driven non-inductively, R_0 is the major radius of the plasma, and P_{CD} is the power available to drive the current. In the scenario with H-mode-like profiles a current drive figure-of-merit of $\gamma_{CD} \geq 0.21 \times 10^{20}$ A/W-m^2 is required Such values of γ_{CD} have been achieved with lower hybrid current drive, and are generally consistent with theoretical projections for electron cyclotron or neutral beam current drive in ITER.

Table 8.2.4-I demonstrates that some enhancement in energy confinement and MHD stability relative to the 'standard' ITER ELMy H-mode case assumptions of $H_H = 1$ and $\beta_N = 2.2$ is also required. For the H-mode-like profiles case, the respective confinement enhancement factor is $H_H = 1.2$ and $\beta_N = 3.8$. These values suggest that the confinement enhancement required is relatively modest: however, the required β_N is about 1.5-times the wall-at-infinity ideal MHD

limit, and hence active resistive wall mode (external kink mode in the presence of a resistive wall) stabilization will likely be required (§3.2.4). In addition, more recent simulations that self-consistently examine the RS plasma performance attainable with candidate current drive efficiencies plasma densities and various degrees of transport reduction inside an internal transport barrier located at the zero-shear radius of candidate RS plasmas show that attaining $Q > 5$ (> 0.5 GW power) will require achieving a challenging combination of plasma performance 'enhancement' characteristics including more than 80% reduction in electron and ion transport across the ITB and also β levels that will require wall stabilization [9]. For sustained steady-state operation, it will also be necessary to control the current and pressure profiles on time-scales of > 1000 s.

Finally, both of the ITER advanced steady-state scenarios discussed above assume that operation will be possible in ITER at densities above the Greenwald density limit. The final scenario in Table 8.2.4-I addresses this issue by considering operation with the volume averaged density equal to Greenwald limit. Otherwise the profiles are the same as assumed for the scenario with H-mode like profiles. It is possible to compensate for the lower density to an extent by raising the temperature. However, this pushes the operating point past the peak in $<\sigma v>/T^2$, so that the plasma reactivity and the total fusion power are correspondingly reduced (to 1000 MW in the low-density scenario). Confinement and beta enhancement factors are otherwise similar to the higher-density H-mode-like scenario. It is quite clear that high-density ($\geq n_{GW}$) is an essential requirement for successfully steady-state operation in ITER at rated fusion power.

8.2.4.2. Advanced performance control in present experiments and projections to ITER

The parameters presented in the previous section are intended to illustrate the characteristics of candidate steady-state operation modes for ITER and also to show to some degree the uncertainties (owing largely to present lack of definitive understanding of the physics basis of reverse-shear and other advanced-performance plasma operation modes) in what may be required in ITER. Because of these uncertainties, it is premature to draw definitive conclusions about exactly how advance performance will be obtained and controlled in ITER. However, the are certain aspects of advanced performance operation and control that can already be foreseen. These operation and control considerations are:

i) Setting up of the required current profile and transport barrier during the low-β phase of the discharge,

ii) Maintenance of this current density profile during the plasma current ramp-up to about 12-13 MA and during the burn,

iii) Control of the transport barrier throughout the evolution of the discharge towards steady-state equilibrium.

The pressure gradients must also be controlled in order to maintain MHD stability at high β, since in present experiments, excessive pressure gradient frequently leads to growing MHD instability and loss of the ITB and/or disruption (see §3.2.7). The control of the burn—through DT fueling and He exhaust—is expected to be more difficult than in the standard ELMy H-mode regime, because of the strong coupling between the current density profile and the transport coefficients, and also because the barrier provides for some decoupling between the core and edge plasmas.

Present experiments mostly address aspect (*i*), the setting-up of the current density profile and formation of the transport barrier: Various techniques have been used to affect the current penetration, in order to obtain the required target current profile. The main actuators are the plasma current ramp-up rate, plasma density and additional heating power waveforms. Each of these primarily affects the ratio between the current rise time and the current penetration time. Thus some freedom is available in finding the most appropriate route to the optimized shear configuration. However, there are also additional and machine-dependent constraints, such as the minimum electron density for avoiding m=2, n=1 locked mode formation (see §3.2.5) and in avoiding excessive NBI 'shine-through (see §6), the effect of the initial density on the subsequent H-mode behavior (see §2.4), and current-rise MHD instabilities of the external kink type (see §8.2.3).

All the tokamaks cited have found satisfactory recipes for setting up the target q-profile with a limited risk of disruption. In particular, the current rise rates are relatively fast, but are still essentially free of MHD. The techniques used can, to some extent, be extrapolated to ITER. However, due to voltage limitations, off-axis non-inductive current drive assist may be necessary for ITER current ramp-up, with nevertheless some caution in view of the total grid power requirement.

Maintaining the optimized current profile—aspect *(ii)*—during the start of burn, while a large bootstrap current component is generated, and during the relaxation towards a steady-state equilibrium with zero applied electric field, will require a large amount of experimental work on present long-pulse machines and also presumably on ITER where magnetic relaxation times are comparable to the standard inductive-pulse duration. In Tore Supra, first attempts to control the current density profile have been partially successful and produced LH-driven steady-state discharges with a required internal inductance [10]. This involves actuating either the launched LH power or the phasing of the launcher in order to modify the wave power deposition pattern. In JT-60U, generating and maintaining the negative central magnetic shear were demonstrated by LHCD

alone [7] and a negative central shear has been sustained for 7.5 s. When the steep internal transport barrier was formed, a high bootstrap current component carrying 70% of the total plasma current was transiently induced [11].

Given the stiffness of the current density profile and the relatively small leverage exercised by the current drive systems, it will be important that the self-generated bootstrap current has a high degree of alignment with the pre-formed current profile, and this will probably require advanced model-based predictive control right from the early stage of the discharge and during the ramp-up phase. Up to now, the transient results are all obtained while the plasma current is being ramped up at a relatively high rate (0.3 MA/s in JET), implying large edge currents. Combining the poloidal field system control with efficient off-axis current drive at low temperature is therefore thought to be most valuable in order to provide the desired control capability.

Controlling the heat transport barrier— aspect *(iii)*—together with the current profile is required in order to avoid MHD instabilities as found on DIII-D, JET and JT-60U. Typically, MHD instabilities arise when the pressure profile becomes too peaked. In DIII-D, this is counteracted by allowing an L to H-mode transition to take place at the appropriate time. The pressure profile then broadens, and a disruption is avoided. In JET [12], this is also a possibility, but it is found that the H-mode phase does not lead to an enhanced performance. The present control technique is rather to adjust the neutral beam heating power, through a feedback loop, in order to obtain a pre-programmed waveform of the D-D reaction rate. In JT-60U, control of the barrier is exercised by moving the NBI heating off-axis, which is done by changing the major radius of the discharge, or by applying high-parallel-wavenumber LH waves for off-axis current drive.

At present there is no universal recipe for the control of the transport barrier and this must be the object of R&D. The optimum scenario appears to be machine-dependent. Machine dependencies come in via factors such as NBI shine-through, error-field density limits, recycling characteristics, etc. We thus conclude that while some of these techniques may have their equivalents in ITER, it is likely that a significant amount of effort will be required to produce steady-state optimized shear burning plasmas.

In addition to the control issues found on present experiments, ITER will have to provide control of the D-T ratio, helium exhaust, heat removal through radiation. Recent JET experiments with residual tritium on the walls, showed that the optimised shear regime has a significantly lower interaction with the walls than the standard ELMy H-mode. In fact, nearly all of the fuelling of the enhanced core comes from NBI but it is not clear yet whether the extrapolation to core fueling in ITER is possible. Alternative pellet fueling would also have to be proven compatible with off-axis current drive. Recent experiments in JT-60U with helium beam core fueling suggest a significant diffusion of helium across the heat transport barrier [13]. As far as radiation is concerned,

controlling the location of the transport barrier may turn out to provide a better decoupling between the high confinement region and the highly radiating edge.

8.2.4.3. Energy confinement considerations

In advanced performance scenarios, energy confinement (ITB effect) and the resulting pressure profile and bootstrap current profile are intimately coupled. Hence it is not possible to fully separate current and pressure control. The excellent global confinement seen in reversed shear discharges has motivated extensive analysis of the experimental data. This analysis has focused on the paradigm of turbulence suppression via E×B flow shear [14]. The E×B flow shear (which is produced mainly by internal pressure gradients) can give rise to transport barriers. Barriers to both electron [15] and ion [16] transport have been reported, and it has been inferred from transport analysis of TFTR and DIII-D discharges that the ion thermal transport is reduced to neoclassical levels in the reversed shear region. Such turbulence suppression is expected on theoretical grounds [17] and is currently the subject of much theoretical research (for an excellent review of this subject, see Ref. [18]).

While the ExB model can explain experimental data, its predictive application is still limited and making predictions for barrier characteristics and control methods in ITER requires better physics understanding. However, eventual understanding of the underlying details of transport barrier formation may make it possible to control the temperature and/or density profiles in ITER advanced steady-state operating modes with the application of modest amounts of auxiliary power. This would enable better control of plasma temperature and density profiles. Such profile control is particularly important in ITER advanced steady-state operating modes with large bootstrap current fractions because the total current profile is largely determined by the density and temperature profiles through the neoclassical bootstrap effect. Hence, transport control would enable operation with lower disruptivity, and with higher bootstrap current fractions, thereby greatly reducing the non-inductive current drive power requirements (e.g., the optimised case in Table 8.2.4-I). There has been some success in this area through the use of IBW waves to create sheared poloidal flows within the plasma which, in turn, created barriers to the transport of particles and energy [19], [20], [21]. Further progress in the demonstration of the formation and active control transport barriers could greatly enhance the performance of ITER advanced steady-state operating modes and the attractiveness of a steady-state demonstration reactor based on these operating modes.

8.2.4.4. Simulations of ITER current drive and plasma operating point control

In steady-state operation off-axis current drive is required. Off-axis current drive is possible with ECRF power at a current drive figure-of-merit $\gamma_{ECRH} \approx 0.20 \times 10^{20}$ A/W-m^2; with Lower hybrid (LH) waves ($\gamma_{LH} = 0.34 \times 10^{20}$ A/W-m^2); and possibly even with mode-converted ICRF power. Assuming the density and temperature profiles from the optimized operating point of Table 8.2.4-I, the ACCOME code has been used to develop scenarios in which a combination of 50 MW of LH and 40 MW of neutral beam power can, in combination with the bootstrap effect, support the full plasma current, providing a total plasma current profile that is stable to ballooning modes and n=1,2, and 3 ideal kink modes up to $\beta_N = 3.0$ even in the absence of a conducting wall [22].

Time-dependent scenarios involving LH and fast wave power have been studied with the transport codes JETTO and ASTRA [8]. The transport code results are analyzed with the MHD stability code CASTOR, to study the behavior of ballooning, kink and infernal modes. The LHCD deposition profiles are determined with codes validated on existing experimental results (BARANOV and BANDIT3D). Practical means of controlling the current density profile and fusion power by appropriate feedback loops are also investigated with ASTRA and CRONOS. In an advanced scenario of steady-state operation at 13 MA plasma current, off-axis LHCD in the region r/a = 0.5 - 0.8 is used to create a wide magnetic shear reversal zone and to provide full current drive together with the bootstrap current. A consistent scheme is obtained with a bootstrap fraction $I_{bs}/I_p \approx 0.7$, $I_{LH}/I_p \approx 0.25$, $I_{FW}/I_p \approx 0.05$ (Fig. 8.2.4-4). A fusion power output of about 1 GW is produced in steady state.

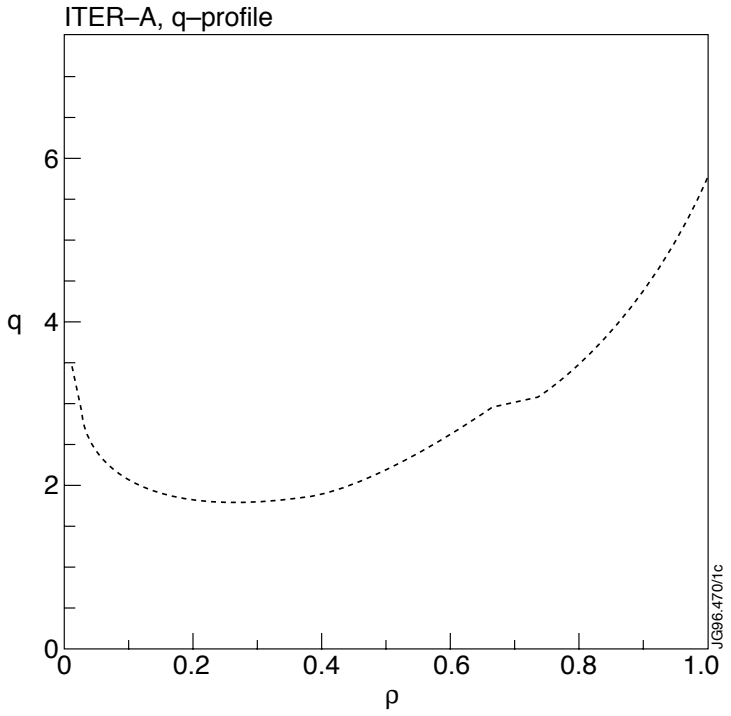

FIG. 8.2.4-4. JETTO simulation of the q-profile during the current flat-top in an advanced scenario with LHCD current profile control in ITER

The sensitivity of these results to various assumptions on the transport models regarding, for example, the effect of shear reversal has been studied by running similar scenarios on codes such as ASTRA and CRONOS. In the case of strongly non-linear shear dependence in the advanced scenarios, feedback schemes may be necessary to control the discharge against MHD collapse and undesired evolution to other steady-state equilibria. This is due to the strong coupling loops which exist between the current profile, heat transport, alpha-particle heating, bootstrap current and resistive diffusion, which in turns determines the current profile evolution [23] Thus, access to optimized MHD-stable profiles and prescribed fusion yields may require simultaneous control, on a slow resistive time scale, of the off-axis (LH) current generation, of the central heating and current drive power (e.g. FWCD), and of the plasma fuel density. It is found that real-time calculations of the internal electric field from magnetic reconstruction are very advantageous for control purposes in order to avoid strong relaxation oscillations and collapses during transitions of the transport coefficients.

8.2.4.5. Summary and future R&D recommendations

'Advanced performance' plasma operation modes based upon modified or optimized shear profiles that exhibit enhanced energy confinement and sometimes enhanced MHD stability have been obtained in a wide range of present tokamaks. Plasma with weak or reversed magnetic shear profiles are common to all of the experiments: other plasma operation features, including plasma shape and divertor vs. limiter operation appear to be unimportant to the attainment of at least some degree of performance enhancement. To date, studies of such modes have concentrated primarily on the attainment of the requisite conditions, which typical combine a weak or reversed magnetic shear profile—usually created by current or plasma shape ramping—with formation of an auxiliary-heating-induced internal transport barrier, and the 'advanced performance' phase so-obtained is usually transient owing either to the eventual magnetic relaxation of the shear profile or to the eventual onset of MHD instability owing to rising plasma pressure. However, sustained (potentially steady-state) reversed-shear modes have also been obtained by using lower hybrid current drive to create a reversed-shear profile.

Present experimental investigations of advanced performance have tended to concentrate on attainment of the required plasma conditions and optimization of plasma performance rather than on exploring explicit control of the shear and/or pressure profiles or transport barrier properties. This present limitation on the study of control can be ascribed to a great degree to the fact that experimental means — e.g., powerful rf heating and current drive systems with good radial deposition control and agility — to actively varying control the current and pressure profiles are only now becoming available in the present generation of tokamak experiments. So at present understanding of underlying physics mechanisms that control internal transport barrier formation and efficacy is lacking, and empirical data on active shear profile and barrier control are only now starting to become available. Hence the physics design of advanced performance scenarios for ITER and for the control of such advanced-performance operation are provisional. However, the ITER design incorporates the basic hardware provisions — including sufficient PF system flexibility and plasma magnetics control capability and also various options for radially-localized heating and current drive — that are anticipated to be necessary to support steady-state operation sustained by non-inductive current drive and bootstrap current. Assessments of the feasibility of achieving such operation in ITER confirm that the capabilities of the design are consistent with known requirements for the reversed-shear (RS) plasma operation modes that are now obtained (mostly on a transient basis) in present tokamaks. But since the physics understanding of these modes and the operation features required to sustain and control them on a steady-state basis are still subjects of on-going physics R&D, at the present time the degree to which steady-state

operation can be ultimately be achieved in ITER and the details of how such operation will be controlled largely remain as questions to be answered by research to be undertaken in the future.

A number of considerations related to ITER plasma operation and control in an RS mode have emerged. First, weak or negative magnetic shear plasmas can be produced in ITER by the same method of current and/or shape ramping combined with early auxiliary heating that has been used to obtain enhanced-performance RS plasmas in present tokamaks. Such 'transient' operation in ITER will likely be useful as an alternate to standard ELMy H-mode operation to obtain ignition and study approach to equilibrium thermal helium levels. Experiment durations are estimated to exceed 100 s. Second, the ITER PF system and divertor system are compatible on a steady-state basis with a high-q, high-elongation, high-triangularity plasma that can be obtained by shifting the plasma radially outward with decreased minor radius ($R_O \cong 8.5$ m, $a \cong 2.4$ m, $\kappa_{95} \cong 2.0$, $I_p \cong 12$ MA, $q_{95} \cong 5$). Third, non-inductive sustainment of a reverse-shear current profile and 12-MA current (~80% bootstrap-driven) is consistent to first approximation with 100 MW of current drive power apportioned between on-axis and off-axis current drive deposition. Fourth, the ideal MHD stability of such current profiles and the plasma pressure profile required for up to 1.5 GW fusion power is adequate if stabilization of external kink modes by an ideally-conducting wall located at $r/a \cong 1.3$ is assumed.

However, considerations 3) and 4) are based upon *ad hoc* assumptions that it will be possible to simultaneously obtain near-optimal plasma pressure, current density and safety factor profiles, MHD wall stabilization and also reduction in plasma energy transport relative to transport observed in positive-shear H-mode plasmas. In contrast, simulations that self-consistently examine the RS plasma performance attainable with candidate current drive efficiencies plasma densities and various degrees of transport reduction inside an internal transport barrier located at the zero-shear radius of candidate RS plasmas show that attaining $Q > 5$ (> 0.5 GW power) will require obtaining a challenging combination of plasma performance 'enhancement' characteristics including beta levels that will require wall stabilization.

There are also significant uncertainties as to how well RS plasmas can be controlled in a steady-state regime. Magnetic control of the high-elongation plasmas needed for RS operation will be less robust than magnetic control of similar full-bore ITER plasmas. Control of the current profile is also more problematical in the physics sense, since the bootstrap current profile is determined by the pressure profile (which in turn may be determined by the shear and/or rotation profiles and ITB efficacy in a manner that is not yet fully understood), and also in the practical sense that the ability to arbitrarily control on-axis and off-axis current drive profiles is subject to physics and technological limitations. In addition, how plasma rotation affects wall stabilization and whether 'active' stabilization of the resistive wall MHD mode (the result of resistance in the kink-stabilizing wall) will be required to obtain adequate beta in RS plasmas both remain as open

physics issues that need to be resolved by future research. These considerations and present uncertainties make design of a RS plasma control system and drawing conclusions about its adequacy premature. It is clear, however, that at a minimum, accurate real-time measurement of the q(r) or j(r) profiles and also of the electron and ion p(r) profiles of ITER RS plasmas will be critical to their successful control, and that candidate current drive systems will have to have some degree of active control capability that can be used to first optimize the current profile and then to respond to changes in the bootstrap current profile that confinement effects produce. Finally, the time scale of ultimate relaxation to true equilibrium steady-state is expected to approach 10,000 s, so all ITER control means used must be capable of operating for essentially indefinite duration periods. This will put certain operational constraints on the various hardware and diagnostic systems involved and will also mandate the development of non-magnetic diagnostics for plasma configuration control in very-long/steady-state duration pulses.

References to Section 8.2.4

[1] T. S. Taylor, *Physics of advanced tokamaks*, Plasma Phys. Controlled Fusion **39** B47-B73 (1997).

[2] J. R. Ferron, L. L. Lao, T. S. Taylor, Y. A. Kim, E. J. Strait, D. Wroblewski, *Improved Confinement and Stability in the DIII-D Tokamak Obtained Through Modification of the Current Profile*, Phys. Fluids B **5** (1993) 2532-2539.

[3] F. M. Levinton, M. C. Zarnstorff, S. H. Batha, M. Bell, R. E. Bell, R. V. Budny, C. Bush, Z. Chang, E. D. Fredrickson, A. Janos, J. Manickam, A. Ramsey, S. A. Sabbagh, G. L. Schmidt, E. J. Synakowski, G. Taylor, *Improved Confinement with Reversed Magnetic Shear in TFTR*, Phys. Rev. Lett. **75** (1995) 4417-4420.

[4] JET Team (presented by C. Gormezano), *Optimisation of JET Plasmas with Current Profile Control*, in *Fusion Energy 1996* (Proceedings 16th IAEA Conference, Montreal 1996, IAEA Vienna 1997) **Vol. 1** 487-495.

[5] T. Fujita, S. Ide, H. Shirai, M. Kukuchi, O. Naitio, Y. Koide, S. Takeji, H. Kubo, S. Ishida, *Internal Transport Barrier for Electrons in JT-60U Reversed Shear Discharges*, Phys. Rev. Lett. **78** (1997), 2377-2380.

[6] G. T. Hoang, C. Gil, E. Joffrin, D. Moreau, A. Becoulet, P. Bibet, J. P. Bizarro, R. V. Bundy, J. Carrasco, J. P. Coulon, C. De Michelis, T. Dudok De Wit, P. Monier-Garbet, M. Goniche, R. Guirlet, T. Hutter, S. M. Kaye, J. LaSalle, L. Laurent, P. LeCoustey, X. Litaudon, M. Mattioli, Y. Peysson, A.-L. Pecquet, G. Rey, S. A. Sabbagh, B. Saoutic, G. Tonon, J. C. Vallet, *Improved Confinement in High l_i Lower Hybrid Driven Steady State Plasmas in Tore Supra*, Nucl. Fusion **34** (1994) 75-85.

[7] S. Ide, O. Naito, T. Fujita, T. Oikawa, M. Seki, JT-60 Team, *Application of LHCD to Sustainment and Control of a Reversed Magnetic Shear Plasma in JT-60U*, in *Fusion Energy 1996* (Proceedings 16th IAEA Conference, Montreal 1996, IAEA Vienna 1997) **Vol. 3** 253-264.

[8] Boucher, D., Y. Baranov, B. Fischer, X. Litaudon, D. Moreau, W. M. Nevins, V. Parail, F. X. Söldner, I. Voitsekhovitch, ITER Joint Central Team, *ITER scenarios including non-inductive steady state operation,* in *Fusion Energy 1996* (Proceedings 16th IAEA Conference, Montreal 1996, IAEA Vienna 1997) **Vol. 2** 945-952.

[9] Boucher, D., *et al*, *Assessment and Modeling of Inductive and Non-Inductive Scenarios for ITER*, to be published in *Proceedings 17th IAEA Fusion Energy Conference (Yokohama 1998)* .

[10] Wijnands, T. *et al.,* Nucl. Fus. **37** (1997) 777.

[11] S. Ide, T. Fujita, O. Naito, M. Seki, *Sustainment and modification of reversed magnetic shear by LHCD on JT-60U*, Plasma Phys. Controlled Fusion, **38 (1996)** 1645-1652.

[12] Sips, A.C.C. *et al*., *Operation at High Performance in Optimised Sghear Plasmas in JET*, in *Controlled Fusion and Plasma Physics* (Proceedings 24th European Physical Society Conference, Berchtesgarten 1997, Europhysics Conference Abstracts, Geneva,1997) **21A Part I**, 97-100.

[13] Sakasai, A. H. Kubo, K. Shimizu, T. Fujita, N. Asakura, K. Itami, S. Higashijima, S. Sakurai, H. Takenaga, N. Hosogane, *Active control of helium ash exhaust and transport characteristics in JT-60U,* in *Fusion Energy 1996* (Proceedings 16th IAEA Conference, Montreal 1996, IAEA Vienna 1997) **Vol. 1** 789-799.

[14] E.J. Doyle, et al., Plasma Physics and Controlled Nuclear Fusion Research (IAEA, Vienna, 1997) paper A6-4; K.M. M^{c}Guire, et al, Plasma Physics and Controlled Nuclear Fusion Research (IAEA, Vienna, 1997) paper O1-2; Y. Koide and the JT-60 Team, Phys. Plasmas **4**, 1623 (1997).

[15] T. Fijuta et al, Plasma Physics and Controlled Nuclear Fusion Research (IAEA, Vienna, 1997) paper A1-4; T. Fujita, et al., Phys. Rev. Lett **78**, 2377 (1997).

[16] F.M. Levington, et al., Phys. Rev. Lett. **75**, 4417 (1995); E.J. Strait, et al., Phys. Rev. Lett. **75**, 4421 (1995).

[17] see, for example, H. Biglari, et al, Phys. Fluids B **2**, 1 (1990); R. Waltz, et al., Phys. Plasmas **2**, 2408 (1995).

[18] K.H. Burrell, Phys. Plasmas **4**, 1499 (1997).

[19] M. Ono, Phys. Fluids B **5**, 241 (1993).

[20] G.G. Craddock, et als, Phys. Plasmas **1**, 1944 (1994).

[21] M. Ono, et al., Phys. Plasmas **2QA**, 741 (1995).

[22] P. Bonoli, et al. **…**

[23] X. Litaudon, et al, Plasma Physics and Controlled Nuclear Fusion Research 1996 (IAEA, Vienna, 1995) paper AP1-11.